



**NTNU – Trondheim**  
Norwegian University of  
Science and Technology

# Statistics of surf parameter and wave power for individual waves

**Hongtao Li**

Marine Technology

Submission date: July 2014

Supervisor: Dag Myrhaug, IMT

Norwegian University of Science and Technology  
Department of Marine Technology





**MASTER THESIS IN MARINE TECHNOLOGY**

**SPRING 2014**

**FOR**

**STUD. TECHN. HONGTAO LI**

**STATISTICS OF SURF PARAMETER AND WAVE POWER FOR INDIVIDUAL WAVES**

The surf parameter, also often referred to as the surf similarity parameter or the Iribarren number, is used to characterize surf zone processes. Shallow water regions where waves break are referred to as the surf zone, and the different breakers on slopes are defined and classified in terms of the surf parameter. It also appears that the surf parameter enters in many empirical and theoretical models for wave-induced phenomena in the surf zone. Statistics of the surf parameter for individual waves are appropriate in formulating risks of e.g. damage of breakwaters, seawalls and artificial reefs.

The wave power is defined as the transport of wave energy per unit crest length of the progressive wave front. The statistics of wave power for individual waves is relevant for e.g. making assessments of wave power devices and their potential for converting energy from waves.

The thesis will focus on using the Longuet-Higgins (1983) joint distribution of wave height and wave period to establish the statistics of the surf parameter as well as the wave power, and to compare these statistics with those obtained earlier by Myrhaug and Fouques (2012) for the surf parameter and by Myrhaug et al. (2009) for the wave power.

The student shall:

1. Give a background of the surf parameter and wave power including previous work on their statistics
2. Give a brief description of the Longuet-Higgins (1983) distribution
3. Present the statistics of surf parameter and wave power based on the Longuet-Higgins distribution
4. Compare the present results with the previous results by Myrhaug and Fouques (2012) and Myrhaug et al. (2009).

The work scope may prove to be larger than initially anticipated. Subject to approval from the supervisor, topics may be deleted from the list above or reduced in extent.

In the thesis the candidate shall present his personal contribution to the resolution of problem within the scope of the thesis work.

Theories and conclusions should be based on mathematical derivations and/or logic reasoning identifying the various steps in the deduction.

The candidate should utilize the existing possibilities for obtaining relevant literature.

The thesis should be organized in a rational manner to give a clear exposition of results, assessments, and conclusions. The text should be brief and to the point, with a clear language. Telegraphic language should be avoided.

The thesis shall contain the following elements: A text defining the scope, preface, list of contents, summary, main body of thesis, conclusions with recommendations for further work, list of symbols and acronyms, reference and (optional) appendices. All figures, tables and equations shall be numerated.

The supervisor may require that the candidate, in an early stage of the work, present a written plan for the completion of the work. The plan should include a budget for the use of computer and laboratory resources that will be charged to the department. Overruns shall be reported to the supervisor.

The original contribution of the candidate and material taken from other sources shall be clearly defined. Work from other sources shall be properly referenced using an acknowledged referencing system.

The thesis shall be submitted:

- Signed by the candidate
- The text defining the scope included
- In bound volume(s)
- Drawings and/or computer prints which cannot be bound should be organized in a separate folder.

Deadline: 10.06.2014

  
Dag Myrhaug  
Supervisor

## Abstract

In this thesis, the theoretical bivariate distribution of surf parameter and wave height is derived from a theoretical joint distribution of wave height and wave period based on narrow band approximation. Statistical properties of the derived bivariate probability density function are sensitive to the bandwidth parameter, which is reflected by appreciable spread in its contour. Based on theoretical solutions given by Matlab and Mable which also are verified by numerical calculations, the peak value of this distribution decreases exponentially. However the position of the peak value varies around characteristic wave height as bandwidth parameter increases in the range of interest. The resultant conditional distribution of surf parameter given small wave height is rather broad-banded.

By employing same bandwidth parameter and dimensionless quantities, the derived theoretical probability model of surf parameter and wave height is compared with best-fit parametric probability model to data from Norwegian Continental Shelf. It is found that the two models do not compare well with each other but give same statistical qualitative behaviour for statistical quantities of surf parameter such as conditional probability, expected value and variance. Resultant probabilities of four breakers also display same variation pattern for the two models.

During the recent two decades the interest of green energy has increased, and wave energy is among the area of interest. Due to the necessity to assess the appropriateness of a wave power farm, there is an urgent need for reliable statistical models to give credible predication of expected wave power in the field of interest. Hence, a theoretical bivariate distribution of wave power and wave height as well as wave power and wave period is compared with that of parametric probability model based on the same data for developing parametric probability model of surf parameter and wave height.

By pursuing the same methodology for investigation of statistical properties of theoretical distribution of surf parameter, it is shown that singularities appear in both theoretical distributions for wave power. In comparison with parametric probability model for wave power, it is shown that the marginal distribution of wave power is in good agreement. Contour plots of two models show that the theoretical model is much more broad banded. The computed conditional expected value and standard deviation of wave power given wave height from

two models show almost same increasing trend and correspond to the interpretation of the contour plots. Similarly, the two conditional characteristic quantities of wave power given wave period from two models both increase firstly then decrease with wave period.

Several numerical integration methods, including trapezoidal, Simpson and Romberg method implemented by author, are applied to obtain credible result. Adaptive Gauss quadrature is comprehensively employed to carry out validation against unity for transformed theoretical probability model of surf parameter and wave power as well as for their marginal distributions and conditional distributions. Convergence study has been conducted and results are presented either in figures or by tabulated values.

## Preface

This master thesis is completed under the supervision of Prof. Dag Myrhaug in Department of Marine Technology and submitted to NTNU for the partial fulfilment of requirements for the degree of Master of Science. The thesis work is also an integral part of two year International master programme. Much of the demanding computation work is performed on supercomputer Vilje HPC of NTNU.

Out of enthusiasm about contributing to the wave statistics, I pursue this thesis topic and benefit greatly. Programming skill turns out very essential for this task. Hence, Matlab, Maple, bash script as well as visual basic are utilized to either perform the main work or increase the efficiency. Through the whole process, I gradually realize the power and beauty of theoretical mathematics, since some problems can be solved by theoretical methods in maybe 20 minutes but numerical methods in hours. Additionally, it should be noted that there is an appreciable potential by intermediate executer to produce not meaningful results with hundred hours of work.

Therefore, this thesis work is a combination of theoretical and numerical study. The distributions of surf parameter, related quantities and wave power presented in this thesis are validated at least three times by manual derivations if possible, by numerical tool either Matlab or Maple. Convergence study is always performed to attempt to deliver credible result. As for concrete problems, several integration methods are employed to obtain converged results.

At the end of my master student life, I would like firstly to express my sincere gratitude towards my supervisor Prof. Dag Myrhaug for his patient guidance and stimulating discussions. I would also like to give special thanks to Prof. Bernt Leira for his valuable input. I appreciate the helpful discussions with Hong Wang and Prof. Håvard Holm about programming. I acknowledge the insights for verification and validation concepts provided by my project thesis supervisor Prof. Tor Einar Berg, during the completion of project thesis at last autumn. I also would like to thank my previous supervisor Prof. Yi Huang at DUT, my teachers Prof. Ye Li, Prof. Yushan Sun and Prof. Hai Huang at HEU and PhD Mun Chen Ong at MARINTEK for their encouragements to begin my academic journey.

I would like to extend my thanks to my officemates, Torleif Bertelsen, Sindre Dahl, Andreas

Bergstad, Christian Andersson and Arild Matland for the motivating studying environment. In addition, I wish to thank friends here and elsewhere, in particular post-doc Ekaterina Kim, PhD Fachri Panusunan Nasution, Long Chen, Jie Zhang, Bowen Zhang, Ke Gao, Quentin Pallato, Ségolène Méjean, Tianjiao Dai, Boyang Zhao, Xu Han, Xin Lv, Ping Fu, Annika Laks, Chunqi Zhou, Meilin Ma, Chongyao Zhou, Tianzuo Yao and Jing Zhao. You share my memory and fun.

Lastly, I feel much grateful towards my parents Zhiwen Li, Chunmei Tang and elder brother Chuan Li for your love, care and support. Without you, I would never ever realize my beautiful dreams one by one.

Trondheim, July 1st, 2014

Hongtao Li



## Nomenclature

$\alpha_d$	deepwater model parameter
$B$	coefficient for connecting $t$ with $\hat{t}_{MK}$
$C_g$	wave group velocity
$C_\omega$	wave profile velocity
$d_b$	water depth at wave breaking
$h_b$	breaker index
$E$	total average wave energy per unit surface area
$E(j_{MK} \hat{h}_{MK})$	expected value of normalized wave power given normalized wave height
$E(j_{MK} \hat{t}_{MK})$	expected value of normalized wave power $j_{MK}$ given normalized wave period $\hat{t}_{MK}$
$E(R \hat{h}_{MK})$	expected value of runup $R$ given $\hat{h}_{MK}$
$E(\hat{\xi}_{MK} \hat{h}_{MK})$	expected value of $\hat{\xi}_{MK}$ given $\hat{h}_{MK}$
$f$	wave frequency
$F(\hat{h}/\nu)$	correction factor to Rayleigh distribution of $\hat{h}$ in LH83 model
$g$	acceleration of gravity
$\gamma_T$	coefficient for connecting $T_{rms}$ with $T_z$
$\gamma_\xi$	coefficient used for connecting $\hat{\xi}_{MK}$ with $\hat{h}_{MK}$ and $\hat{t}_{MK}$
$G(\nu)$	parameter dependent on $\nu$
$\hat{h}_{IN}$	normalized wave height by $\sqrt{m_o^f}$
$\hat{h}$	normalized wave height by characteristic wave height $H_{cr}$
$\hat{S}$	normalized wave steepness by characteristic wave steepness $S_{cr}$
$\hat{\xi}$	normalized surf parameter by characteristic surf parameter $\xi_{cr}$

$\hat{h}_b$	normalized breaker index that is dependent on $\hat{\xi}$
$H_b$	wave height at wave breaking
$\hat{h}_{max}$	value of $\hat{h}$ corresponding to $p_{max}$
$\hat{h}_{MK}$	wave height normalized by $H_{rms}$
$H_{rms}$	root mean square value of wave height from data
$H_s$	significant wave height
$j$	normalized wave power corresponding with $\hat{h}$ and $t$
$J$	dimensional wave power of per unit crest length
$j_{MK}$	normalized wave power corresponding with $\hat{h}_{MK}$ and $\hat{t}_{MK}$
$K$	empirical coefficients for connecting $R$ with $\xi$ and $H$
$k_1$	one of two empirical coefficients for connecting breaker index $hb$ with surf parameter $\xi$
$k_2$	the other empirical coefficient for connecting breaker index $hb$ with surf parameter $\xi$
$L(\nu)$	parameter dependent on bandwidth parameter $\nu$ and defined in LH83 model
$\lambda$	wave length
$m$	slope
$m_n^f$	$n$ th spectral moment expressed in wave frequency $f$
$\mu_R$	expected value of $\ln R$ from MF12 model
$\mu_{\hat{\xi}}$	expected value of $\ln \hat{\xi}_{MK}$ from MF12 model
$n$	parameter used in MB09 probability model for wave power
$p(\hat{h}_b, \hat{h})$	joint probability density function of $\hat{h}_b$ and $\hat{h}$
$p(\hat{h}_{bMK}, \hat{h}_{MK})$	joint probability density function of $\hat{h}_{bMK}$ and $\hat{h}_{MK}$
$\phi$	cumulative distribution function of standard normal distribution

$p(\hat{h}_{MK})$	marginal probability density function of normalized wave height $\hat{h}_{MK}$
$p\left(\hat{t}_{MK} \hat{h}_{MK} = \sqrt{\frac{j_{MK}}{\hat{t}_{MK}}}\right)$	probability density function obtained by substituting $\sqrt{\frac{j_{MK}}{\hat{t}_{MK}}}$ for $\hat{h}_{MK}$ in $p\left(\hat{t}_{MK} \hat{h}_{MK}\right)$
$p(H, \xi)$	joint probability density function of wave height $H$ and surf parameter $\xi$
$p(j, \hat{h})$	joint probability density function of $j$ and $\hat{h}$
$p(j_{IN}, \hat{h}_{IN})$	joint probability density function of normalized wave power $j_{IN}$ and normalized wave height $\hat{h}_{IN}$
$p(\hat{j}_{IN}, \tau)$	joint probability density function of normalized wave power $\hat{j}_{IN}$ and normalized wave period $\tau$
$p(j_{MK} \hat{h}_{MK})$	conditional probability density function of normalized wave power $j_{MK}$ given normalized wave height $\hat{h}_{MK}$
$p(j_{MK}, \hat{h}_{MK})$	joint probability density function of normalized wave power $j_{MK}$ and normalized wave period $\hat{h}_{MK}$
$p(j, t)$	joint probability density function of $j$ and $t$
$p_{max}$	maximum value of probability density function
$p(R, H)$	joint probability density function of $R$ and $H$
$p(R \hat{h}_{MK})$	conditional probability density function of $R$ given $\hat{h}_{MK}$
$p(\hat{t}_{MK} \hat{h}_{MK})$	conditional probability density function of $\hat{t}_{MK}$ given $\hat{h}_{MK}$
$p(\xi, H)$	joint probability density function of $\xi$ and $H$
$p(\hat{\xi}_{MK} \hat{h}_{MK})$	conditional probability density function of $\hat{\xi}_{MK}$ given $\hat{h}_{MK}$
$p(\hat{\xi}_{MK}, \hat{h}_{MK})$	joint probability density function of $\hat{\xi}_{MK}$ and $\hat{h}_{MK}$
$p(\xi, R)$	joint probability density function of $\xi$ and $R$
$Q(v)$	parameter dependent on $v$
$r$	parameter used in MB09 probability model for wave power

$R_a$	normalized wave amplitude
$\rho$	water density
$S$	wave steepness
$S(f)$	wave spectrum expressed in wave frequency $f$
$\sigma(j_{MK} \hat{h}_{MK})$	standard deviation of normalized wave power $j_{MK}$ given normalized wave height $\hat{h}_{MK}$
$\sigma(j_{MK} \hat{t}_{MK})$	standard deviation of normalized wave power $j_{MK}$ given normalized wave period $\hat{t}_{MK}$
$\sigma_R^2$	variance of $\ln R$ from MF12 model
$\sigma_{\hat{\xi}}^2$	variance of $\ln \hat{\xi}_{MK}$ from MF12 model
$\sigma(\hat{\xi}_{MK} \hat{h}_{MK})$	conditional standard deviation of $\hat{\xi}_{MK}$ given $\hat{h}_{MK}$
$S_{rms}$	root mean square value of wave steepness from data
$T$	wave period
$\hat{t}_{MK}$	wave period normalized by $T_{rms}$
$\tau$	wave period normalized by $\bar{T}$
$\theta$	angle relative to horizontal level
$T_z$	mean zero crossing period
$\nu$	bandwidth parameter
$W(\nu)$	parameter dependent on $\nu$
$\xi$	surf parameter
$\hat{\xi}_{max}$	value of $\hat{\xi}$ corresponding to $p_{max}$
$\hat{\xi}_{MK}$	surf parameter normalized by $\xi_{rms}$
$A$	coefficient bridges different normalized procedures for wave height
$C_m$	coefficient bridges different normalized procedures for surf parameter

$\gamma_H$	coefficient used for defining root mean square value of wave height
$\gamma_s$	coefficient used for defining rms value of wave steepness
$\hat{h}_{bMK}$	normalized breaker index that is dependent on $\hat{\xi}_{MK}$
$H_{cr}$	characteristic wave height for normalization
hMK	$hMK \equiv \hat{h}_{MK}$
jMK	$jMK \equiv j_{MK}$
$p_{max}$	maximum value of joint distribution $p(\hat{\xi}, \hat{h})$ as $v$ varies
$p_{max_{fit}}$	best fit to maximum value of joint probability density function $p(\hat{\xi}, \hat{h})$ as $v$ varies
$p(\hat{\xi}, \hat{h})$	joint probability density function of $\hat{\xi}$ and $\hat{h}$
$S_{cr}$	characteristic wave steepness for normalization
$t$	normalized wave period by characteristic period $T_{cr}$
$T_{cr}$	characteristic wave period
$x_d$	limit for various types of wave breakers
$\xi_{cr}$	characteristic surf parameter for normalization

## Abbreviations

cdf	cumulative distribution function
DUT	Dalian University of Technology
HEU	Harbin Engineering University
NTNU	Norwegian University of Science and Technology
pdf	probability density function
rms	root mean square value
SWL	still water level
WEC	wave energy converter

# Contents

- 1 Introduction** **1**
- 1.1 Background . . . . . 1
  - 1.1.1 surf parameter . . . . . 1
  - 1.1.2 Wave power . . . . . 2
- 1.2 Notes for numerical method . . . . . 3
- 1.3 Objectives and scope of work . . . . . 4
- 1.4 Thesis outline . . . . . 4
  
- 2 Statistics of surf parameter for individual waves** **7**
- 2.1 Theoretical bivariate distribution of surf parameter and wave height . . . . . 7
- 2.2 Parametric joint distribution of surf parameter and wave height . . . . . 11
- 2.3 Comparison between parametric probability and theoretical probability model 13
  - 2.3.1 Using same normalized quantities . . . . . 13
  - 2.3.2 Comparison of statistical quantities of interest . . . . . 14
  - 2.3.3 Application examples . . . . . 18
  
- 3 Statistics of wave power for individual waves** **33**
- 3.1 Basic mathematics background for wave power . . . . . 33
- 3.2 Theoretical probability model for wave power . . . . . 34
- 3.3 Parametric probability model for wave power . . . . . 37
- 3.4 Comparison between theoretical and parametric probability model for wave power . . . . . 38
  - 3.4.1 Comparison of peak values from two models . . . . . 38
  - 3.4.2 Comparison of other properties from two models . . . . . 40
  
- 4 Conclusions and Recommendations** **47**

4.1	Conclusions . . . . .	47
4.2	Recommendation for further work . . . . .	48
	<b>Bibliography</b>	<b>50</b>
<b>A</b>	<b>Derivation and numerical stability study of the theoretical</b>	<b>55</b>
A.1	Erratum in Longuet - Higgins 83 Model . . . . .	55
A.2	Maximum value of theoretical joint distribution of surf parameter and wave height . . . . .	56
A.3	Connection between different normalized procedure . . . . .	57
A.4	Another approach to derive theoretical models for different quantities of interest	59
A.4.1	Normalized quantities . . . . .	59
A.4.2	Dimensional quantities . . . . .	60
A.5	Numerical Stability Study for surf parameter and runup . . . . .	60
A.5.1	surf parameter . . . . .	60
A.5.2	Runup . . . . .	69
<b>B</b>	<b>Derivation and numerical stability study of the theoretical</b>	<b>71</b>
B.1	Numerical stability study for MB09 model . . . . .	71
B.2	Numerical Stability Study for IN11 model . . . . .	72
<b>C</b>	<b>Matlab Scripts</b>	<b>79</b>
<b>D</b>	<b>Example of visual basic code for Excel</b>	<b>87</b>
<b>E</b>	<b>Example of bash script for using on supercomputer</b>	<b>88</b>



# List of Figures

2.1	The value and position of $p_{max}$ vary with $\nu$ in the range of 0.05:0.03:0.8 . . . . .	10
2.2	Isocontours of derived LH83 model $p(\hat{h}_{MK}, \hat{\xi}_{MK})$ , $p$ takes peak value (indicated as $\times$ ), 0.8, 0.3, 0.1, 0.01, 0.001 and 0.0001 respectively from the centre outwards . . . . .	14
2.3	Isocontours of MF12 model $(\hat{h}_{MK}, \hat{\xi}_{MK})$ , $p$ takes peak value (indicated as $\times$ ), 0.8, 0.3, 0.1, 0.01, 0.001 and 0.0001 respectively from the centre outwards (adapted from Myrhaug and Fouques (2012)) . . . . .	15
2.4	$p(\hat{h}_{MK})$ versus $\hat{h}_{MK}$ . . . . .	16
2.5	Marginal cdf $P(\hat{h}_{MK})$ versus $\hat{h}_{MK}$ . . . . .	17
2.6	Marginal cdf $P(\hat{\xi}_{MK})$ versus $\hat{\xi}_{MK}$ . . . . .	17
2.7	$P(\hat{\xi}_{MK} \hat{h}_{MK})$ versus $\hat{\xi}_{MK}$ in Weibull-scale . . . . .	18
2.8	$E[\hat{\xi}_{MK} \hat{h}_{MK}]$ . . . . .	19
2.9	$\sigma(\hat{\xi}_{MK} \hat{h}_{MK})$ . . . . .	19
2.10	Probability of breaker index $\hat{h}_{bMK}$ in Weibull scale . . . . .	20
2.11	Conditional probability of breaker index $\hat{h}_{MKb}$ in Weibull scale . . . . .	21
2.12	Sketches of different wave breakers (after Sorensen (1993)) . . . . .	21
2.13	Probability of spilling breakers as $S_m$ and slopes $m$ vary . . . . .	23
2.14	Probability of plunging breakers as $S_m$ and slopes $m$ vary . . . . .	23
2.15	Probability of collapsing breakers as $S_m$ and slope $m$ vary . . . . .	24
2.16	Probability of surging breakers as $S_m$ and slope $m$ vary . . . . .	24
2.17	Marginal probability density of $\xi_{MK}$ for $S_m = 0.010$ and different slopes $m$ . . . . .	25
2.18	Marginal probability density of $\xi_{MK}$ for $S_m = 0.035$ and different slopes $m$ . . . . .	25
2.19	Marginal probability density of $\xi_{MK}$ for $S_m = 0.070$ and different slopes $m$ . . . . .	26
2.20	Isocontours of joint density $p(H, \xi)$ for slope $m = 0.10$ . $p$ takes peak value(indicated as $\times$ ), 0.1, 0.01, 0.001 and 0.0001 from center outwards . . . . .	26

2.21	Isocontours of joint density $p(H, \xi)$ for slope $m = 0.30$ . $p$ takes peak value (indicated as $\times$ ), 0.1, 0.01, 0.001 and 0.0001 from center outwards . . . . .	27
2.22	Isocontours of joint density $p(H, \xi)$ for slope $m = 0.50$ . $p$ takes peak value(indicated as $\times$ ), 0.1, 0.01, 0.001 and 0.0001 from center outwards . . . . .	27
2.23	Sketch for runup . . . . .	27
2.24	Conditional cumulative distribution of wave run-up given wave height $P(R H)$	30
2.25	Conditional cumulative distribution of wave run-up given wave height $P(R H)$	31
3.1	Isocontour of $p(\hat{t}_{MK}, j_{MK})$ from MB09 model, $p$ takes 0.001, 0.01, 0.1, 0.25, 0.75, 1.25, 1.75 and 2 from outermost to the centre (adapted from Myrhaug et al. (2009)) . . . . .	39
3.2	Isocontour of $p(\hat{t}_{MK}, j_{MK})$ from IN11 model, $p$ takes 0.001, 0.01, 0.1, 0.25, 0.75, 1.25, 1.75 and 2 from the outermost to the centre . . . . .	39
3.3	Isocontour of joint probability density $(\hat{h}_{MK}, j_{MK})$ from MB09 model, $p$ takes 1, 0.7, 0.3, 0.1, 0.01, 0.001 from center outwards . . . . .	40
3.4	Isocontour of joint probability density $(\hat{h}_{MK}, j_{MK})$ from IN11 model, $p$ takes 1, 0.7, 0.3, 0.1, 0.01, 0.001 from center outwards . . . . .	40
3.5	Marginal distribution of $j_{MK}$ . . . . .	41
3.6	$E(j_{MK} \hat{h}_{MK})$ versus $\hat{h}_{MK}$ . . . . .	42
3.7	$\sigma(j_{MK} \hat{h}_{MK})$ . . . . .	42
3.8	Contour of $\hat{h}_{MK}^2 \hat{t}_{MK} p(\hat{h}_{MK}, \hat{t}_{MK})$ . . . . .	43
3.9	$E(j_{MK} \hat{h}_{MK}) p(\hat{h}_{MK})$ versus $\hat{h}_{MK}$ . . . . .	44
3.10	$E(j_{MK} \hat{t}_{MK})$ versus $\hat{t}_{MK}$ . . . . .	45
3.11	$\sigma(j_{MK} \hat{t}_{MK})$ versus $\hat{t}_{MK}$ . . . . .	45
3.12	$E(j_{MK} \hat{t}_{MK}) p(\hat{t}_{MK})$ versus $\hat{t}_{MK}$ . . . . .	46
3.13	Marginal pdf $p(\hat{t}_{MK})$ versus $\hat{t}_{MK}$ . . . . .	46
A.1	Variation of $p_{max}$ as $v$ is close to 0 and 1, respectively . . . . .	57
A.2	$E(\hat{\xi}_{MK} \hat{h}_{MK})$ versus $\hat{h}_{MK}$ $\hat{\xi}_{MK} = 0.0005 : 0.0005 : 400.0005$ . . . . .	61
A.3	$E(\hat{\xi}_{MK} \hat{h}_{MK})$ versus $\hat{h}_{MK}$ $\hat{\xi}_{MK} = 0.0005 : 0.0005 : 600.0005$ . . . . .	61
A.4	$\delta E(\hat{\xi}_{MK} \hat{h}_{MK})$ versus $\hat{h}_{MK}$ $\hat{\xi}_{MK} = 0.0005 : 0.0005 : 600.0005$ and $\hat{\xi}_{MK} = 0.0002 : 0.0002 : 600.0002$ , respectively . . . . .	62
A.5	$E(\hat{\xi}_{MK} \hat{h}_{MK})$ versus $\hat{h}_{MK}$ $\hat{\xi}_{MK} = 0.0005 : 0.0005 : 1000.0005$ . . . . .	62

A.6	$\delta E(\hat{\xi}_{MK} \hat{h}_{MK})$ versus $\hat{h}_{MK} \hat{\xi}_{MK} = 0.0005 : 0.0005 : 600.0005$ and $\hat{\xi}_{MK} = 0.0005 : 0.0005 : 1000.0005$ , respectively . . . . .	63
A.7	$\delta E(\hat{\xi}_{MK} \hat{h}_{MK})$ caused by using Simpson and Romberg integration method, respectively . . . . .	63
A.8	Comparison of $E(\hat{\xi}_{MK} \hat{h}_{MK})$ between derived LH83 model and MF12 model $\hat{\xi}_{MK} = 0.0005 : 0.0005 : 1000.0005$ . . . . .	64
A.9	$\sigma(\hat{\xi}_{MK} \hat{h}_{MK})$ versus $\hat{h}_{MK} \hat{\xi}_{MK} = 0.0005 : 0.0005 : 400.0005$ . . . . .	65
A.10	$\sigma(\hat{\xi}_{MK} \hat{h}_{MK})$ versus $\hat{h}_{MK} \hat{\xi}_{MK} = 0.0005 : 0.0005 : 600.0005$ . . . . .	65
A.11	$\delta\sigma(\hat{\xi}_{MK} \hat{h}_{MK})$ versus $\hat{h}_{MK} \hat{\xi}_{MK} = 0.0005 : 0.0005 : 600.0005$ and $\hat{\xi}_{MK} = 0.0002 : 0.0002 : 600.0002$ , respectively . . . . .	66
A.12	$E(\hat{\xi}_{MK} \hat{h}_{MK})$ versus $\hat{h}_{MK} \hat{\xi}_{MK} = 0.0005 : 0.0005 : 1000.0005$ . . . . .	66
A.13	$\delta\sigma(\hat{\xi}_{MK} \hat{h}_{MK})$ versus $\hat{h}_{MK} \hat{\xi}_{MK} = 0.0005 : 0.0005 : 600.0005$ and $\hat{\xi}_{MK} = 0.0005 : 0.0005 : 1000.0005$ , respectively . . . . .	67
A.14	$\delta\sigma(\hat{\xi}_{MK} \hat{h}_{MK})$ caused by using Simpson and Romberg integration method, respectively . . . . .	67
A.15	Comparison of $\sigma(\hat{\xi}_{MK} \hat{h}_{MK})$ between derived LH83 model and MF12 model $\hat{\xi}_{MK} = 0.0005 : 0.0005 : 1000.0005$ . . . . .	68
A.16	Numerical stability study for calculation of $E(R \hat{h}_{MK})$ from derived LH83 model	69
A.17	Conditional cumulative distribution of wave run-up given wave height $P(R H)$ from derived LH83 model by integration step corresponding with $\text{Rend} = 100.0005$ in Fig. A.16 . . . . .	70
A.18	Conditional cumulative distribution of wave run-up given wave height $P(R H)$ from derived LH83 model by integration step indicated with $\text{Rend} = 200.0005$ in Fig. A.16 . . . . .	70
B.1	Isocontour of $p(\hat{t}_{MK}, j_{MK})$ from MB09 model $p$ takes 0.25, 0.75, 1.25, and 2.0 from outermost to center, respectively . . . . .	76
B.2	$\delta E(j_{MK} \hat{t}_{MK})$ versus $\hat{t}_{MK}$ from MB09 model . . . . .	77
B.3	$\delta\sigma(j_{MK} \hat{t}_{MK})$ versus $\hat{t}_{MK}$ from MB09 model . . . . .	77
B.4	$E(j_{MK} \hat{h}_{MK})$ from IN11 model versus $\hat{h}_{MK}$ ( $\text{hMK} \equiv \hat{h}_{MK}$ and $\text{jMK} \equiv j_{MK}$ ) . . . . .	77
B.5	$\sigma(j_{MK} \hat{h}_{MK})$ from IN11 model versus $\hat{h}_{MK}$ ( $\text{hMK} \equiv \hat{h}_{MK}$ and $\text{jMK} \equiv j_{MK}$ ) . . . . .	78
B.6	$\delta E(j_{MK} \hat{t}_{MK})$ versus $\hat{t}_{MK}$ from IN11 model . . . . .	78
B.7	$\delta\sigma(j_{MK} \hat{t}_{MK})$ versus $\hat{t}_{MK}$ from IN11 model . . . . .	78

E.1 Example of bash script . . . . . 88

# List of Tables

2.1	Peak values and their positions of MF12 and derived LH83 model . . . . .	14
2.2	Classification of wave breaker in terms of surf parameter . . . . .	22
A.1	Numerical integration by matlab trap built-in function and Simpson method .	61
B.1	Numerical peak value of $p(\hat{h}_{MK}, j_{MK})$ from MB09 model . . . . .	72
B.2	Numerical peak value of $p(\hat{t}_{MK}, j_{MK})$ from MB09 model . . . . .	72
B.3	Numerical peak value of $p(\hat{h}_{MK}, j_{MK})$ from IN11 model . . . . .	72
B.4	Numerical peak value of $p(\hat{t}_{MK}, j_{MK})$ from IN11 model . . . . .	73
B.5	Integration steps for numerical stability study of $\delta E(j_{MK} \hat{t}_{MK})$ from MB09 model	73
B.6	Numerical integration by matlab built-in function and trapzoidal method for IN11 model . . . . .	73
B.7	Numerical integration by matlab built-in function and Simpson method for IN11 model . . . . .	73
B.8	Numerical integration by matlab built-in function and Romberg method - ba- sic construction for IN11 model . . . . .	73
B.9	Numerical integration by matlab built-in function and Simpson method for IN11 model . . . . .	74
B.10	Comparison of numerical integration by matlab integral built-in function and recursive Romberg method for IN11 model . . . . .	75
B.11	Integration steps for numerical stability study of $\delta E(j_{MK} \hat{t}_{MK})$ and $\delta\sigma(j_{MK} \hat{t}_{MK})$ from IN11 model . . . . .	75

# Chapter 1

## Introduction

In this chapter, the previous work for surf parameter and wave power is reviewed. Objective is defined based on the time and resources available. The organization of the thesis is given for reader to have an overview about the methodologies used and work completed.

### 1.1 Background

#### 1.1.1 surf parameter

Surf parameter, also mentioned as surf similarity parameter or Iribarren number is firstly introduced by [Iribarren Cavanilles and Nogales \(1949\)](#) and applied later by [Battjes \(1974\)](#). It is defined as the slope of either beach or face of structure to the square root of the wave steepness. A number of surf zone phenomena can be represented by quantities related to surf parameter, such as breakers, sediment transport as a result of wave breaking as well as runup. One application of runup is in determination of position of a beach setback line for restricted construction ([Sorensen \(1993\)](#)).

A lognormal distribution of surf parameter is presented by [Tayfun \(2006\)](#) by following a lognormal form of wave steepness from theoretical arguments. Conversely, [Myrhaug and Fouques \(2007\)](#) found that the surf parameter normalized by rms (root mean square) value is distributed in Fréchet form as being less than 0.913 otherwise a lognormal distribution based on data from North Sea. [Myrhaug and Fouques \(2010\)](#) exemplified the transforma-

tion of a joint pdf of significant wave height and peak period based on data from Northern North Sea to obtain the bivariate probability model of surf parameter and significant wave height. More recently, [Myrhaug et al. \(2011\)](#) derived joint pdf of surf parameter and wave height from parametric model of wave height and wave period given by [Myrhaug and Kjeldsen \(1984\)](#) and demonstrated thoroughly the statistical properties of derived model.

### 1.1.2 Wave power

The wave energy in the ocean is considered as a promising energy source. Existing wave conversion technologies and concepts have been comprehensively examined by many publications (such as [Clément et al. \(2002\)](#), [Falnes \(2007\)](#) [Cruz \(2008\)](#), and [Falcão \(2010\)](#)). [Mørk et al. \(2010\)](#) evaluated the wave power distribution around the globe and seasonality of it from data given by global wind - wave model and measurements from buoy. More recently, [Gunn and Stock-Williams \(2012\)](#) suggested annual best direction for harvesting wave energy worldwide. Specifically, [Vicinanza et al. \(2013\)](#) gave a review of the total wave power in the oceans close to several European countries.

Compared to already commercialized offshore wind power exploitation, wave energy extraction is still in the immature phase ([Mørk et al. \(2010\)](#)). One of the remaining challenges is the reliable estimate of the wave power in the potential wave power farm. To quantify the wave energy conversion for economically appealing site, sea state parameters such as significant wave height, energy period and wave propagation direction are usually utilized. It is noted that sea states appearing most frequently does not have to contribute most significantly to the total incident wave energy but would be essential for fatigue analysis ([Lenée-Bluhm et al. \(2011\)](#)).

The optimal performance of the WECs (wave energy converters) are strongly frequency dependent. As a consequence of variability of sea state, WECs have to be designed or selected to give maximum output in an average sense. [Smith et al. \(2006\)](#) demonstrated that a hypothetical WEC works most effectively when it is tuned to individual waves. [Saulnier et al. \(2011\)](#) carried out the sensitivity analysis of WEC performance towards wave groupiness and spectral width parameter.

[Myrhaug et al. \(2011\)](#) presented two joint distributions of wave power and wave period for

sea states by random variable transformation from bivariate probability distribution of  $H_s$  and  $T_p$  and  $H_s$  and  $T_z$ , respectively.

Myrhaug et al. (2009) investigated the statistical properties of parametric model for wave power and primary wave parameters (i.e. wave height and wave period). This model is developed from transformation of parametric probability model for wave height and wave period by best fit to measurements on Norwegian Continental Shelf (Myrhaug and Kjeldsen (1984)).

In the utilization of same methodology, Izadparast and Niedzwecki (2011) derived theoretical model of wave power and primary wave parameters for individual waves from joint probability model of wave height and wave period given by Longuet-Higgins (1983). They found that narrow banded approximation for wave power is appropriate as bandwidth parameter  $(v) < 0.4$  if triangular spectrum is employed to approximate a more complicated practically used spectrum.

## 1.2 Notes for numerical method

Since the credibility of results obtained in this thesis is strongly dependent on the numerical integration method, some discussions are necessary.

Each numerical integration method may only be applicable for specific problems. Hence, sometimes trial and error process cannot be circumvented. Engineers and scientists have to be aware of the limitation of numerical method. Critical assessment of the results delivered by numerical method is always necessary. Potential risk is high for inexperienced user of mathematics tool such as Matlab and Maple. As stated by Davis and Rabinowitz (1984), *Whenever possible, a problem should be analyzed and put into a proper form before it is run on a computer and one good thought may be worth a hundred hours on the computer.* This becomes apparent during this thesis work. Therefore, numerical integration methods should never be employed in a blind fashion. It is advisable that proficient programmers have acquainted themselves with analytical results for integrals.

In concrete application, one common problem faced by many analysts would be the truncation of the infinite interval. Then, adequate estimate of the upper integral limit for numerical implementation requires analyst to be capable of estimating the tail appropriately. Addi-



tionally, it would be desirable to conduct numerical stability analysis for verification. Prior to evaluation of particular integral, [Abramowitz \(1954\)](#) suggested the following important points to take into consideration:

- *Confirm the existence of the integral*
- *Ascertain the important ranges of the parameters involved*
- *Reduce the integral to its simplest forms*
- *Determine the essential parameters which are involved*
- *Determine the accuracy to which numerical values (if desired) are to be given*

As for the probability analysis, another powerful tool is to check the unity of cdf (cumulative distribution of function) as integrating over the whole valid range of integration variables in the probability model.

### **1.3 Objectives and scope of work**

1. Investigate the statistical properties of joint distribution of surf parameter and wave height derived from bivariate distributions of individual wave height and wave period developed by [Longuet-Higgins \(1983\)](#).
2. Examine the effects of the bandwidth parameter on the behaviour of the derived bivariate distribution of surf parameter and wave height
3. Compare the theoretical distribution of surf parameter and wave height with the parametric model presented in [Myrhaug and Fouques \(2012\)](#)
4. Compare the theoretical bivariate distribution of wave power and wave height as well as wave power and wave period from [Izadparast and Niedzwecki \(2011\)](#) with the parametric model given by [Myrhaug et al. \(2009\)](#)

### **1.4 Thesis outline**

1. Chapter 2 presents the derivation and the statistical properties of theoretical distribution of surf parameter and wave height. Comparison is made between parametric

model and theoretical model by focusing on the quantities of interest for surf parameter. Then, a number of application examples are given to serve the purpose of demonstration.

2. Chapter 3 compares the theoretical and parametric model for wave power by comparing marginal and conditional quantities of wave power
3. Chapter 4 makes a summary of contributions as well as suggestions for further work
4. Appendix A gives detailed alternative derivation way for equations given in Chapter 2. Numerical convergence study for results given in Chapter 2 is present in a concise way.
5. Appendix B covers the comparison of results from by application of different numerical integration methods and convergence study for results given in Chapter 3. Romberg integration method is depicted in details herein.
6. Appendix C, D and E give examples of Matlab scripts, visual basic and bash script.



# Chapter 2

## Statistics of Surf Parameter for individual waves

In this chapter, a theoretical bivariate distribution of surf parameter and wave height is derived from theoretical joint distribution of wave height and wave period from [Longuet-Higgins \(1983\)](#) (given in section 2.1). Properties of the derived model will be exhibited in sections 2.1 and 2.3. Detailed comparisons between derived model and the parametric model given by [Myrhaug and Fouques \(2012\)](#) are made in subsection 2.3.2. Then, some examples of practical applications of derived model are shown in subsection 2.3.3.

### 2.1 Theoretical bivariate distribution of surf parameter and wave height

According to [Myrhaug and Fouques \(2012\)](#), the surf parameter  $\xi$  is defined as  $m/\sqrt{s}$ , where  $m$  is the slope and is computed by  $\tan\theta$  with  $\theta$  as the angle referred to horizontals.  $S$  is the wave steepness with definition as  $S = H/\lambda$  ( $\lambda = gT^2/(2\pi)$ ), where  $g, \lambda$  and  $T$  is the acceleration of gravity, wave length and wave period, respectively.

Characteristic values used herein for normalisations are  $H_{cr}$  for wave height,  $T_{cr}$  for wave period,  $S_{cr}$  for wave steepness and  $\xi_{cr}$  for surf parameter. The definitions of these values are

given by

$$T_{cr} = 2\pi \frac{m_0^\omega}{m_1^\omega} \quad (2.1)$$

$$H_{cr} = 2\sqrt{2m_0^\omega} \quad (2.2)$$

$$S_{cr} = \frac{H_{cr}}{gT_{cr}^2/(2\pi)} \quad (2.3)$$

$$\xi_{cr} = m/\sqrt{S_{cr}} \quad (2.4)$$

Normalized wave period, wave height, wave steepness and surf parameter then are denoted as  $t$ ,  $\hat{h}$ ,  $\hat{S}$  and  $\hat{\xi}$ , respectively (D. Myrhaug, personal communication, 26 February 2014). Aforementioned  $m_0^\omega$  and  $m_1^\omega$  are calculated by:

$$m_n^\omega = \int_0^\infty \omega^n S(\omega) d\omega; n = 0, 1, 2, \dots \quad (2.5)$$

where  $S(\omega)$  is the one sided wave spectrum expressed in terms of circular wave frequency  $\omega$ . Based on foregoing definition,  $\hat{\xi}$  can be expressed as

$$\hat{\xi} = \frac{t}{\sqrt{\hat{h}}} \quad (2.6)$$

Longuet-Higgins (1983) gave joint probability density function of  $\hat{h}$  and  $t$  (hereafter denoted as LH83 model) as the following:

$$p(\hat{h}, t) = \frac{2}{v\sqrt{\pi}} \frac{\hat{h}^2}{t^2} \exp\left[-\hat{h}^2\left(1 + (1 - 1/t)^2/v^2\right)\right] L(v) \quad (2.7)$$

where  $v$  is the bandwidth parameter, and  $L(v)$  is a normalization factor as a consequence of only positive  $t$  being taken into account.  $v$  and  $L(v)$  are given as

$$L(v) = \frac{2}{1 + (1 + v^2)^{-1/2}} \quad (2.8)$$

$$v = \left( \frac{m_0^\omega m_2^\omega}{(m_1^\omega)^2} - 1 \right)^{1/2} \quad (2.9)$$

LH83 model is derived from the joint distribution of wave envelope amplitude and the rate of change of total phase. If the surface wave elevation is considered as narrow banded process,

the wave envelope amplitude can be approximated as wave amplitude. Thus, with further assumption for the time derivative of total phase, the Eq. 2.7 is obtained. Hereafter, the distinguish will not be made and wave amplitude will be used. It should be noted that the value of normalized wave amplitude defined by Longuet-Higgins (1983) is identical with normalized wave height  $\hat{h}$  defined herein. Furthermore, Eq.(2.17) given in Longuet-Higgins (1983) should have a leading factor with  $2/(\sqrt{\pi}v)$  instead of  $2/(\sqrt{\pi})$  (see section A.1 for details).

By transformation of pdf (probability density function), Eq. 2.7, with argument  $(\hat{h}, t)$  into  $(\hat{h}, \hat{\xi})$ , joint pdf  $p(\hat{\xi}, \hat{h})$  is shown as:

$$p(\hat{\xi}, \hat{h}) = \frac{2}{v\sqrt{\pi}} \frac{\hat{h}^{3/2}}{\hat{\xi}^2} \exp \left[ -\hat{h}^2 \left( 1 + \left( 1 - \frac{1}{\hat{\xi}\sqrt{\hat{h}}} \right)^2 / v^2 \right) \right] L(v) \quad (2.10)$$

where  $L(v)$  can also be given as another form if corrected form of Eq. (2.17) in Longuet-Higgins (1983) is utilized

$$\frac{1}{L(v)} = \frac{2}{v\sqrt{\pi}} \int_0^\infty \int_0^\infty \frac{\hat{h}^{3/2}}{\hat{\xi}^2} \exp \left[ -\hat{h}^2 \left( 1 + \left( 1 - \frac{1}{\hat{\xi}\sqrt{\hat{h}}} \right)^2 / v^2 \right) \right] d\hat{h} d\hat{\xi} \quad (2.11)$$

Actually,  $L(v)$  keeps the same form in transformation of variables due to its independence of  $\hat{h}$  and  $t$  as seen in Eq. (2.8). Also, it is reasonable to take analytical integral result shown above rather than numerical solution of Eq. (2.11).

The maximum value of  $p(\hat{h}, \hat{\xi})$  is found by taking its partial differentiation with respect to  $\hat{h}$  and  $\hat{\xi}$ , respectively, and enforcing them being zero. Additionally,  $\hat{h} \geq 0$ ,  $\hat{\xi} \geq 0$  and  $p(\hat{\xi}, \hat{h}) > 0$  should be satisfied simultaneously. Thus the position  $(\hat{h}_{max}, \hat{\xi}_{max})$  of maximum value is obtained.

$$\hat{h}_{max} = \frac{\sqrt{2}}{4} G(v) \quad (2.12)$$

$$\hat{\xi}_{max} = 2^{-13/4} \frac{v^2 + 1}{v^2} G(v)^{7/2} - 2^{-9/4} \frac{v^2 + 5}{v^2} G(v)^{3/2} \quad (2.13)$$

where  $G(v)$  is a factor only dependent on  $v$ , and takes the form

$$G(v) = \sqrt{\frac{\sqrt{16v^2 + 25} + (5 + 2v^2)}{v^2 + 1}} \quad (2.14)$$

By substituting Eqs. (2.12), (2.13) and (2.14) in Eq. (2.10), the value of  $p(\hat{h}, \hat{\xi})$  at mode (maximum value) is therefore

$$p_{max} = 2^{-11/4} \exp\left(-\frac{5}{4} \frac{G(v)^2 W(v)}{Q(v)}\right) \frac{L(v) G(v)^{5/2} W(v)^2}{Q(v) v \sqrt{\pi}} \quad (2.15)$$

where  $W(v)$  and  $Q(v)$  are factors dependent on  $v$  only and given by

$$Q(v) = (\sqrt{16v^2 + 25} + 5)^2 \quad (2.16)$$

$$W(v) = 8v^2 + \sqrt{16v^2 + 25} + 5 \quad (2.17)$$

From Eq. (2.15), it seems that the maximum value of  $p(\hat{h}, \hat{\xi})$  decreases exponentially for increasing  $v$ . This statement is verified by fitting to the data generated by Eq. (2.15) (shown by Fig. 2.1a). Maximum value after being fitted  $p_{max_{fit}}$  is given by

$$p_{max_{fit}} = 14.91 \exp(-17.89v) + 2.214 \exp(-1.317) \quad (2.18)$$

Take first derivative of Eq. (2.15) with respect to  $v$  and enforce it to be zero, it is found that  $v = 0.969086$  gives the minimum peak value. With the increase of  $v$ , the projection of point  $p_{max}$  on  $\hat{\xi} - \hat{h}$  plane moves on a straight line (see Fig. 2.1b produced by using Eqs. (2.12) and (2.13)) to smaller wave height (varying around character wave height  $H_{cr}$ ) and surf parameter. By fitting, the corresponding track projected is given as

$$\hat{h} = 0.6054\hat{\xi} + 0.5459 \quad (2.19)$$

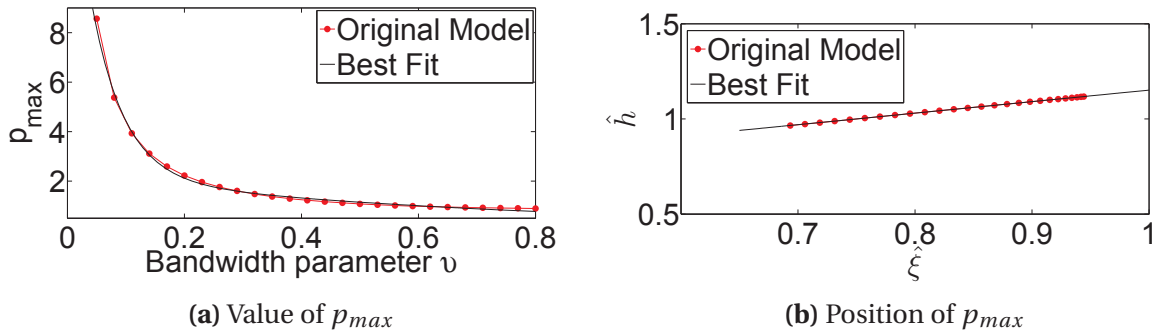


**Figure 2.1:** The value and position of  $p_{max}$  vary with  $v$  in the range of 0.05:0.03:0.8

More investigation with respect to the effect of bandwidth parameter on the statistical quan-

tities of interest is given in subsection 2.3.2.

## 2.2 Parametric joint distribution of surf parameter and wave height

By best fitting to measurements on the Norwegian continental shelf, [Myrhaug and Kjeldsen \(1984\)](#) (hereafter denoted as MK84) gave parametric joint distribution of normalized wave height and wave steepness. Through transformation of variables, [Myrhaug and Fouques \(2012\)](#) derived the parametric bivariate distribution of normalized wave height  $\hat{h}_{MK}$  and surf parameter  $\hat{\xi}_{MK}$ , given as

$$p(\hat{\xi}_{MK}, \hat{h}_{MK}) = p(\hat{\xi}_{MK} | \hat{h}_{MK}) p(\hat{h}_{MK}) \quad (2.20)$$

where  $p(\hat{h}_{MK})$  and  $p(\hat{\xi}_{MK} | \hat{h}_{MK})$  are given as a 2-parameter Weibull pdf and a lognormal pdf, respectively and take the forms

$$p(\hat{h}_{MK}) = \frac{2.39 \hat{h}_{MK}^{1.39}}{1.05^{2.39}} \exp \left[ - \left( \frac{\hat{h}_{MK}}{1.05} \right)^{2.39} \right] \quad (2.21)$$

$$p(\hat{\xi}_{MK} | \hat{h}_{MK}) = \frac{1}{\sqrt{2\pi} \sigma_{\hat{\xi}_{MK}} \hat{\xi}_{MK}} \exp \left[ - \frac{(\ln(\hat{\xi}_{MK}) - \mu_{\hat{\xi}_{MK}})^2}{2\sigma_{\hat{\xi}_{MK}}^2} \right] \quad (2.22)$$

Here,  $\mu_{\hat{\xi}_{MK}}$  and  $\sigma_{\hat{\xi}_{MK}}$  are mean value and variance of  $\ln(\hat{\xi}_{MK})$  respectively, given by

$$\mu_{\hat{\xi}_{MK}} = \begin{cases} -0.048 + 0.5105 \hat{h}_{MK} - 0.279 \hat{h}_{MK}^2 & \text{for } \hat{h}_{MK} \leq 1.7 \\ -0.125 \arctan[4(\hat{h}_{MK} - 1.7)] + 0.0135 & \text{for } \hat{h}_{MK} > 1.7 \end{cases} \quad (2.23)$$

$$\sigma_{\hat{\xi}_{MK}}^2 = -0.0375 \arctan[1.75(\hat{h}_{MK} - 1.20)] + 0.05625 \quad (2.24)$$

where normalized wave height  $\hat{h}_{MK}$  and normalized surf parameter  $\hat{\xi}_{MK}$  are defined by

$$\hat{h}_{MK} = \frac{H}{H_{rms}} \quad (2.25)$$

$$\hat{\xi}_{MK} = \frac{\xi}{\xi_{rms}}; \quad \xi_{rms} = \frac{m}{\sqrt{S_{rms}}} \quad (2.26)$$



Normalized wave steepness herein is defined as  $hat{S}_{MK} = S/S_{rms}$ . Connections between  $S_{rms}$ ,  $H_{rms}$  and sea state parameter  $H_s$ ,  $T_z$  are found by performing linear regression analysis, given by

$$H_{rms} = 0.714 H_s \quad (2.27)$$

$$S_{rms} = 0.7 S_m; \quad S_m = \frac{H_s}{\frac{g}{2\pi} T_z^2} \quad (2.28)$$

where significant wave height  $H_s$  and mean zero crossing period  $T_z$  are defined in terms of spectral moments  $m_n^f$

$$T_z = \sqrt{\frac{m_0^f}{m_2^f}} \quad (2.29)$$

$$H_s = 4\sqrt{m_0^f} \quad (2.30)$$

Here  $m_0^f$  and  $m_2^f$  are zeroth and second moment of single sided wave spectrum  $S(f)$ , which is defined as

$$m_n^f = \int_0^\infty f^n S(f) df; \quad n = 0, 1, 2, \dots \quad (2.31)$$

It is noted that  $n^{th}$  spectral moments  $m_n^f$  expressed by wave frequency  $f$  with unit  $Hz$  are defined in the same manner as for  $m_n^\omega$  (see Eq. (2.5)). As  $\omega = 2\pi f$  and area under spectra (represents energy) given as  $S(f)$  and  $S(\omega)$  should be the same, following connection is established

$$S(\omega) = \frac{1}{2\pi} S(f) \quad (2.32)$$

Further, relation between spectral moments expressed in  $f$  and  $\omega$  are derived as

$$m_n^\omega = (2\pi)^n m_n^f \quad (2.33)$$

It is noted that the definition of  $S_{rms}$  in [Myrhaug and Kjeldsen \(1984\)](#) is identical with that in [Myrhaug and Fouques \(2012\)](#) but extra factor  $4\pi^2$  exists in Eq. (12) given by [Myrhaug and Kvålsvold \(1995\)](#), since wave spectrum is expressed in terms of circular wave frequency  $\omega$  there ([personal discussion with Dag Myrhaug on June 10th, 2014](#)).

## 2.3 Comparison between parametric probability and theoretical probability model

In [Longuet-Higgins \(1983\)](#),  $\nu \leq 0.6$  is used as the basis for deriving narrow band approximation Eq. (2.7). Hence, typical values of bandwidth parameter within the range are selected to serve the purpose of investigating the its effect on the properties of derived LH83 model.

### 2.3.1 Using same normalized quantities

To make results comparable with those presented in [Myrhaug and Fouques \(2012\)](#), their definitions of normalized wave height and slope are employed and bandwidth parameter  $\nu$  is limited to 0.504 ([Myrhaug and Fouques \(2012\)](#)), which is the bandwidth of surface wave elevation process the MF12 model is based on. From Eqs. (14) and (16) in [Myrhaug and Kvålsvold \(1995\)](#), the relation between normalized procedures employed in [Myrhaug and Kjeldsen \(1984\)](#) and [Longuet-Higgins \(1983\)](#) is given as

$$\hat{h} = \frac{\gamma_H \hat{h}_{MK}}{2\sqrt{2}}; \quad \gamma_H = 2.8582 \quad (2.34)$$

$$\hat{\xi} = \xi_{MK} \sqrt{\frac{4\pi\sqrt{2}}{\gamma_S(1+\nu^2)}}; \quad \gamma_S = 17.6 \quad (2.35)$$

Hereafter,  $\gamma_H/(2\sqrt{2})$  and  $\sqrt{4\pi\sqrt{2}/\gamma_S(1+\nu^2)}$  are denoted as  $A$  and  $C_m$  ( see section A.3 for detailed derivations of  $C_m$  ), respectively.

Theoretical joint distribution of  $(\hat{\xi}_{MK}, \hat{h}_{MK})$  is then derived from Eq. (2.10) by using Jacobian  $\left| \frac{\partial \hat{\xi}}{\partial \xi_{MK}} \cdot \frac{\partial \hat{h}}{\partial h_{MK}} \right| = C_m A$  and becomes

$$p(\hat{\xi}_{MK}, \hat{h}_{MK}) = \frac{2A^{5/2}}{C_m \sqrt{\pi} \nu} \left( \frac{\hat{h}_{MK}^{3/2}}{\hat{\xi}_{MK}^2} \right) \exp \left[ - (A \hat{h}_{MK})^2 \left( 1 + \left( 1 - \frac{1}{C_m \hat{\xi}_{MK} \sqrt{A \hat{h}_{MK}}} \right)^2 / \nu^2 \right) \right] L(\nu) \quad (2.36)$$

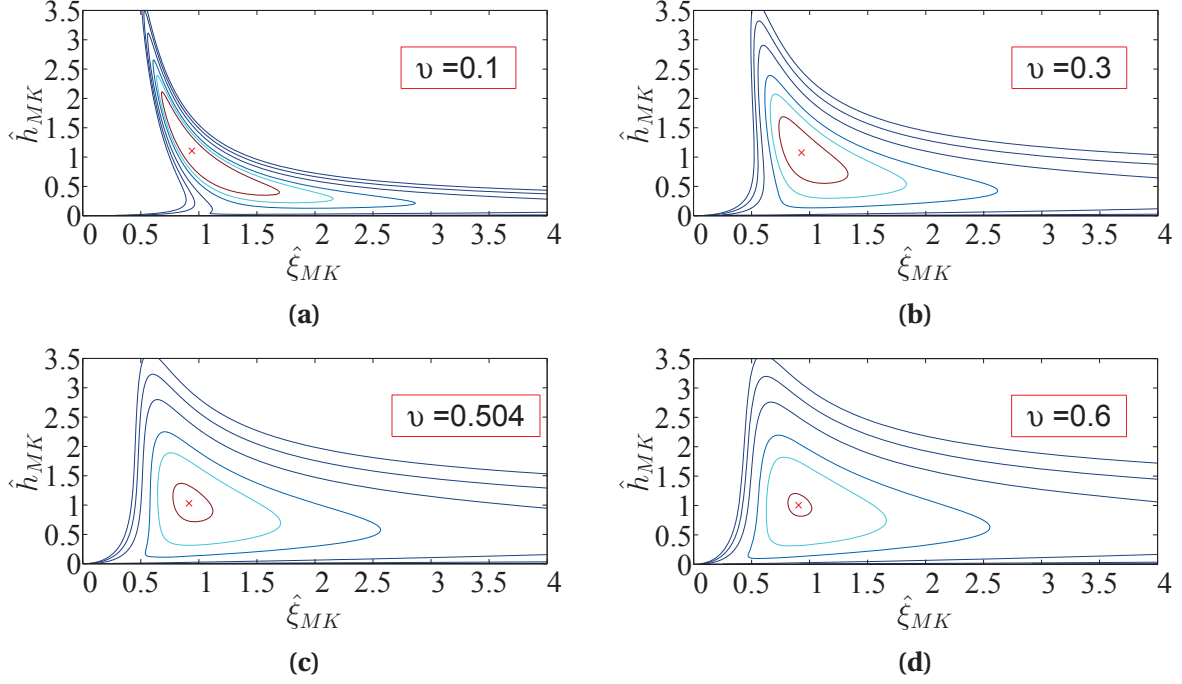


**Figure 2.2:** Isocontours of derived LH83 model  $p(\hat{h}_{MK}, \hat{\xi}_{MK})$ ,  $p$  takes peak value (indicated as  $\times$ ), 0.8, 0.3, 0.1, 0.01, 0.001 and 0.0001 respectively from the centre outwards

It is also feasible firstly to make a change of variables for LH83 model from  $(\hat{h}, \hat{t})$  into  $(\hat{h}_{MK}, \hat{t}_{MK})$  through the use of Eqs. (2.34) and (3.11). Then, obtained pdf can further be transformed to theoretical joint distribution of  $(\hat{\xi}_{MK}, \hat{h}_{MK})$ , which is identical with Eq. (2.36) (details can be found in section A.4).

### 2.3.2 Comparison of statistical quantities of interest

Compared with derived LH83 model( Fig 2.2c), MF12 model (Fig 2.3) gives more even distribution. The positions and the values of the peak from two models are close to each other as seen in Table 2.1.

**Table 2.1:** Peak values and their positions of MF12 and derived LH83 model

Model	$\nu$	$\hat{h}_{MK}$	$\hat{\xi}_{MK}$	peak value
MF12	–	0.905	1.120	1.160
Derived LH83	0.1	1.105	0.940	4.362
Derived LH83	0.3	1.075	0.930	1.516
Derived LH83	0.504	1.030	0.915	0.974
Derived LH83	0.6	1.005	0.905	0.855

Symmetry with respect to wave height is observed as  $\hat{h}_{MK} \approx 0.6$  for MF12 model given  $\hat{\xi}_{MK} > 2$ . Asymmetry with respect to surf parameter is observed for derived LH83 model while symmetry is presented for MF12 model as  $\hat{h}_{MK} > 2$ .

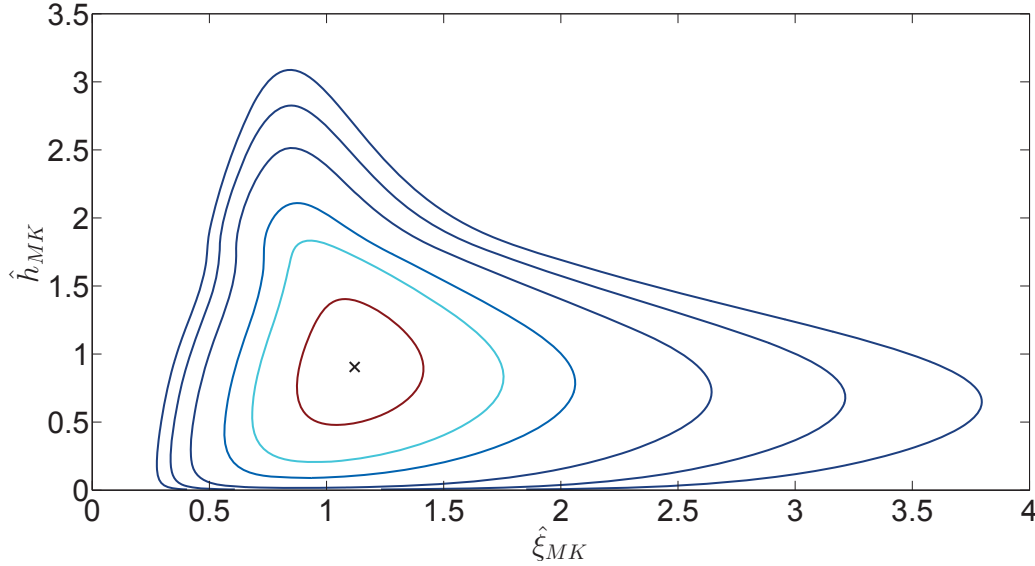


**Figure 2.3:** Isocontours of MF12 model ( $\hat{h}_{MK}, \hat{\xi}_{MK}$ ),  $p$  takes peak value (indicated as  $\times$ ), 0.8, 0.3, 0.1, 0.01, 0.001 and 0.0001 respectively from the centre outwards (adapted from [Myrhaug and Fouques \(2012\)](#))

It is observed from Fig. 2.2 that the broadening of spectrum lowers the probability density gradient. And the point with maximum probability density is almost fixed as illustrated by Fig. 2.2 as well as by Table 2.1. In the lower range of wave height, the conditional distribution of  $\hat{\xi}_{MK}$  given  $\hat{h}_{MK}$  is skewed to the right and broad-banded compared to large wave height (e.g.  $\hat{h}_{MK} > 2$ ). Same feature is also inherent in MF12 model (see e.g Figs 14 - 16 [Myrhaug and Fouques \(2012\)](#)). Fig. 2.9 also illustrates the branded-band feature as  $\hat{h}_{MK}$  less than 1.5. Fig. 2.2a shows that the isocurve possesses longer tail in comparison with other values of bandwidth parameter as  $\hat{h}_{MK} < 1.5$ . [Longuet-Higgins \(1983\)](#) gave the theoretical marginal distribution of non-dimensional wave amplitude  $R_a$  with Eq. (5.4). As mentioned previously,  $R_a = \hat{h}$ , and therefore the marginal distribution of  $\hat{h}$  take the same form as that of  $R_a$  and as shown below.

$$p(\hat{h}) = \frac{2\hat{h}}{\sqrt{\pi}} e^{-\hat{h}^2} L(v) \int_{-\infty}^{\hat{h}/v} e^{-\eta^2} d\eta \quad (2.37)$$

$$= 2\hat{h} e^{-\hat{h}^2} L(v) F(\hat{h}/v) \quad (2.38)$$

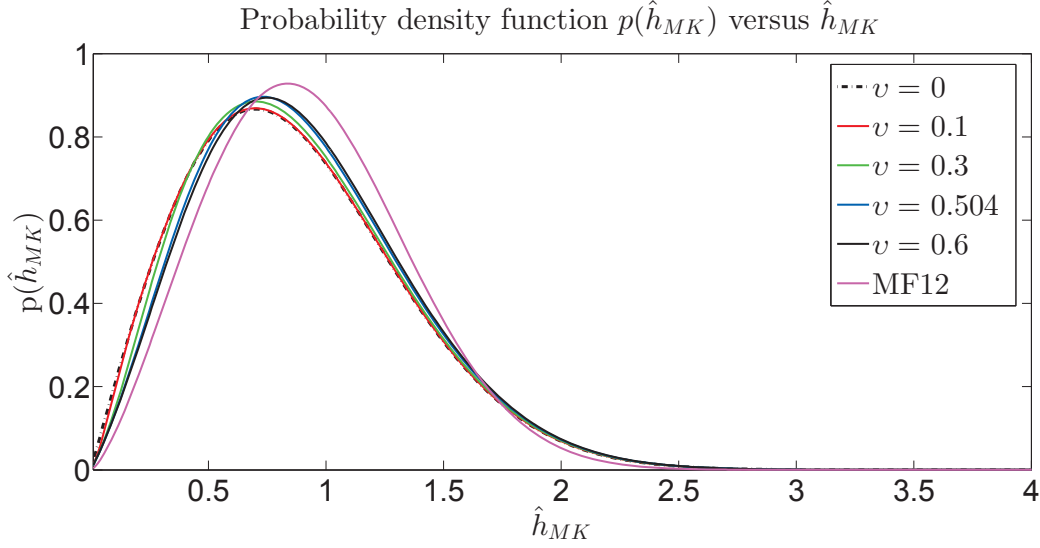


**Figure 2.4:**  $p(\hat{h}_{MK})$  versus  $\hat{h}_{MK}$

where  $L(v)$  and  $F(\hat{h}/v)$  are correction factors to Rayleigh distribution.  $F(\hat{h}/v)$  and  $\eta$  are given by

$$F(\hat{h}/v) = \frac{1}{\sqrt{\pi}} \int_{-\infty}^{\hat{h}/v} e^{-\eta^2} d\eta \quad (2.39)$$

$$\eta = \frac{\hat{h}}{v} (1 - 1/t) \quad (2.40)$$

Note that  $F(\hat{h}/v)$  is not the same as mostly common error function with leading factor  $\frac{2}{\sqrt{\pi}}$ . Transforming Eq. (2.37) into the distribution of  $\hat{h}_{MK}$ , Fig. 2.4 is produced by also including results from integrating Eq. (2.36) with respect to  $\hat{\xi}_{MK}$ . Fig. 2.4 illustrates that the marginal distribution of  $\hat{h}_{MK}$  is not sensitive to the variation of bandwidth, which is also presented in Fig. 2 by Longuet-Higgins (1983) and supported by Fig. 2.5. It is observed that MF12 model gives higher peak value, which shifts to the right compared to model derived from LH83. The distinguish between these two models are clearly seen as  $v = 0.504$ .

Weibull scale probability paper (Fig. 2.5) is used to better illustrate the difference of these two models, especially between Rayleigh distribution ( $v = 0$ ) and the distribution with  $v = 0.1$ . Both Fig. 2.5 and Fig. 2.4 shows the higher and lower probability given by transformed LH83 model and Rayleigh distribution in small and large wave height relative to MF12 model, respectively. Thus, cautions should be taken for utilizing Rayleigh and MF12 model in severe sea state. Another feature is very small curvature observed in Weibull probability paper for transformed LH83 model. As what Longuet-Higgins (1983) stated, correction from

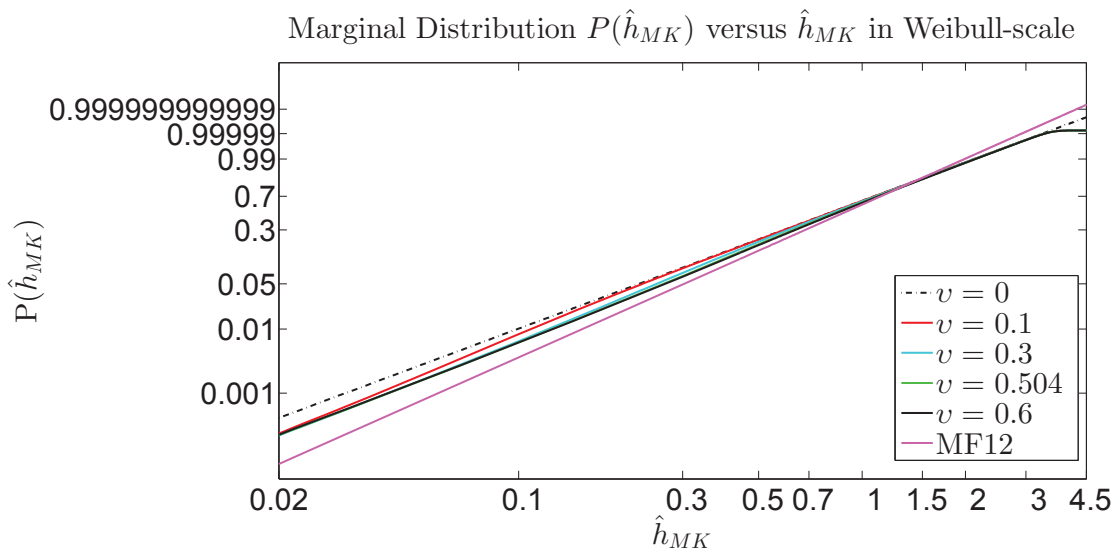


**Figure 2.5:** Marginal cdf  $P(\hat{h}_{MK})$  versus  $\hat{h}_{MK}$

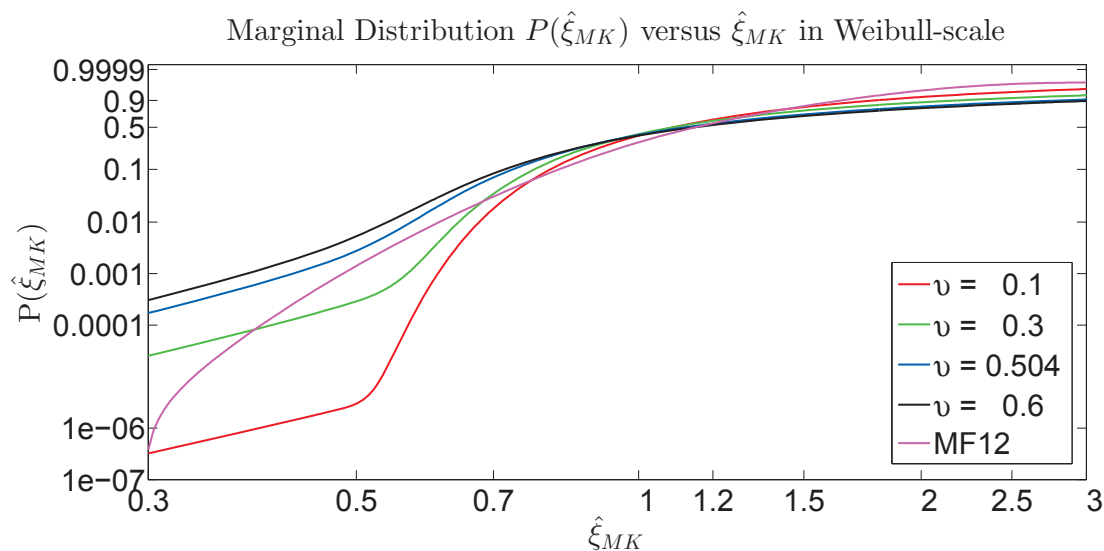
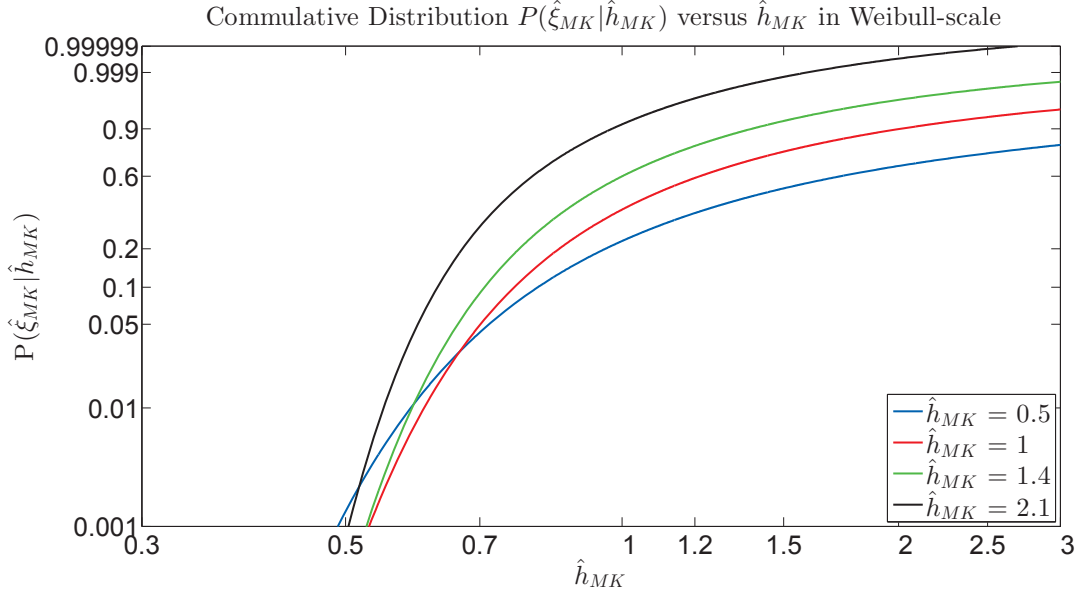


**Figure 2.6:** Marginal cdf  $P(\hat{\xi}_{MK})$  versus  $\hat{\xi}_{MK}$

$L(\nu)F(R/\nu)$  to Rayleigh model is obvious in the order of  $\nu$  and small as  $\hat{h}_{MK}$  is in the order of 1.5. Tail behaviour is observed for transformed LH83 model, which further implies incapability of this model for predicting probability of extremely large wave height. With no analytical expression of cdf for marginal wave height distribution, numerical integration has to be used to evaluate the integral of Eq. (2.37). The probability of  $\hat{h}_{MK}$  corresponds to the tail of transformed LH83 model and is sensitive to the steps for integration. Thus, step with maximum numerical error of cdf in the magnitude of  $10^{-8}$  is applied. Fig 2.6 shows decreasingly evident concavity of  $P(\hat{\xi}_{MK})$  curve by transformed LH83 model as broadening of spectrum. By contrast, the curve generated by MF12 model has the same sign of curvature the throughout all slopes. From Fig. 2.7, it is seen that the conditional probability of  $\hat{\xi}_{MK}$  is



increased with  $\hat{h}_{MK}$  for  $\hat{\xi}_{MK}$  being approximately larger than 0.7.

Fig. 2.8 shows the expected value of  $\hat{\xi}_{MK}$  given wave height  $\hat{h}_{MK}$  ( $E(\hat{\xi}_{MK}|\hat{h}_{MK})$ ). It appears that the values increase with decreasing bandwidth parameter  $\nu$  as  $\hat{h}_{MK}$  is small for distribution derived from LH83, However, the trend reverses with large  $\hat{h}_{MK}$ . It is also observed that all curves follow the same pattern, that is, they increase firstly and then reduce as  $\hat{h}_{MK}$  grows. Fig. 2.9 shows the lower variability for MF12 model than corresponding transformed LH83 model. It also implies that dispersion increases with bandwidth parameter  $\nu$  as expected.

It should be noted that the numerically computed  $E(\hat{\xi}_{MK}|\hat{h}_{MK})$  and  $\sigma(\hat{\xi}_{MK}|\hat{h}_{MK})$  are only converged as  $\hat{h}_{MK} > 2$  for derived LH83 model (see Figs. A.8 and A.15 for details). However the trends reflected in 2.8 and 2.9 remain the same even by utilizing different integration steps (see Figs.A.2 - A.6 and Figs.A.9 - A.12 for details).

### 2.3.3 Application examples

For the purpose of facilitating comparison, application examples of derived LH83 model are presented in the foregoing text with the same manner utilized in Myrhaug and Fouques (2012). One quantity of interest in coastal engineering is breaker index  $h_b$ . It is defined as  $H_b/d_b$ , where  $H_b$  and  $d_b$  are wave height and water depth at breaking, respectively. Empirically,  $h_b$  can be related with  $\xi$  by  $h_b = k_1 \xi^{k_2}$  as suggested by Myrhaug and Fouques (2007).

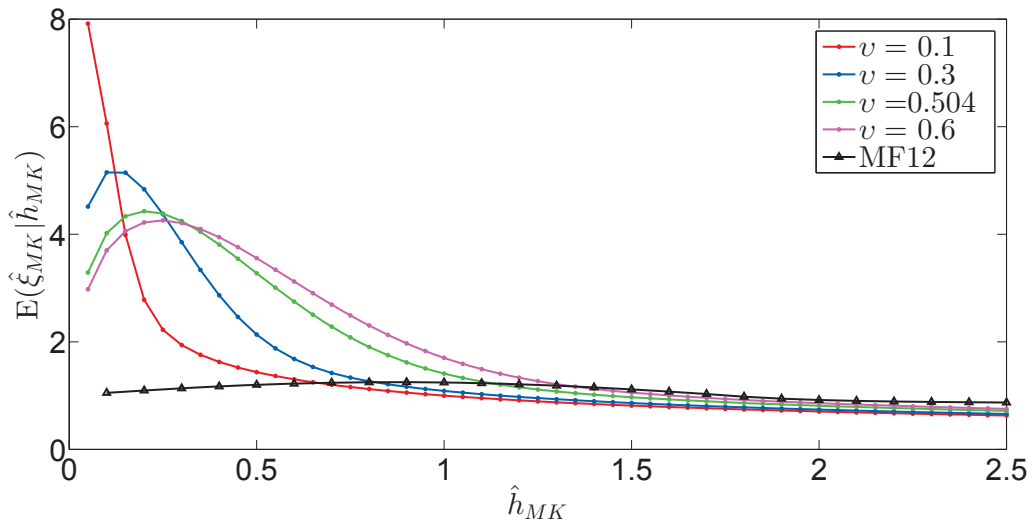


Figure 2.8:  $E[\hat{\xi}_{MK} | \hat{h}_{MK}]$

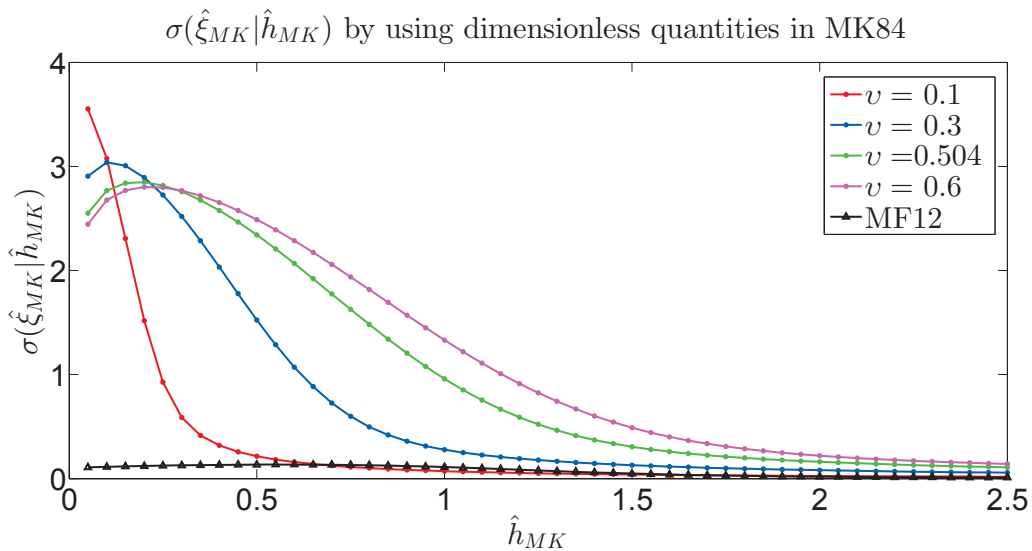
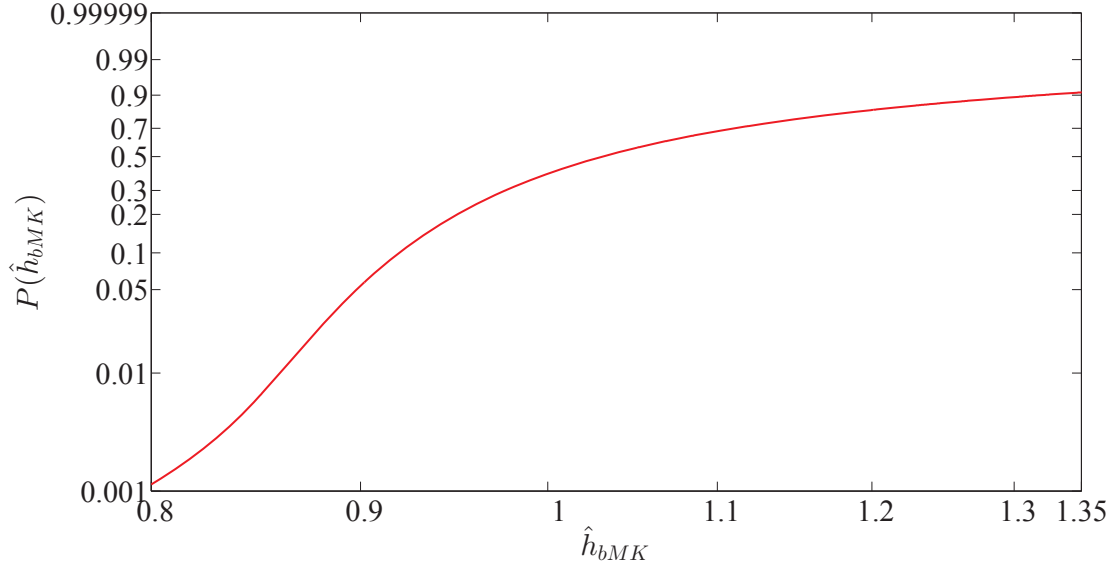


Figure 2.9:  $\sigma(\hat{\xi}_{MK} | \hat{h}_{MK})$





**Figure 2.10:** Probability of breaker index  $\hat{h}_{bMK}$  in Weibull scale

$k_1$  and  $k_2$  are empirical coefficients and one possible set of values ( $k_1 = 1.20, k_2 = 0.27$ ) are proposed by Kaminsky and Kraus (1994). Normalized form of  $h_b$  consistent with Myrhaug and Fouques (2012) is defined as  $\hat{h}_{bMK} = h_b / (k_1 \xi_{rms}^{k_2}) = \hat{\xi}_{MK}^{k_2}$ . Through a change of variables from Eq. (2.36) by using Jacobian  $\left| \frac{\partial \hat{\xi}_{MK}}{\partial \hat{h}_{bMK}} \right| = \hat{h}_{bMK}^{1/k_2 - 1} / k_2$ , joint distribution  $p(\hat{h}_{bMK}, \hat{h}_{MK})$  is obtained as

$$p(\hat{h}_{bMK}, \hat{h}_{MK}) = \frac{2L(v) A^{5/2} \hat{h}_{MK}^{3/2}}{k_2 C_m \sqrt{\pi v} \hat{h}_{bMK}^{(k_2+1)/k_2}} \exp \left[ - (A \hat{h}_{MK})^2 \left( 1 + \left( 1 - \frac{1}{C_m \hat{h}_{bMK}^{1/k_2} \sqrt{A \hat{h}_{MK}}} \right)^2 / v^2 \right) \right] \quad (2.41)$$

Fig. 2.10 shows the marginal probability  $P(\hat{h}_{bMK})$  in Weibull-scale. Similar to what is observed in Fig. 2.7, the exceeding conditional probability of  $\hat{h}_{bMK}$  given  $\hat{h}_{MK}$  decreases as  $\hat{h}_{MK}$  increases for a given value of  $\hat{h}_{bMK}$  as shown in Fig. 2.11.

According to the change of surface profile in the process of breaking, breaking waves are divided into four categories, whose main features are illustrated in Fig. 2.12 and described as follows (Sorensen (1993) and Myrhaug (2006))

- Spilling breaker : Foam firstly appears at the crest where air is entrapped and spread to the front face of the wave as it moves forward. Its profile nearly horizontally symmetric.

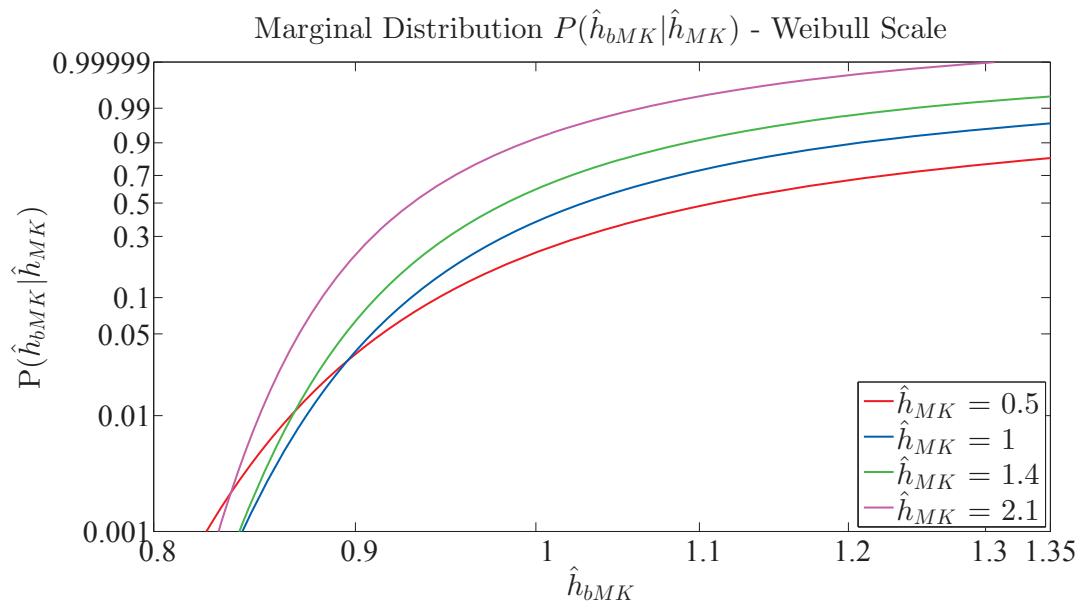


**Figure 2.11:** Conditional probability of breaker index  $\hat{h}_{MKb}$  in Weibull scale

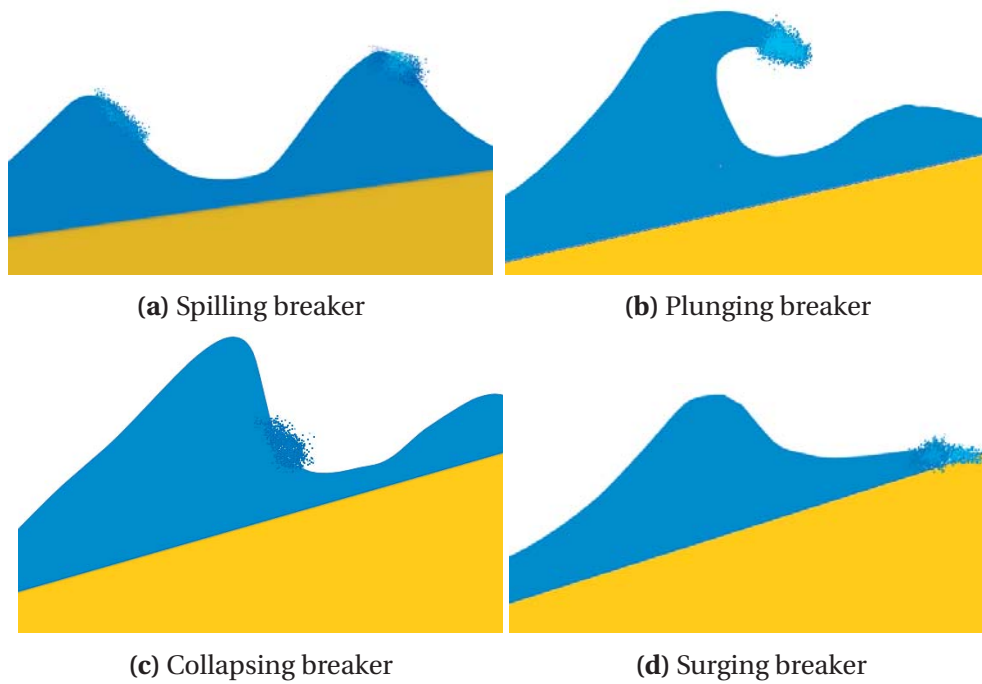


**Figure 2.12:** Sketches of different wave breakers (after Sorensen (1993))

- Plunging breaker : Overhanging crest formed due to gravity shows evident horizontal asymmetry profile of plunging breaker. Afterwards, the crest plunges at the base of the front face of the wave.
- Collapsing breaker : Crest overtakes lower parts and forms vertical front. The lower portion of the front face plunges forward and collapses.
- Surging Breaker : Steepness of wave front increases as the wave propagates towards shallower water. In the close proximity of shoreline, lower portion of the wave ejects forward.

Spilling breaker and plunging breaker happen both in deep water and shallow water, while collapsing breaker and surging breaker are only observed in shallow water. With decreasing wave steepness and the increase of slope, progression from plunging breaker, collapsing breaker to surging breaker is found.

Further, [Battjes \(1974\)](#) classifies wave breakers based on the quantities of surf parameter, as given in [Table 2.2](#).

**Table 2.2:** Classification of wave breaker in terms of surf parameter

wave breaker	surf parameter ( $\xi$ ) <sup>1</sup>
Spilling breaker	0 – 0.5
Plunging breaker	0.5 – 3.0
Collapsing breaker	3 – 3.5
Surging breaker	> 3.5

The normalized surf parameters corresponds to different types of wave breakers can be given as in the form

$$\hat{\xi}_{MKd} = \left( x_d \sqrt{S_{rms}} \right) / m \quad (2.42)$$

where  $x_d$  is in correspondence with limits of various wave breakers(i.e.  $x_d = 0$  and  $x_d = 0.5$  for the lower and upper limit of spilling breaker, respectively).

The probability for these breakers then can be computed by integrating [Eq. \(2.10\)](#) in the interval given by  $\hat{\xi}_{MKd}$  and range of  $\hat{h}$  of interest.

It should be noted that every point on the curves of the [Figs. 7-10](#) given in [Myrhaug and](#)

<sup>1</sup>Lowerlimit is not included in each range except for spilling breaker

Fouques (2012) can be interpreted as the marginal probability of  $\hat{\xi}_{MK}$  in an interval, since the joint density probability function of  $(\hat{\xi}_{MK}, \hat{h}_{MK})$  is integrated over the whole range of  $\hat{h}_{MK}$ .

Fig. 2.13 gives the probability of spilling breakers independent of wave height with varying sea state parameter  $S_m$ . It is clearly seen that probability increases with  $S_m$  and probability of a spilling breaker is higher with smaller slope  $m$ . Contrastingly, probability of a surging breaker drops with the increase of slope (shown by Fig. 2.16).

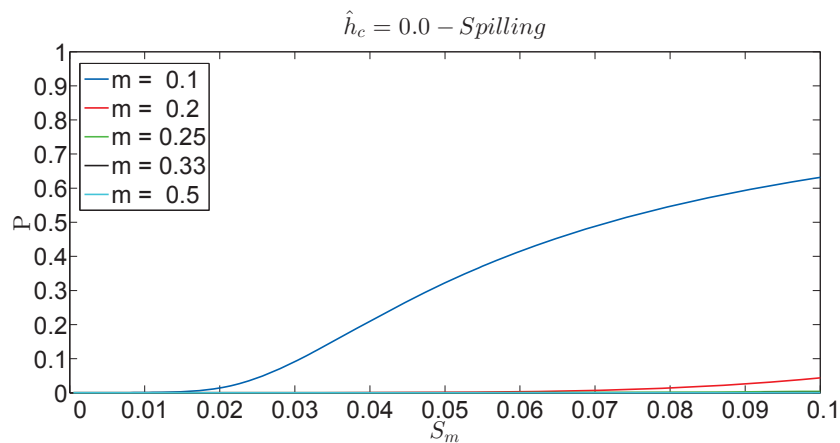


Figure 2.13: Probability of spilling breakers as  $S_m$  and slopes  $m$  vary

Similar probability variation pattern of each mentioned wave breaker can be found in Figs. 7-10 in Myrhaug and Fouques (2012). However, derived LH83 model gives higher probability for spilling breaker and lower probability for plunging breaker.

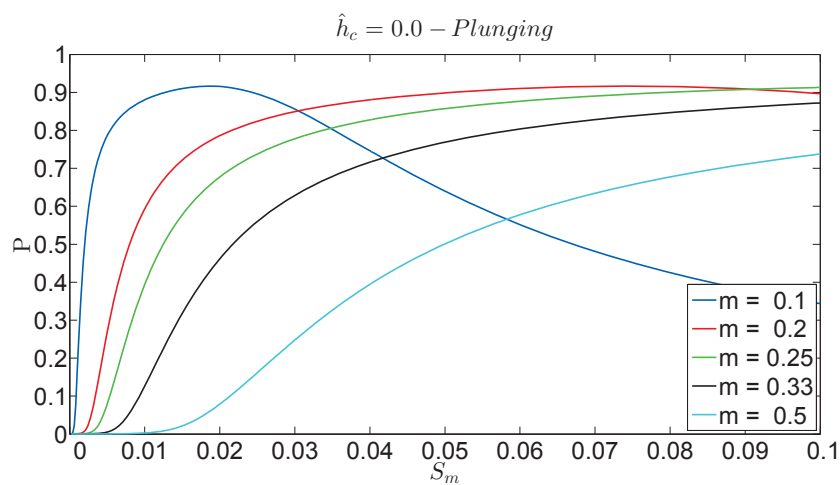
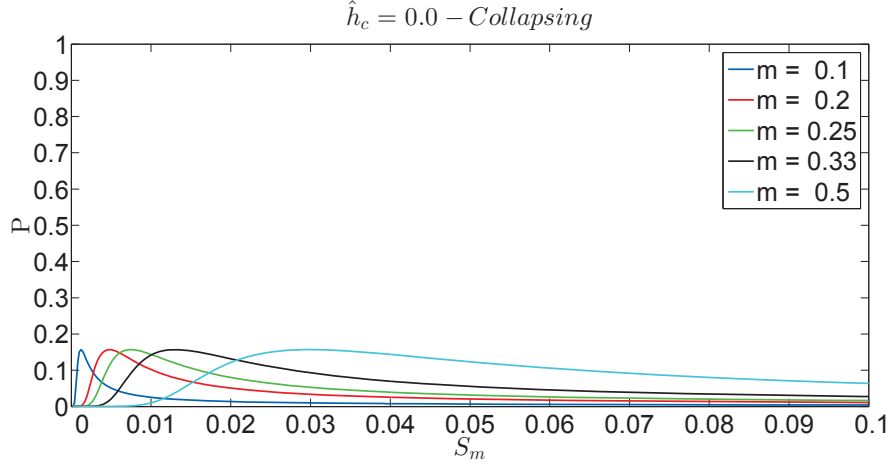
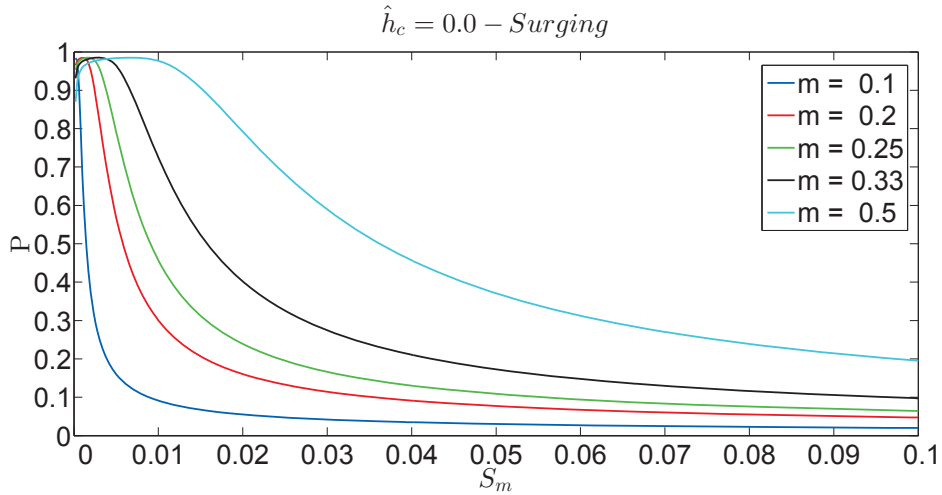


Figure 2.14: Probability of plunging breakers as  $S_m$  and slopes  $m$  vary



**Figure 2.15:** Probability of collapsing breakers as  $S_m$  and slope  $m$  vary

Every point on curves in Figs. 2.13 - 2.16 can be interpreted as the area under the pdf curve which is truncated by the limits of each wave breaker (e.g. 0.5 and 3 for plunging breaker) for a given  $S_m$ . Take collapsing breaker (i.e.  $3 \leq \xi \leq 3.5$ ) as an example, the area under curves corresponding to slope  $m = 0.25$  and  $m = 0.33$  is the same as seen in Fig. 2.17, which is displayed by intersection of the green and black line in Fig. 2.15 as  $S_m = 0.01$ .



**Figure 2.16:** Probability of surging breakers as  $S_m$  and slope  $m$  vary

Joint probability density function of  $(\xi, H)$  is derived from Eq. (2.36) by transformation and is given as

$$p(\xi, H) = \frac{2A^{2.5} \xi_{rms} H^{1.5}}{\sqrt{\pi} \nu C_m H_{rms}^{2.5} \xi^2} \exp\left[-(AH/H_{rms})^2 \left[1 + \left(1 - \frac{\xi_{rms} H_{rms}^{0.5}}{C_m \xi (AH)^{0.5}}\right)^2 / \nu^2\right] L(\nu)\right] \quad (2.43)$$

In principle, altering  $S_m$  and  $m$  directly changes the distribution of dimensional wave surf parameter  $\xi$ . Actually, all distributions mentioned in this thesis should be interpreted as short term distribution in one sea state. In other words, probability models relevant for discussion here are conditional distributions that are dependent on sea state. As  $S_m$  is a sea state parameter, the change of it varies conditional distribution of related short term parameters. Figs. 2.17 - 2.19 support the statement.

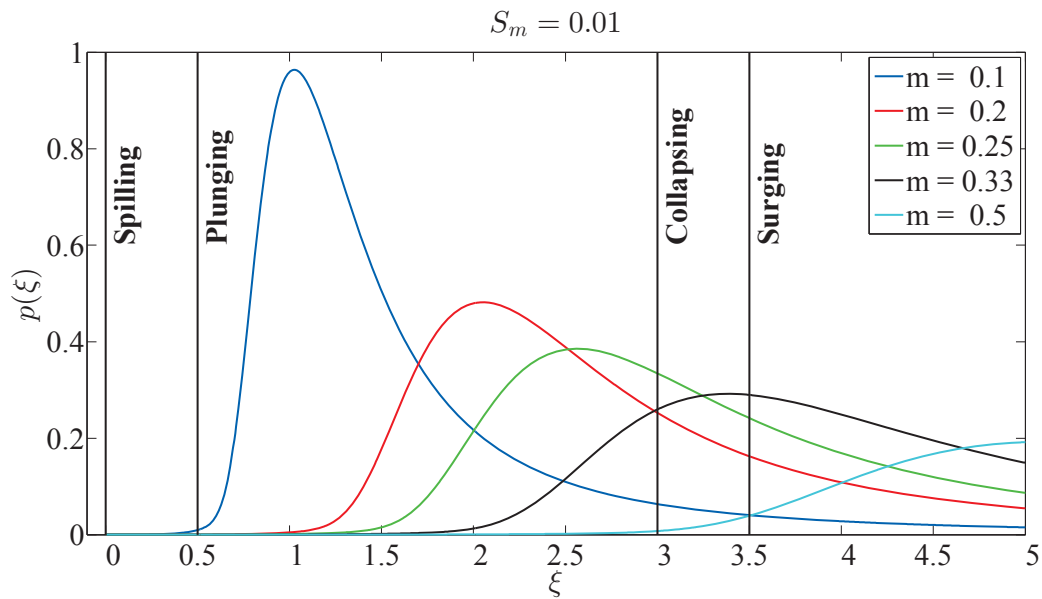


**Figure 2.17:** Marginal probability density of  $\xi_{MK}$  for  $S_m = 0.010$  and different slopes  $m$

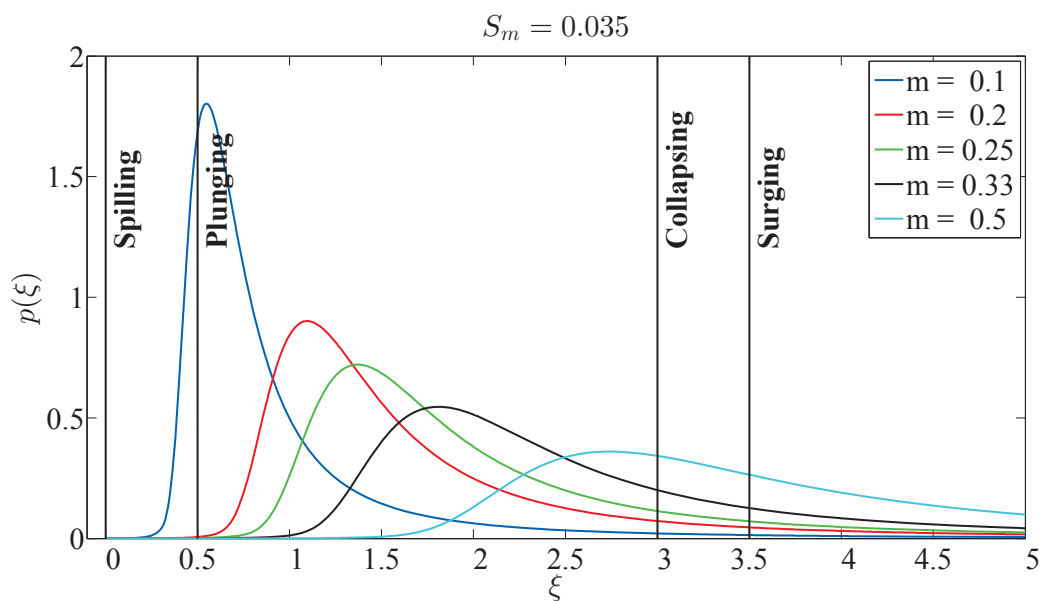


**Figure 2.18:** Marginal probability density of  $\xi_{MK}$  for  $S_m = 0.035$  and different slopes  $m$

Figs 2.20 - 2.22 give isodensity curve of  $p(H, \xi)$  for different slopes  $m$  and for sea state ( $H_s = 7.5 m, T_p = 9.5 s$ ) corresponding to one year return period according to measurements from Northern North Sea (details can be found in Myrhaug et al. (2009)).

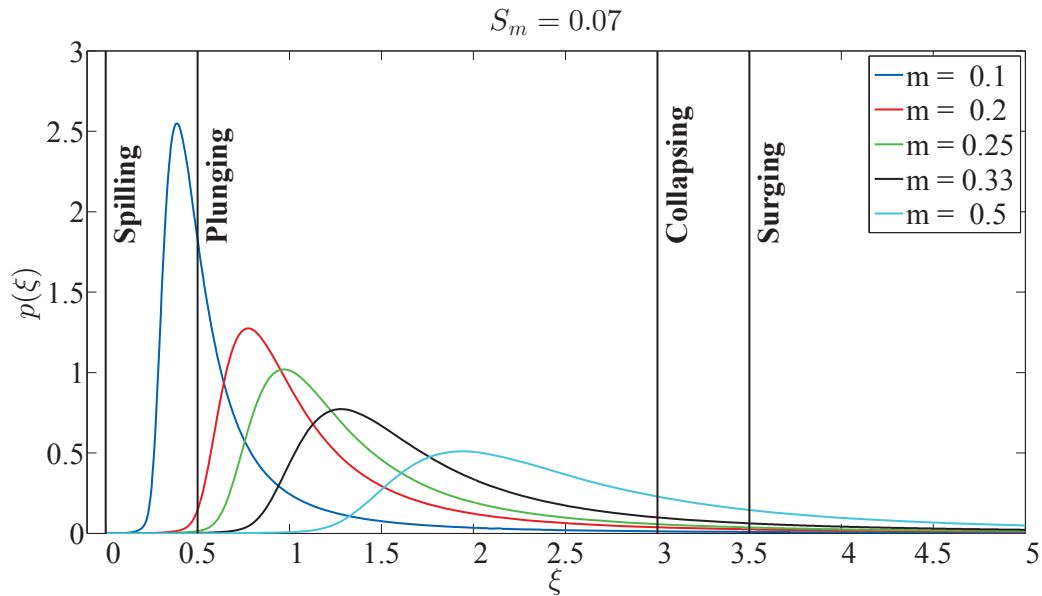


**Figure 2.19:** Marginal probability density of  $\xi_{MK}$  for  $S_m = 0.070$  and different slopes  $m$

Vertical lines represent the limit of each wave breaker and corresponding probabilities are also presented. It appears that surging breaker occur more frequently than collapsing breaker for each given slope. Spilling breaker only dominates as  $m = 0.1$  while plunging breaker dominates for other two slopes.

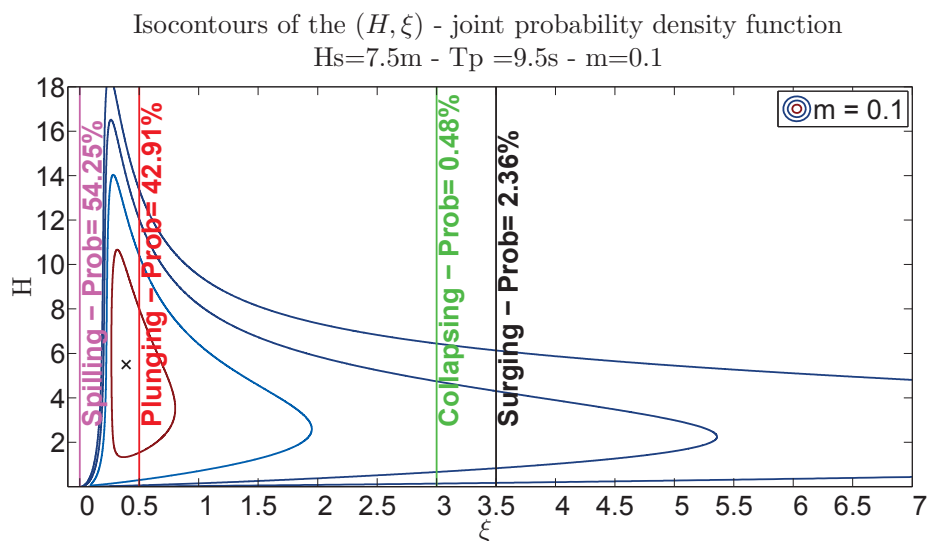


**Figure 2.20:** Isocontours of joint density  $p(H, \xi)$  for slope  $m = 0.10$ .  $p$  takes peak value (indicated as  $\times$ ), 0.1, 0.01, 0.001 and 0.0001 from center outwards

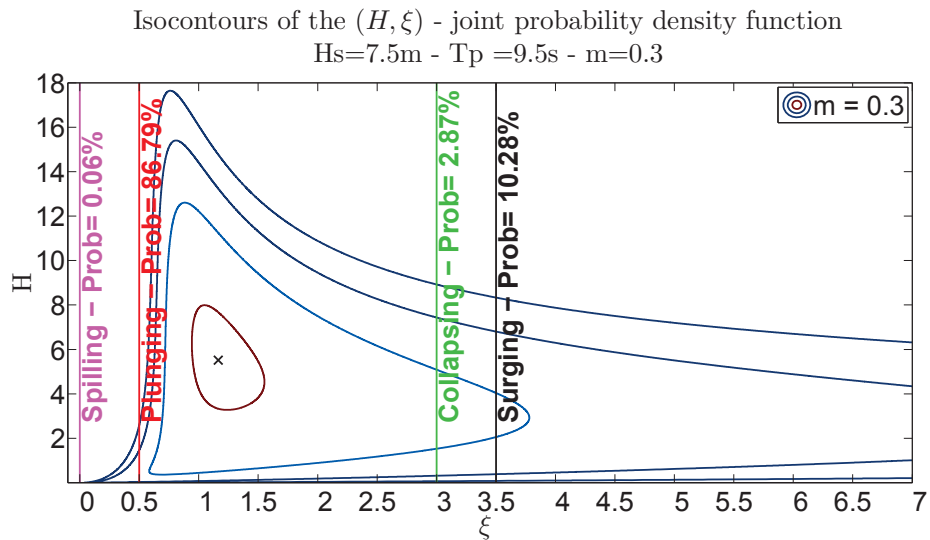


**Figure 2.21:** Isocontours of joint density  $p(H, \xi)$  for slope  $m = 0.30$ .  $p$  takes peak value (indicated as  $\times$ ), 0.1, 0.01, 0.001 and 0.0001 from center outwards

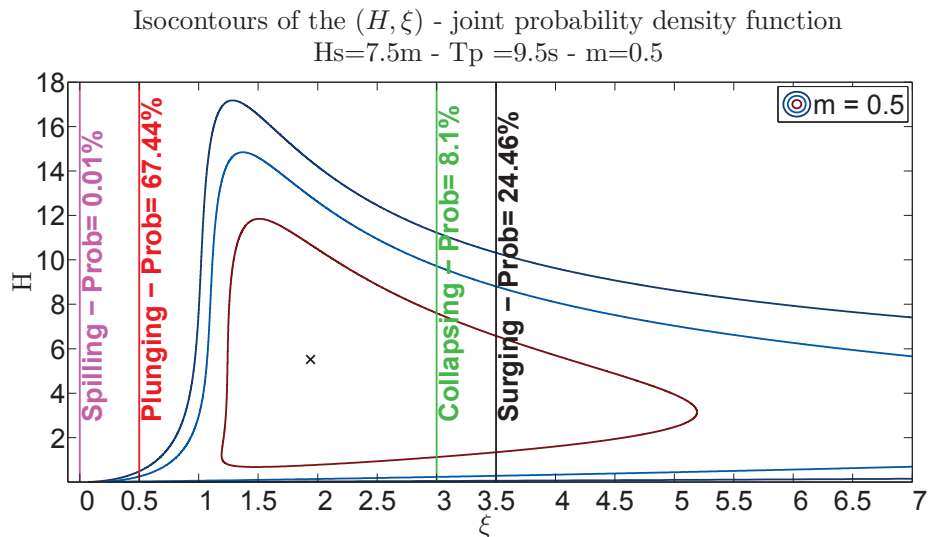


**Figure 2.22:** Isocontours of joint density  $p(H, \xi)$  for slope  $m = 0.50$ .  $p$  takes peak value (indicated as  $\times$ ), 0.1, 0.01, 0.001 and 0.0001 from center outwards

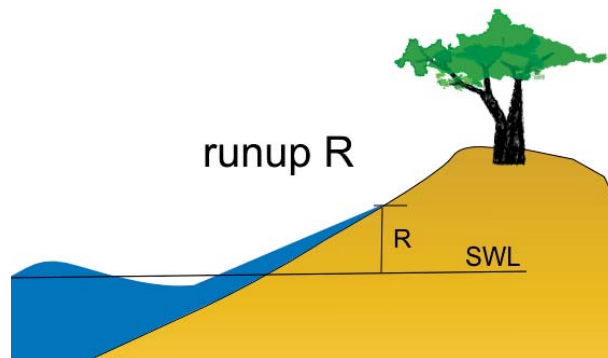


**Figure 2.23:** Sketch for runup



Move focus to breaking waves now. According to [Sorensen \(1993\)](#), runup  $R$  is defined as the maximum vertical elevation above SWL (still water level) as water rises to the beach or structure face, which is depicted in Fig. 2.23.

[Hunt, I.A. \(1959\)](#) made estimation of run-up above sea water level at wave breaking for periodic monochromatic waves, which is based on experimental data from many laboratory tests performed in Europe and United States ([Sorensen \(1993\)](#)). Hunt's formula is given by

$$R = H\xi = H \tan\theta \sqrt{\lambda/H} = \tan\theta \sqrt{H\lambda} = \tan\theta \sqrt{H \frac{gT^2}{2\pi}} \quad (2.44)$$

It should be noted that Eq. (2.44) is only valid for breaking waves at  $\xi \leq 2$  that is correspondence with  $R \leq 2H$  ([Nielsen \(2009\)](#)). In addition,  $H$  herein is restricted to deep wave height. Then  $\lambda$  can be expressed as  $gT^2/(2\pi)$  by using deep water dispersion relation  $\omega^2 = gk$ , where  $k$  is wave number and defined as  $k = 2\pi/\lambda$ .

Eq. (2.44) also implies that runup increases with slope for given incident waves and depends more on the period than on the wave height ([Nielsen \(2009\)](#)).

As for waves do not break, the relation among runup, slope and wave height is formulated in [Meyer \(1971\)](#) from the solution given in [Carrier and Greenspan \(1958\)](#):

$$\frac{R}{H} = \sqrt{\frac{2\pi}{\tan\beta}} \quad \text{for } \xi > 4 \quad (2.45)$$

[Baldock et al. \(2009\)](#) provided with an alternative form of Hunt's formula that delivers better correlation with their experimental data and it takes the form

$$\frac{R}{H} = K\xi \quad (2.46)$$

where  $K$  is empirical coefficients and  $K = 1$  corresponds with original Hunt's formula.  $H$  is deep wave height.

By focusing on the occurrence frequency of wave runup corresponding with breaking waves, theoretical joint distribution of wave runup  $R$  and wave height  $H$  is derived from Eq. (2.43),

given as

$$p(R, H) = \frac{2KA^{2.5}\xi_{rms}}{C_m\sqrt{\pi\nu}H_{rms}^{2.5}} \frac{H^{2.5}}{R^2} \cdot \exp\left[-(AH/H_{rms})^2\left(1 + \left(1 - \frac{K\xi_{rms}(H_{rms}H)^{0.5}}{C_m\sqrt{AR}}\right)^2/\nu^2\right)\right] L(\nu) \quad (2.47)$$

Afterwards,  $K = 1$  is taken as in original form of Hunt's formula for concrete calculations. Even though the validity of Hunt's formula is questionable as  $\xi > 2$ , the example given herein is much simplified for demonstration of the application of the derived LH83 model. As  $p(R|\hat{h}_{MK} = 1)dR = p(R|h = H_{rms})dR$ , an alternative way of investigating the conditional distribution of  $R$  given wave height is using (Dag Myrhaug, personal communication, 12 March, 2014).

$$p(R, \hat{h}_{MK}) = \frac{1}{K\hat{h}_{MK}H_{rms}\xi_{rms}} p(\hat{\xi}_{MK}(R, \hat{h}_{MK}), \hat{h}_{MK}) \quad (2.48)$$

Specifically, the conditional probability density function of  $R$  given non-dimensional wave height  $\hat{h}_{MK}$ ,  $p(R|\hat{h}_{MK})$ , using (2.48) is elaborated as

$$p(R|\hat{h}_{MK}) = \frac{1}{\sqrt{2\pi}R\sigma_R} \exp\left[-\frac{(\ln R - \mu_R)^2}{2\sigma_R^2}\right] \quad (2.49)$$

where  $\mu_R$  and  $\sigma_R^2$  are the mean value and variance of  $R$  and given by

$$\mu_R = \ln(KH\xi_{rms}) + \mu_{\hat{\xi}}; \quad \sigma_R^2 = \sigma_{\hat{\xi}}^2 \quad (2.50)$$

where  $\mu_{\hat{\xi}}$  and  $\sigma_{\hat{\xi}}^2$  are the mean value and variance of non-dimensional surf parameter  $\hat{\xi}$  (see Eqs. (4), (5) and (10) in Myrhaug and Fouques (2012)).

Taking  $(\ln R - \mu_R)/\sigma_R$  as one variable, then Eq. (2.49) after integration can be expressed as standard Gaussian distribution  $\phi$ . Specifically,

$$P(R|\hat{h}_{MK}) = \phi\left[\frac{(\ln R - \mu_R)}{\sigma_R}\right] \quad (2.51)$$

Fig. 2.25 shows the conditional expected value of  $R$  given  $\hat{h}_{MK}$ ,  $E(R|\hat{h}_{MK})$ , where

$$E(R|\hat{h}_{MK}) = \exp\left(\mu_R + \frac{1}{2}\sigma_R^2\right) \quad (2.52)$$

For slope  $m = 1$ , the probability of expected vertical runup given different wave height varies significantly as illustrated in Fig. 2.24 by dots and dash line. By contrast, MF12 results in lower and almost the same probability level of mean wave runup for wave height listed as shown in Fig. 2.25. Though numerical calculated  $E(R|\hat{h}_{MK})$  is only converged for  $\hat{h}_{MK} = 1.4$  and  $\hat{h}_{MK} = 2.1$  as shown in Fig. A.16, nevertheless the same variation pattern is observed even with different integration steps (see Figs. A.17 and A.18 for details)

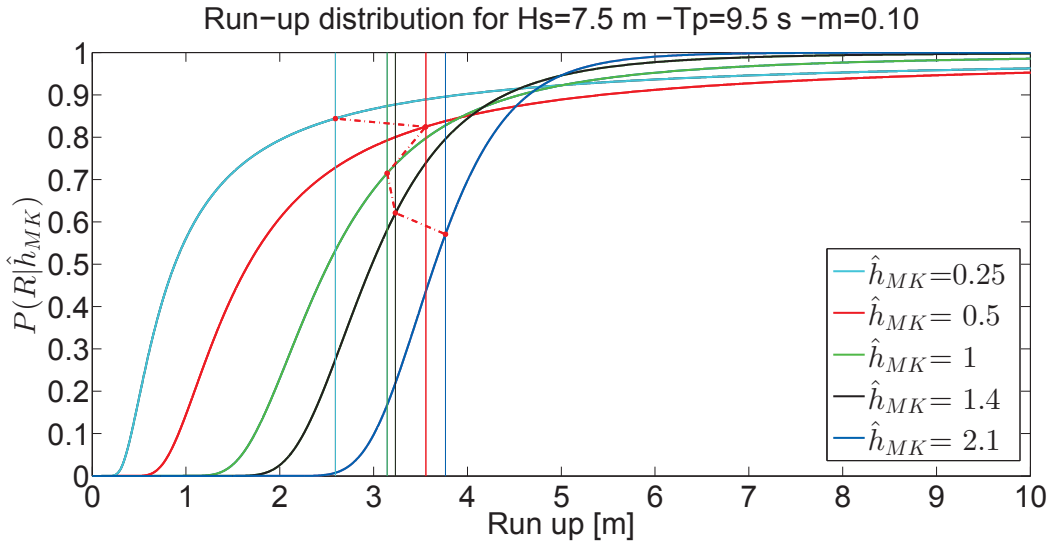


**Figure 2.24:** Conditional cumulative distribution of wave run-up given wave height  $P(R|H)$  from derived LH83 model

It should be noted [Myrhaug and Fouques \(2012\)](#) estimates mean  $R$  given  $\hat{h}_{MK}$  by another method. For example,  $R = H_{rms}\xi_{rms} \cdot E(\hat{\xi}_{MK}|\hat{h}_{MK} = 1.4)$  is employed, which is equal to the value computed by  $E(R|\hat{h}_{MK} = 1.4) = \int_0^\infty R p(R|\hat{h}_{MK} = 1.4) dR$  as well as by Eq. (2.52).

According to [Sorensen \(1993\)](#), runup is connected with the types of breaker. Spilling breaker results in lowest runup while as the breaker develops into the form of plunging, collapsing or surging breaker, the consequent runup may exceed twice the wave height. Hence, it would be of interest to investigate into the conditional probability of runup given different types of wave breakers.

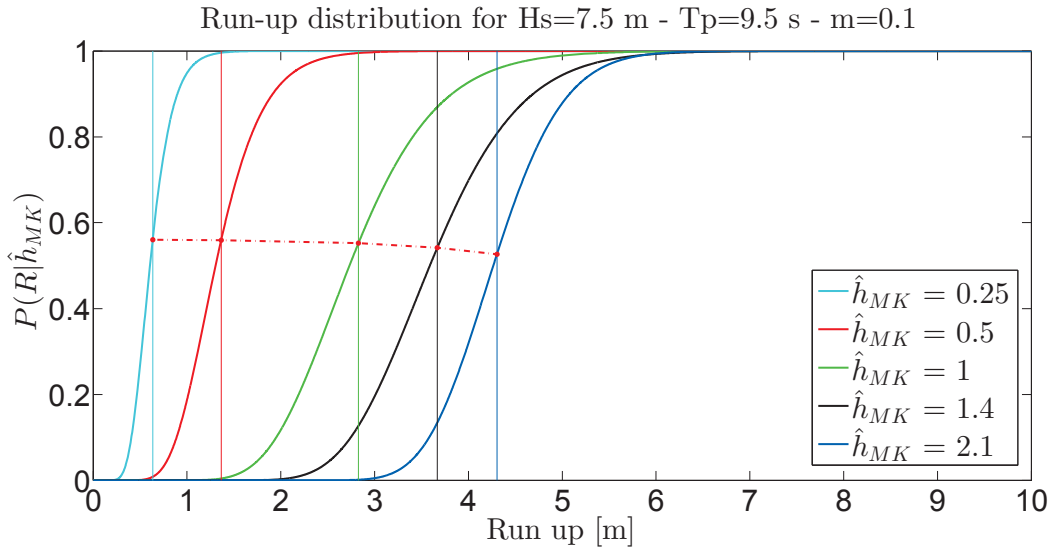


**Figure 2.25:** Conditional cumulative distribution of wave run-up given wave height  $P(R|H)$  based on MF12 model (adapted from Myrhaug and Fouques (2012))

Through making a change of variables from  $(\xi, H)$  to  $(R, \xi)$  by employing Jacobian that is computed in combination with Eq. 2.46,  $\left| \frac{\partial \xi}{\partial R} \cdot \frac{\partial H}{\partial \xi} \right| = (K\xi)^{-1}$ , joint distribution  $p(\xi, R)$  is obtained

$$p(\xi, R) = \frac{2A^{5/2}\xi_{rms}}{C_m\sqrt{\pi\nu}(KH_{rms})^{5/2}} \left( \frac{R^{3/2}}{\xi^{9/2}} \right) \exp \left[ - \left( \frac{AR}{K\xi H_{rms}} \right)^2 \left( 1 + \left( 1 - \frac{\xi_{rms}\sqrt{KH_{rms}}}{C_m\sqrt{A\xi R}} \right)^2 / \nu^2 \right) \right] L(\nu) \quad (2.53)$$

As a result of limited time, the concrete computation is not implemented.



# Chapter 3

## Statistics of wave power for individual waves

In this chapter, the connection between wave power per unit crest length and wave height and in addition to wave power and wave period will be firstly presented in section 3.1. Theoretical probability model from [Izadparast and Niedzwecki \(2011\)](#) and parametric probability model from [Myrhaug et al. \(2009\)](#) for wave power are presented in sections 3.2 and 3.3, respectively. Then, comparison between these two models is conducted in terms of peak values (subsection 3.4.1) before comparing with other properties (subsection 3.4.2).

### 3.1 Basic mathematics background for wave power

Total average wave energy of per unit surface area for regular waves,  $E$  is expressed as

$$E = \frac{1}{2} \rho g \frac{H^2}{4} = \frac{1}{8} \rho g H^2 \quad (3.1)$$

where  $\rho$  is water density. Wave power per unit crest length ( or energy flux, i.e. the rate of energy transferred)  $J$  is defined as

$$J = EC_g \quad (3.2)$$

where  $C_g$  is the wave group velocity. In deep water, following relation is valid

$$C_g = \frac{1}{2}C_\omega = \frac{1}{2}\frac{\omega}{k} = \frac{1}{2}\frac{\omega}{\omega^2/g} = \frac{1}{2}\frac{g}{\omega} = \frac{1}{2}\frac{g}{2\pi/T} = \frac{gT}{4\pi} \quad (3.3)$$

where  $C_\omega$  is phase velocity ( or wave profile velocity ). Combining Eq. (3.2) with Eqs. (3.3) and (3.1), Eq. (3.2) then is rearranged into

$$J = \frac{\rho g^2}{32\pi} H^2 T \quad (3.4)$$

One form of dimensionless wave power  $j$  is defined as

$$j = \frac{J}{\rho g^2 H_{cr}^2 T_{cr} / (32\pi)} = \hat{h}^2 t \quad (3.5)$$

## 3.2 Theoretical probability model for wave power

By means of stochastic variable transformation rule and together with using Eq. (3.5), the joint probability distribution of wave power  $j$  and wave period  $t$  can be formulated through

$$p(j, t) = p\left(\hat{h} = \sqrt{\frac{j}{t}}, t\right) \frac{\partial}{\partial j} \left(\sqrt{\frac{j}{t}}\right) \quad (3.6)$$

Hence, we have  $p(j, t)$  taking the form

$$p(j, t) = \frac{L(v)}{\sqrt{\pi}v} \frac{j^{1/2}}{t^{7/2}} \exp\left[-\frac{j}{t} \left(1 + \left(1 - \frac{1}{t}\right)^2 / v^2\right)\right] \quad (3.7)$$

In the same manner, the joint probability distribution  $p(j, \hat{h})$  is derived from Eq. (2.7) and takes the form

$$p(j, \hat{h}) = \frac{2L(v)}{\sqrt{\pi}v} \frac{\hat{h}^4}{j^2} \exp\left[-\hat{h}^2 \left(1 + \left(1 - \frac{\hat{h}^2}{j}\right)^2 / v^2\right)\right] \quad (3.8)$$

For the purpose of comparing the theoretical bivariate distribution derived herein for wave power with parametric model given in Myrhaug et al. (2009), same normalized procedure is followed (e.g. using the definition of normalized wave period given in Myrhaug and Kjeldsen

(1984), i.e.  $\hat{t}_{MK}$  is defined as  $T/T_{rms}$ . Root mean square value of wave period  $T_{rms}$  is related to  $T_z$  by coefficient  $\gamma_T$  (based on best fit to measurements given by Myrhaug and Kjeldsen (1984) in Eq. (9b))

$$T_{rms} = \gamma_T T_z; \quad \gamma_T = 1.2416 \quad (3.9)$$

Corresponding  $j_{MK}$  is defined as

$$j_{MK} = \frac{J}{\rho g^2 H_{rms}^2 T_{rms} / (32\pi)} = \hat{h}_{MK}^2 \hat{t}_{MK} \quad (3.10)$$

The relation between  $t$  and  $\hat{t}_{MK}$  is given in Myrhaug and Kvålsvold (1995) with coefficient  $B$  as

$$t = B \hat{t}_{MK}; \quad B = \frac{\gamma_T}{\sqrt{1+v^2}} \quad (3.11)$$

Incorporating Eqs. (2.34), (3.5) and (3.10) with (3.11), the connection between  $j$  and  $j_{MK}$  is established:

$$j = A^2 B j_{MK} \quad (3.12)$$

Performing a change of variables for Eq. (3.7) from  $(j, t)$  to  $(j_{MK}, \hat{t}_{MK})$  through the utilization of Jacobian  $\left| \frac{\partial j}{\partial j_{MK}} \cdot \frac{\partial t}{\partial \hat{t}_{MK}} \right| = (AB)^2$ ,  $p(j_{MK}, \hat{t}_{MK})$  is derived as

$$p(j_{MK}, \hat{t}_{MK}) = \frac{A^3 L(v)}{B \sqrt{\pi v}} \frac{j_{MK}^{1/2}}{\hat{t}_{MK}^{7/2}} \exp \left[ -\frac{A^2 j_{MK}}{\hat{t}_{MK}} \left( 1 + \left( 1 - \frac{1}{B \hat{t}_{MK}} \right)^2 / v^2 \right) \right] \quad (3.13)$$

Following same approach, Eq. (3.8), using Jacobian  $\left| \frac{\partial j}{\partial j_{MK}} \cdot \frac{\partial \hat{h}}{\partial \hat{h}_{MK}} \right| = A^3 B$ , is transformed into  $p(j_{MK}, \hat{h}_{MK})$  as

$$p(j_{MK}, \hat{h}_{MK}) = \frac{2A^3 L(v)}{B \sqrt{\pi v}} \frac{\hat{h}_{MK}^4}{j_{MK}^2} \exp \left[ -A^2 \hat{h}_{MK}^2 \left( 1 + \left( 1 - \frac{\hat{h}_{MK}^2}{B j_{MK}} \right)^2 / v^2 \right) \right] \quad (3.14)$$

Izadparast and Niedzwecki (2011) also present the joint distribution of dimensionless wave power and wave period as well as of dimensionless wave power and wave height based on



Longuet-Higgins (1983), but with different normalized procedures. They define dimensionless wave power as

$$j_{IN} = \alpha_d \tau \hat{h}_{IN}^2 \quad (3.15)$$

where  $\alpha_d = (1/8)(\bar{T}/T_p)$  is a sea state parameter for deep water condition,  $T_p$  is peak period for a sea state,  $\tau = T/\bar{T}$  is normalized wave period and  $\hat{h}_{IN} = H/\sqrt{m_0}$  is normalized wave height.

The joint probability density function  $p(j_{IN}, \hat{h}_{IN})$  then is

$$p(j_{IN}, \hat{h}_{IN}) = \frac{\alpha_d \hat{h}_{IN}^4}{8\sqrt{2\pi} v j_{IN}^2} L(v) \exp \left[ \frac{-v^2}{8} \left( 1 + \left( 1 - \frac{\alpha_d \hat{h}_{IN}^2}{j_{IN}} \right) \frac{1}{v^2} \right) \right] \quad (3.16)$$

The joint probability distribution of  $p(\hat{j}_{IN}, \tau)$  takes the form

$$p(\hat{j}_{IN}, \tau) = \frac{j_{IN}^{1/2}}{16v\sqrt{2\pi}(\alpha_d)^{3/2}\tau^{7/2}} L(v) \exp \left[ \frac{-j_{IN}}{8\alpha_d} \left( 1 + \left( 1 - \frac{1}{v^2} \right) \right) \right] \quad (3.17)$$

Connections between  $\hat{h}_{MK}$  and  $\hat{h}_{IN}$ ,  $\hat{t}_{MK}$  and  $\tau$ ,  $j_{MK}$  and  $j_{IN}$  are presented as

$$\hat{h}_{IN} = 2\sqrt{2}A\hat{h}_{MK} \quad (3.18)$$

$$\tau = B\hat{t}_{MK} \quad (3.19)$$

$$j_{IN} = 8\alpha_d A^2 B j_{MK} \quad (3.20)$$

Employing Eqs. (3.18) - (3.20), Eq. (3.14) can alternatively be obtained from Eq. (3.16) by a change of variables with using the Jacobian  $\left| \frac{\partial j_{IN}}{\partial j_{MK}} \cdot \frac{\partial \hat{h}_{IN}}{\partial \hat{h}_{MK}} \right| = (16\sqrt{2}\alpha_d)A^3B$ .

Similarly, Eq. (3.13) can alternatively be derived from Eq. (3.17) with utilizing the Jacobian  $\left| \frac{\partial j_{IN}}{\partial j_{MK}} \cdot \frac{\partial \tau}{\partial \hat{t}_{MK}} \right| = 8\alpha_d (AB)^2$ .

It should be noted that  $T_{cr} = 2\pi m_0^\omega / m_1^\omega$  has the same definition as  $\bar{\tau}$  in Izadparast and Niedzwecki (2011).

Additionally, the Eq. (17) for distribution of wave height given there is missing standard deviation of linear and narrow banded surf wave elevation in the denominator of the leading

factor.

### 3.3 Parametric probability model for wave power

Myrhaug et al. (2009) derives joint probability distribution of  $(\hat{h}_{MK}, j_{MK})$  and  $(\hat{t}_{MK}, j_{MK})$  (hereafter denoted as MB09) from parametric model of  $(\hat{h}_{MK}, \hat{t}_{MK})$  given in Myrhaug and Kjeldsen (1984), which is obtained by best-fitting to data from measurements at sea on Norwegian continental shelf.

Joint pdf  $p(j_{MK}, \hat{h}_{MK})$  is given as

$$p(\hat{h}_{MK}, j_{MK}) = p(j_{MK}|\hat{h}_{MK})p(\hat{h}_{MK}) \quad (3.21)$$

where  $p(\hat{h}_{MK})$  is given as a 2-parameter Weibull model as given in Eq. (2.21).  $p(j_{MK}|\hat{h}_{MK})$  is given as a 3-parameter Weibull model as following

$$p(j_{MK}|h_{MK}) = \frac{\beta}{\rho \hat{h}_{MK}^2} \left( \frac{j_{MK} - \alpha \hat{h}_{MK}^2}{\rho \hat{h}_{MK}^2} \right)^{\beta-1} \exp \left[ - \left( \frac{j_{MK} - \alpha \hat{h}_{MK}^2}{\rho \hat{h}_{MK}^2} \right)^\beta \right]; \quad j_{MK} \geq \alpha \hat{h}_{MK}^2 \quad (3.22)$$

with the parameters

$$\alpha = 0.12 \sqrt{\hat{h}_{MK}} \quad (3.23)$$

$$\beta = 2 \arctan[2(\hat{h}_{MK} - 1.2)] + 5 \quad (3.24)$$

$$\rho = \begin{cases} 0.78 \hat{h}_{MK} + 0.26 & \text{if } \hat{h}_{MK} \leq 0.9 \\ 0.962 & \text{if } \hat{h}_{MK} > 0.9 \end{cases} \quad (3.25)$$

Joint distribution  $p(j_{MK}, \hat{t}_{MK})$  from MB09 is given as

$$p(j_{MK}, \hat{t}_{MK}) = p \left( \hat{t}_{MK} | \hat{h}_{MK} = \sqrt{\frac{j_{MK}}{\hat{t}_{MK}}} \right) \left[ \frac{n}{r} \left( \frac{j_{MK}}{r} \right)^{n-1} \exp \left( - \left( \frac{j_{MK}}{r} \right)^n \right) \right]; \quad j_{MK} \geq 0 \quad (3.26)$$

with the parameters  $r$  and  $n$  are given by

$$r = 1.05^2 \hat{t}_{MK}; \quad n = 2.39/2 \quad (3.27)$$

$p(\hat{t}_{MK}|\hat{h}_{MK} = \sqrt{\frac{j_{MK}}{\hat{t}_{MK}}})$  is obtained by substituting  $\sqrt{j_{MK}/\hat{t}_{MK}}$  for  $\hat{h}_{MK}$  in Eqs. (3.23) – (3.25) and pdf  $p(\hat{t}_{MK}|\hat{h}_{MK})$  in Eq. (3.28).

$$p(\hat{t}_{MK}|\hat{h}_{MK}) = \frac{\beta}{\rho} \left( \frac{\hat{t}_{MK} - \alpha}{\rho} \right)^{\beta-1} \exp \left[ - \left( \frac{\hat{t}_{MK} - \alpha}{\rho} \right)^{\beta} \right]; \quad \hat{t}_{MK} \geq \alpha \quad (3.28)$$

### 3.4 Comparison between theoretical and parametric probability model for wave power

#### 3.4.1 Comparison of peak values from two models

Performing partial differentiation of Eq. (3.7) from IN11 model with regards to  $j$  and  $t$  and enforce them to be zero, following formulae are obtained

$$7j^{0.5}t^3 - 2j^{0.5} \left[ jt^2 + (jt^2 - 4jt + 3j)/v^2 \right] = 0 \quad (3.29a)$$

$$t^3 - 2j \left[ t^2 + (t^2 - 2t + 1)/v^2 \right] = 0 \quad (3.29b)$$

In the similar fashion, following equations are derived from Eq. (3.8) of IN11 model

$$2\hat{h}^3j^2 + \hat{h}^5 \left[ -j^2 + (-j^2 + 4j\hat{h}^2 - 3\hat{h}^4)/v^2 \right] = 0 \quad (3.30a)$$

$$\hat{h}^4j^2 + \hat{h}^4 \left( \hat{h}^4j - \hat{h}^6 \right) \frac{1}{v^2} = 0 \quad (3.30b)$$

As  $\hat{h}$ ,  $j$  and  $t$  are possible to be zero, common factors such as  $\hat{h}^4$  and  $j^{0.5}$  are not cancelled out. No real solutions except zero of Eqs. (3.29) and (3.30) are found. By substituting zero solutions in Eqs. (3.7) and (3.8), singularities are found. Numerically calculated peak values with different meshgrids also support this statement (details can be found in section B.2).

Based on numerical computation results (see Fig 3.1), the peak value of MB09 model for bivariate probability density function of wave power and wave period ( $p(\hat{t}_{MK}, j_{MK})$ ) is found to be extremely close to the  $\hat{t}_{MK}$  axis. Specifically, it is found that the peak value of pdf is 4.807 and it is located at  $\hat{t}_{MK} = 0.235$  and  $j_{MK} = 0.0011$  rather than  $p_{max} = 2.65$ ,  $\hat{t}_{MK} = 0.5$  and  $j_{MK} = 0.072$  given in Myrhaug et al. (2009). Hence, there is dramatic difference of peak value of the bivariate distribution of wave power and wave period between the two models.

It is noted that the contour for bivariate probability distribution without singularity should be enclosed (e.g. see contour of  $p(j_{MK}, \hat{t}_{MK})$  in Fig. B.1b).

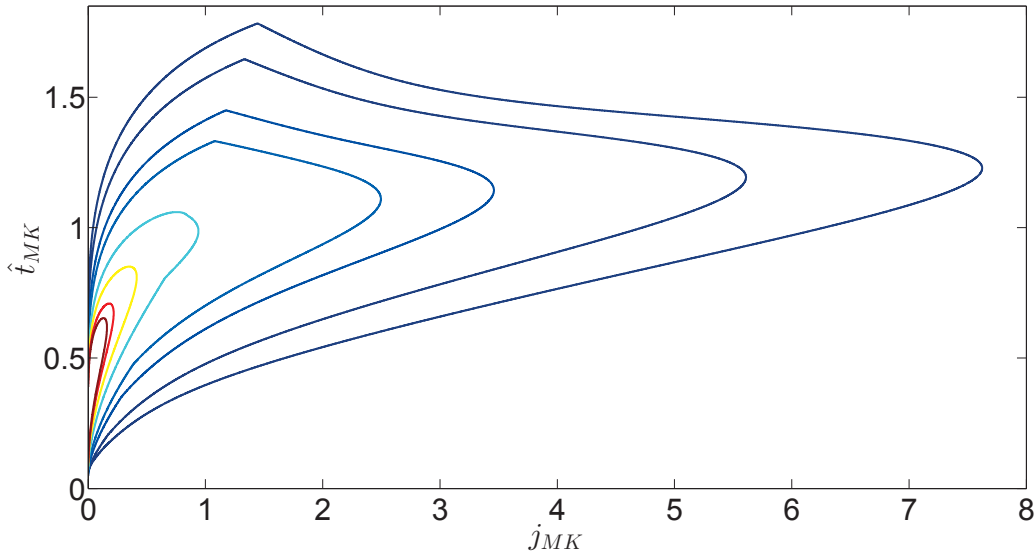


**Figure 3.1:** Isocontour of  $p(\hat{t}_{MK}, j_{MK})$  from MB09 model,  $p$  takes 0.001, 0.01, 0.1, 0.25, 0.75, 1.25, 1.75 and 2 from outermost to the centre (adapted from Myrhaug et al. (2009))

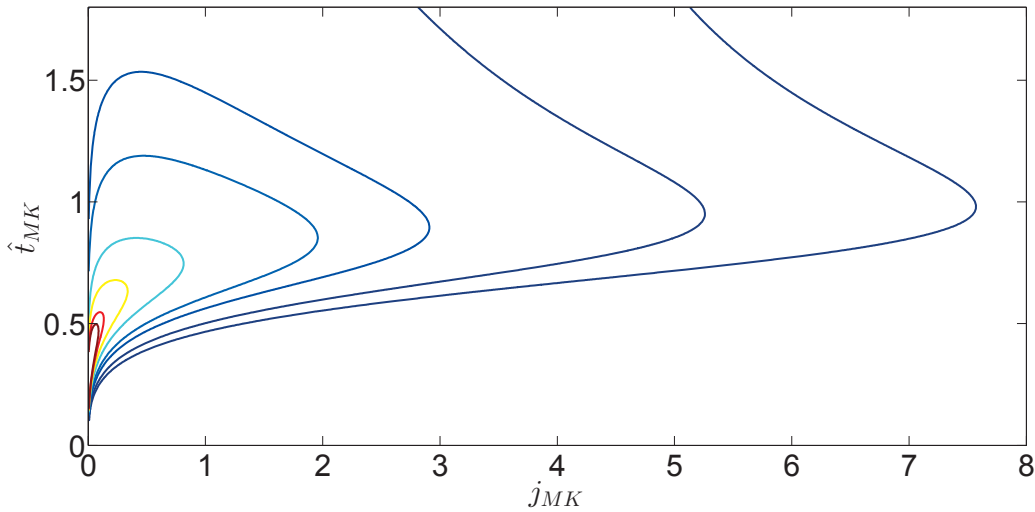


**Figure 3.2:** Isocontour of  $p(\hat{t}_{MK}, j_{MK})$  from IN11 model,  $p$  takes 0.001, 0.01, 0.1, 0.25, 0.75, 1.25, 1.75 and 2 from the outermost to the centre

As for  $p(\hat{h}_{MK}, j_{MK})$ , it is found that singularity seems to appear as  $j_{MK}$  approaches to trivial values (see Table B.1).

It should be noted that the isocontour of  $p(\hat{t}_{MK}, j_{MK})$  (Fig. 7) in Myrhaug et al. (2009) is distinct from Fig. B.1 in the proximity of  $\hat{t}_{MK}$  axis.

### 3.4.2 Comparison of other properties from two models

From Figs. 3.1 and 3.2, it is observed that the conditional distribution of  $j_{MK}$  given  $\hat{t}_{MK}$  seems most broad-banded at  $\hat{t}_{MK} \approx 1$  for both models. However, the conditional distribution of  $\hat{t}_{MK}$  given  $j_{MK}$  from IN11 model is more broad-banded than that of MB09 model. The asymmetry of  $p(j_{MK}, \hat{t}_{MK})$  with regards to  $\hat{t}_{MK}$  is observed for IN11 model, while it appears that the joint distribution from MB09 model is symmetric with respect to  $\hat{t}_{MK}$  at high  $j_{MK}$ .

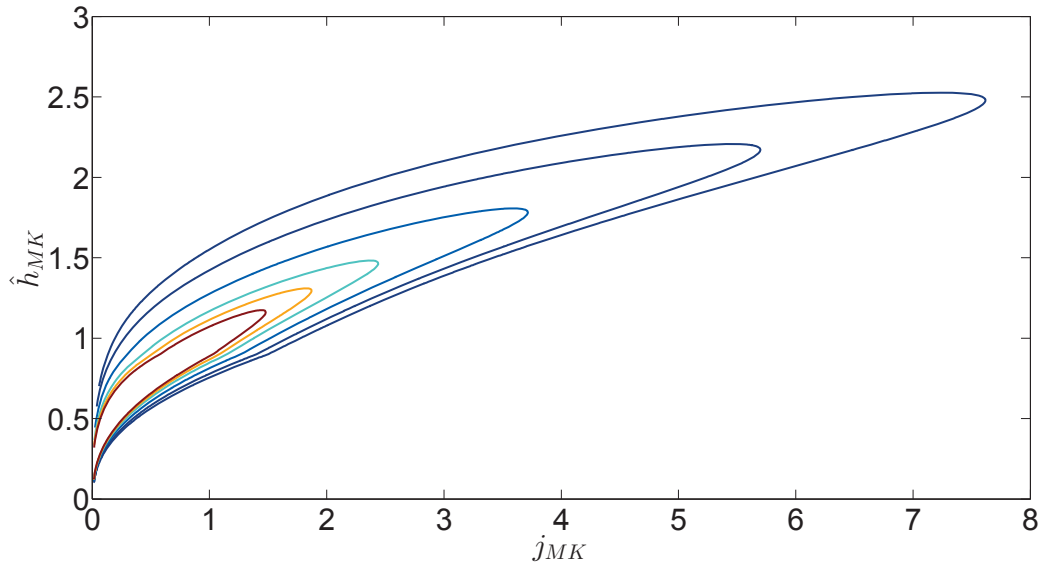


**Figure 3.3:** Isocontour of joint probability density  $(\hat{h}_{MK}, j_{MK})$  from MB09 model,  $p$  takes 1, 0.7, 0.3, 0.1, 0.01, 0.001 from center outwards

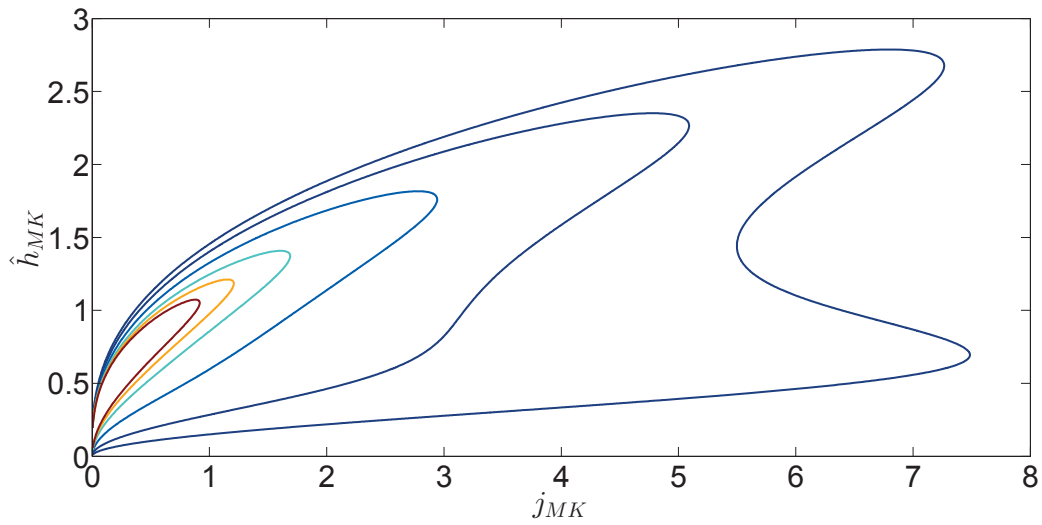
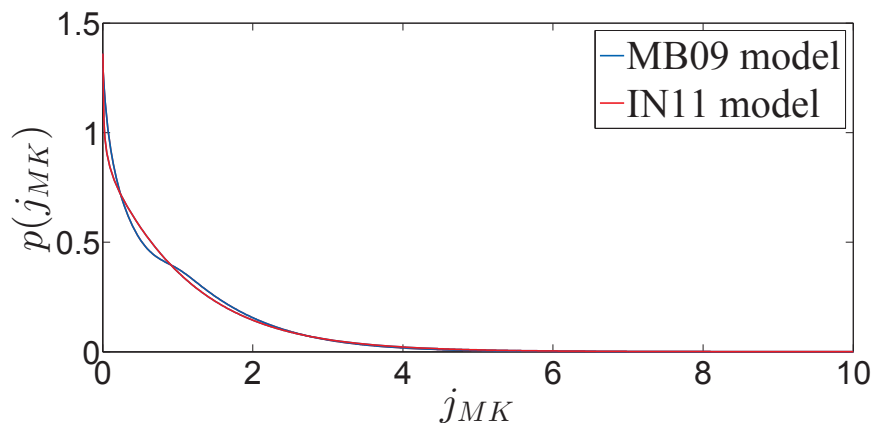
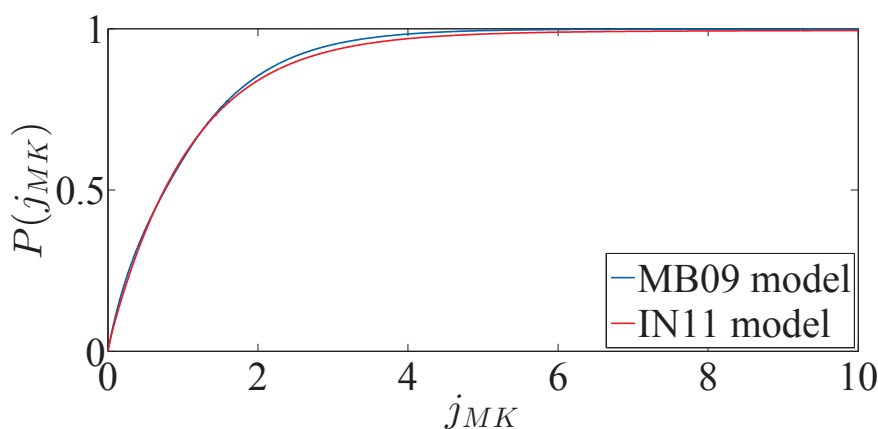


**Figure 3.4:** Isocontour of joint probability density  $(\hat{h}_{MK}, j_{MK})$  from IN11 model,  $p$  takes 1, 0.7, 0.3, 0.1, 0.01, 0.001 from center outwards

It is found from Figs. 3.3 – 3.4, that the contour is not enclosed, though uniform increment of abscissas and ordinates of discrete points with interval  $10^{-5}$  is used. The conditional distribution of  $j_{MK}$  given  $h_{MK}$  given by MB09 model and IN11 model is skewed to the left and right, respectively. Isocurve of IN11 model deviates from MB09 model greatly as joint probability density value is fairly small (i.e. 0.01 and 0.001). Due to  $\rho$  being piecewise function of  $\hat{h}_{MK}$ , obvious discontinuity is observed for MB09 model (see Figs. 3.1 and 3.8a).



(a) Marginal probability density function of  $j_{MK}$



(b) Cumulative distribution function of  $j_{MK}$

**Figure 3.5:** Marginal distribution of  $j_{MK}$

As can be observed from Fig. 3.5a, singularity of marginal distribution of  $j_{MK}$  from two models exist. Hence, sufficiently small steps for integration have to be used, especially as trapezoidal method is utilized. It is also seen that the pdf of  $j_{MK}$  from two models agree well with each other as  $j_{MK} \geq 1$ . However, the cumulative probability functions of  $j_{MK}$  of two models have better agreement for all values of  $j_{MK}$  (see Fig. 3.5b). Same features of pdf and cdf of dimensionless power  $j_{IN}$  were illustrated in Fig. 4 by [Izadparast and Niedzwecki \(2011\)](#).

The conditional expected value of wave power ( $j_{MK}$ ) given wave height ( $\hat{h}_{MK}$ ) is another quantity of interest. As seen from Fig. 3.6, the conditional mean values from two models increase with wave height, which are consistent with the features shown in Figs. 3.3 and 3.4. The difference of  $E(j_{MK}|\hat{h}_{MK})$  from MB09 and IN11 model widens gradually in the high wave heights.

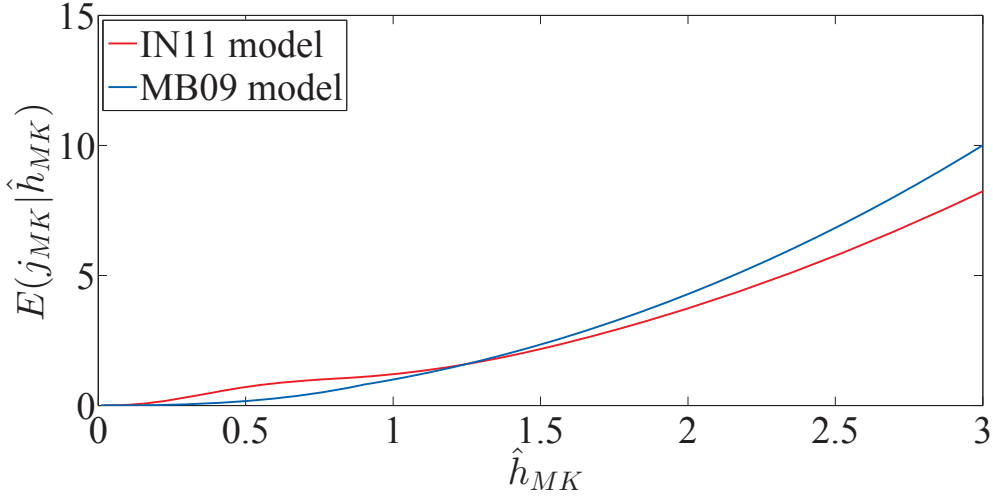


Figure 3.6:  $E(j_{MK}|\hat{h}_{MK})$  versus  $\hat{h}_{MK}$

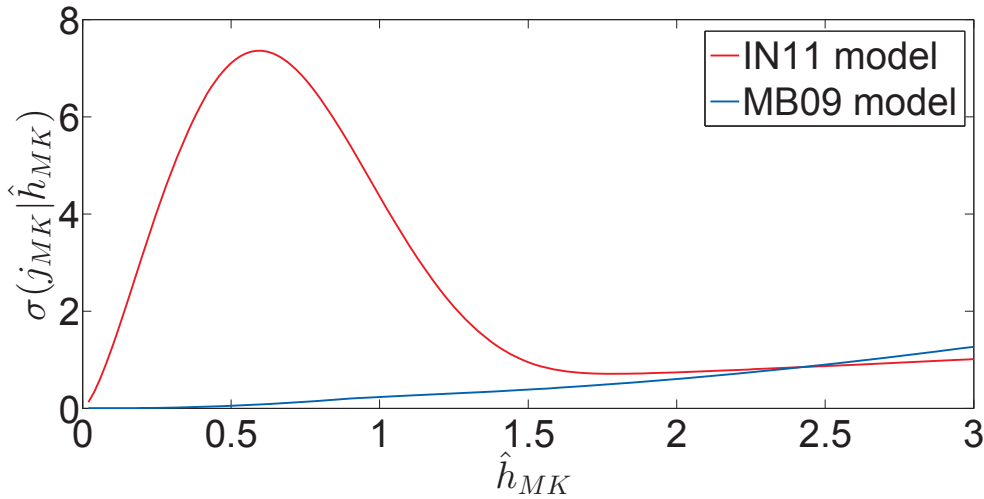


Figure 3.7:  $\sigma(j_{MK}|\hat{h}_{MK})$

Fig. 3.7 shows a noticeable convex feature of curve for  $\sigma(j_{MK}|\hat{h}_{MK})$  from IN11 model, which is reflected by Fig. 3.4 if we examine the conditional distribution of  $j_{MK}$  given  $0 \leq \hat{h}_{MK} \leq 1.5$ . It is found that the numerical calculated  $\sigma(j_{MK}|\hat{h}_{MK})$  is only convergent as  $\hat{h}_{MK}$  is in excess of approximately 1.7, though an amount of efforts have been dedicated to adoption of different numerical integral recipes (see Table B.6 – B.8 and Fig. B.5 for details). However,

the trend of curves in Fig. B.5 is the same as that of curve for IN11 model in Fig. 3.7.

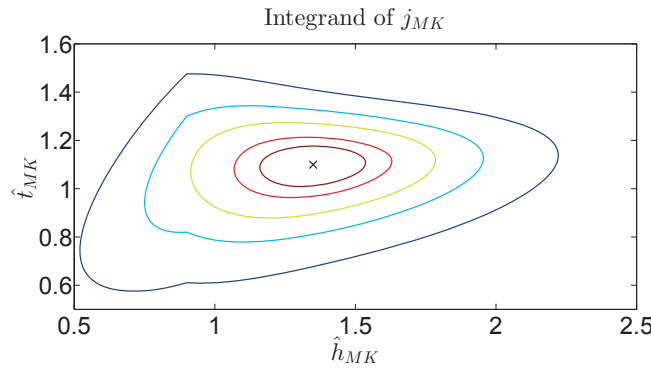
The expected value of  $j_{MK}$  can be obtained by either of following three formulae

$$E(j_{MK}) = \int_0^\infty E(j_{MK}|\hat{t}_{MK}) p(\hat{t}_{MK}) d\hat{t}_{MK} = \int_0^\infty \int_0^\infty j_{MK} p(j_{MK}, \hat{t}_{MK}) dj_{MK} d\hat{t}_{MK} \quad (3.31)$$

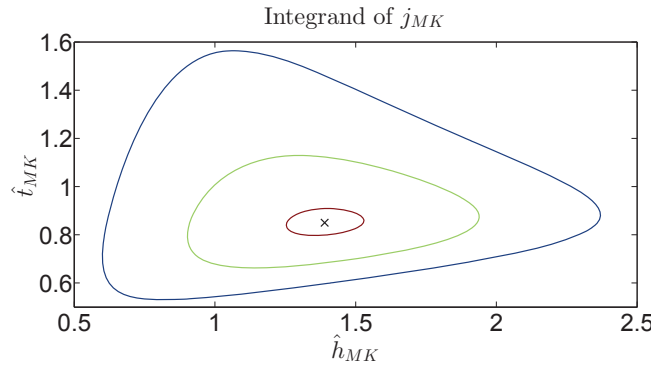
$$E(j_{MK}) = \int_0^\infty \int_0^\infty j_{MK} p(j_{MK}, \hat{h}_{MK}) dj_{MK} d\hat{h}_{MK} \quad (3.32)$$

$$E(j_{MK}) = \int_0^\infty \int_0^\infty \hat{h}_{MK}^2 \hat{t}_{MK} p(\hat{h}_{MK}, \hat{t}_{MK}) d\hat{h}_{MK} d\hat{t}_{MK} \quad (3.33)$$

Note that the Eq. (23) given by Myrhaug et al. (2009) can be rearranged into Eq. (3.31). However, it is found that Eqs. (3.32) and (3.33) for IN11 model cannot be solved by using built-in function *integral2* in Matlab and *int* in Maple with the default accuracy criterion. Routines mentioned above give the same results for Eq. (3.31) to the second decimal,  $E(j_{MK}) = 1.38$ , which is higher than the estimate 1.03 made by Myrhaug et al. (2009).



(a) Contour of  $\hat{h}_{MK}^2 \hat{t}_{MK} p(\hat{h}_{MK}, \hat{t}_{MK})$  from MB09 model. The level is 2, 1.75, 1.25, 0.75 and 0.25 from center outwards, reproduced from Myrhaug et al. (2009)



(b) Contour of  $\hat{h}_{MK}^2 \hat{t}_{MK} p(\hat{h}_{MK}, \hat{t}_{MK})$  from IN11 model. The level is 1.25, 0.75 and 0.25 from center outwards

**Figure 3.8:** Contour of  $\hat{h}_{MK}^2 \hat{t}_{MK} p(\hat{h}_{MK}, \hat{t}_{MK})$



Figs. 3.8a and 3.8b show the integrand of Eq. (3.33) from MB09 and IN11 model, respectively. The forms of contour are similar to each other with IN model being much more spread. Another feature is the lack of levels 1.75 and 2 for IN11 model.

Rearrange Eq. (3.33) into the form shown in Eq. (3.34) as Myrhaug et al. (2009) did.

$$\begin{aligned}
 E(j_{MK}) &= \int_0^\infty \hat{h}_{MK}^2 p(\hat{h}_{MK}) \left( \int_0^\infty \hat{t}_{MK} p(\hat{t}_{MK}|\hat{h}_{MK}) d\hat{t}_{MK} \right) d\hat{h}_{MK} \\
 &= \int_0^\infty \hat{h}_{MK}^2 p(\hat{h}_{MK}) E(\hat{t}_{MK}|\hat{h}_{MK}) d\hat{h}_{MK} \\
 &= \int_0^\infty E(j_{MK}|\hat{h}_{MK}) p(\hat{h}_{MK}) d\hat{h}_{MK}
 \end{aligned} \tag{3.34}$$

Fig. 3.9 shows the integrand in the last line of Eq.(3.34). It appears that the maximum contribution to  $E(j_{MK})$  happens at  $\hat{h}_{MK} \approx 1.2$  and  $\hat{h}_{MK} \approx 1.0$  for MB09 and IN11 model, respectively.

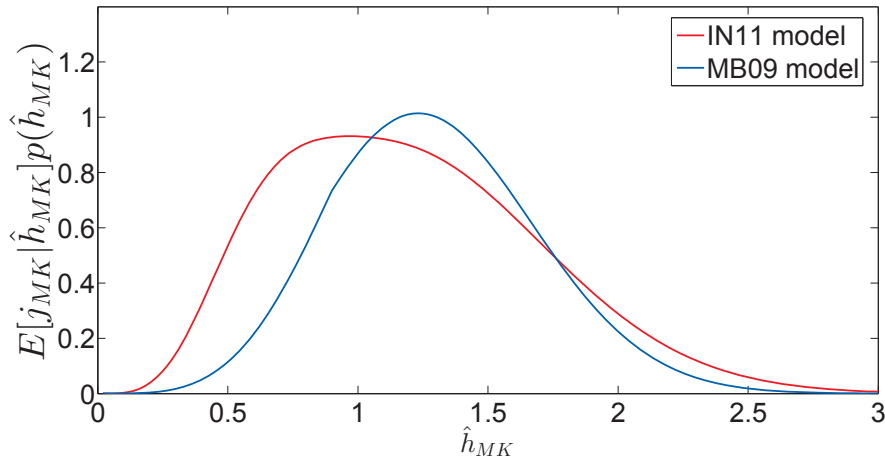


**Figure 3.9:**  $E(j_{MK}|\hat{h}_{MK})p(\hat{h}_{MK})$  versus  $\hat{h}_{MK}$

Figs. 3.10 and 3.11 show that both  $E(j_{MK}|\hat{t}_{MK})$  and  $\sigma(j_{MK}|\hat{t}_{MK})$  of two models possess same qualitative behaviour. Specifically, both  $E(j_{MK}|\hat{t}_{MK})$  and  $\sigma(j_{MK}|\hat{t}_{MK})$  of MB09 model appear to increase to maximum at  $\hat{t}_{MK} \approx 1.3$  before decreasing, while these two quantities of IN11 model rise to peaks at  $\hat{t}_{MK} \approx 1.05$  prior to dropping. They are respectively corresponding to the properties of  $p(j_{MK}, \hat{t}_{MK})$  from two models shown in Figs. 3.1 and 3.2.

Due to high gradient of  $p(j_{MK}|\hat{t}_{MK})$  of IN11 model in the range of 0 – 0.5 for  $\hat{t}_{MK}$  as seen in Fig. 3.2, extremely small integration step has to be employed to reach converged result of  $E(j_{MK}|\hat{t}_{MK})$  and  $\sigma(j_{MK}|\hat{t}_{MK})$ . Even though integration step with  $8 \times 10^{-5}$  is applied, com-

plex number is obtained during calculation of  $\sigma(j_{MK}|\hat{t}_{MK})$  for the values of  $\hat{t}_{MK}$  mentioned above, show by red curve in Fig. 3.11.

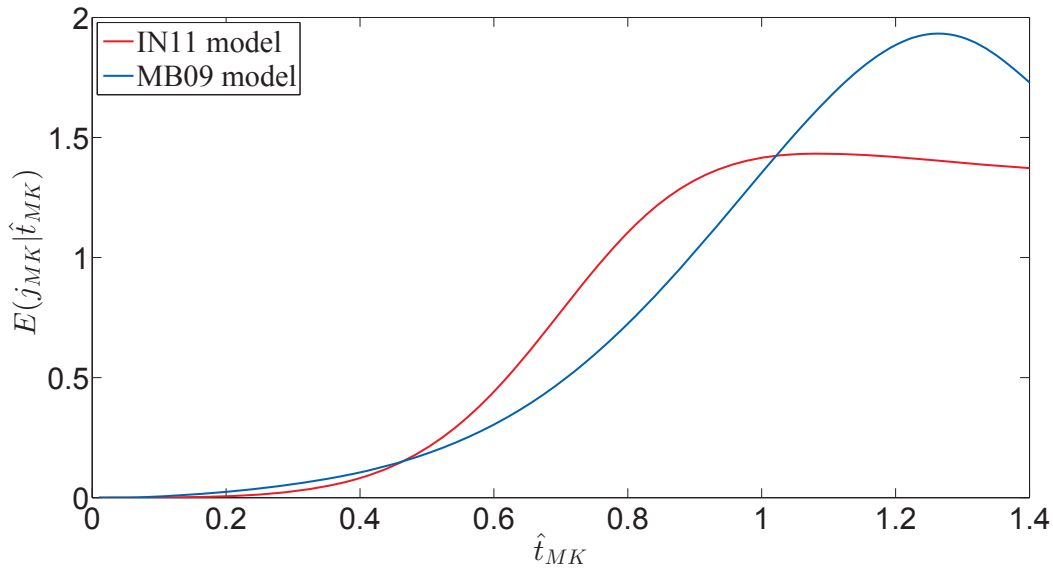


**Figure 3.10:**  $E(j_{MK}|\hat{t}_{MK})$  versus  $\hat{t}_{MK}$

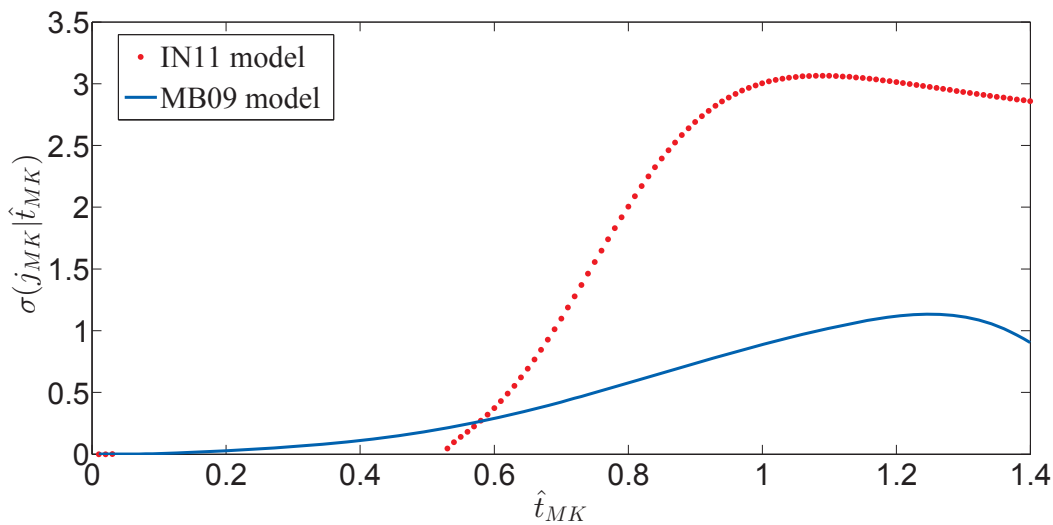


**Figure 3.11:**  $\sigma(j_{MK}|\hat{t}_{MK})$  versus  $\hat{t}_{MK}$

Fig. 3.12 shows the integrand given in the integral after first equal sign in Eq. (3.31). It appears that maximum contribution to  $E(j_{MK})$  is at  $\hat{t}_{MK} \approx 1.1$  for MB09 model while  $\hat{t}_{MK} \approx 0.85$  for IN11 model.

It is seen that the same variation pattern is in presence for  $E(j_{MK}|\hat{t}_{MK})p(\hat{t}_{MK})$  and  $p t_{MK}$  as shown in Figs. 3.11 and 3.13.

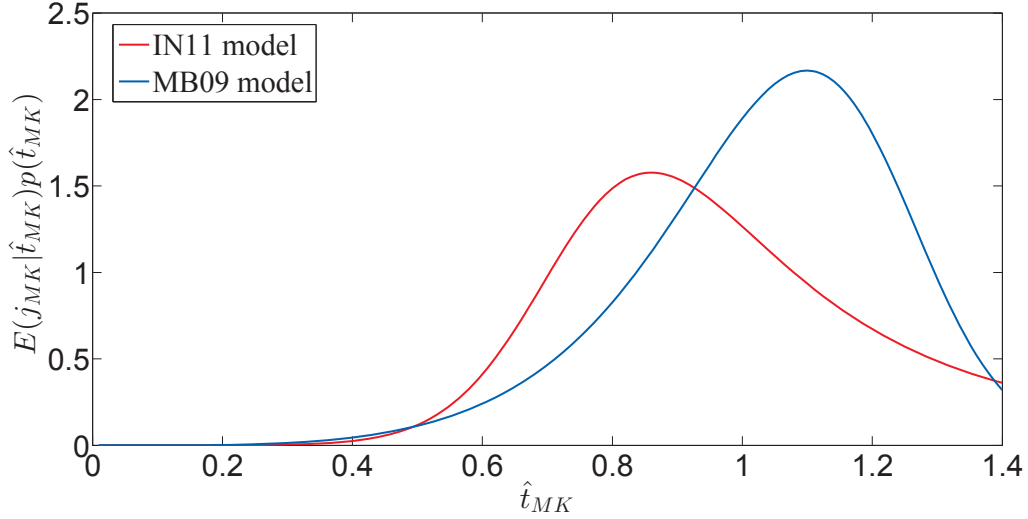


**Figure 3.12:**  $E(j_{MK}|\hat{t}_{MK})p(\hat{t}_{MK})$  versus  $\hat{t}_{MK}$

It should be noted that the blue curves in Figs. 3.10 and 3.11 are different from those given by Myrhaug et al. (2009). It raises the question of the implementation in Matlab by the author of this thesis. However, cdf of  $p(j_{MK}|\hat{t}_{MK})$  reaches unity as integrated over the valid range of  $\hat{t}_{MK}$  for MB09 model. Furthermore, the  $E(j_{MK}|\hat{t}_{MK})$  and  $\sigma(j_{MK}|\hat{t}_{MK})$  computed for MB09 model only have the maximum error to the order of magnitude  $10^{-8}$  (see Figs. B.2 and B.3 for details). Therefore, further discussion with the authors of Myrhaug et al. (2009) is required though some have been done.

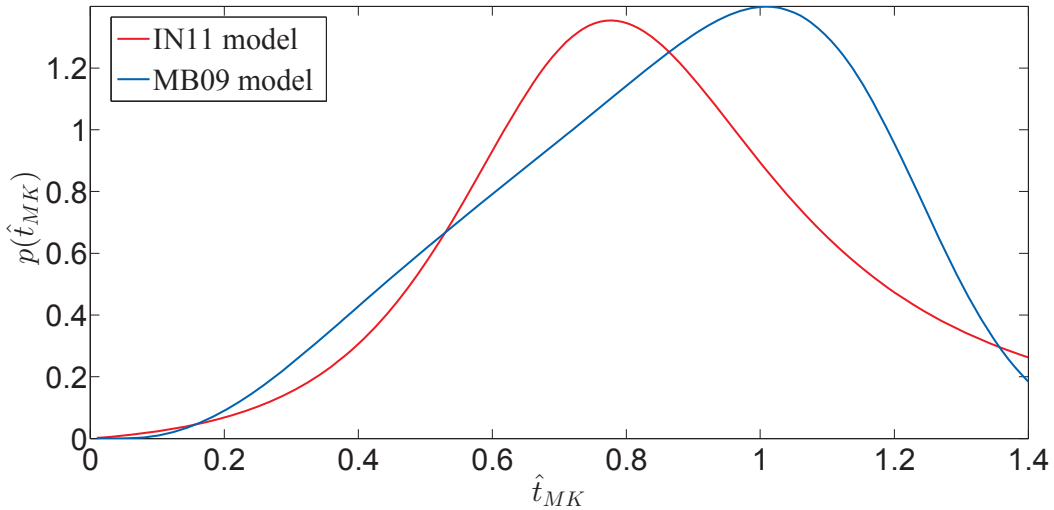


**Figure 3.13:** Marginal pdf  $p(\hat{t}_{MK})$  versus  $\hat{t}_{MK}$

# Chapter 4

## Conclusions and Recommendations

In this thesis, the statistics of surf parameter and wave power for individual waves are focused on. Comprehensive comparisons between theoretical model derived from [Longuet-Higgins \(1983\)](#) and parametric model presented by [Myrhaug and Fouques \(2012\)](#) for surf parameter are made by employing same normalized quantities as well as same scale of plot. Same approach is followed for the comparative study of the theoretic model and parametric model for wave power.

### 4.1 Conclusions

Based on the analysis made in Chapter 2 and Chapter 3, following conclusions are made:

1. Theoretical joint distribution of surf parameter and wave height is derived from theoretical probability model of wave height and wave period from [Longuet-Higgins \(1983\)](#), which is based on narrow banded approximation. The properties of the theoretical bivariate distribution of surf parameter and wave height are then investigated. It is found that the peak value of the derived model decreases exponentially while the its location follows a line. Even though theoretical expressions for peak value as well as its position are presented (Eqs. (2.12) - (2.17)), the simple formulae from best fit to the data generated by those theoretical expressions are suggested to apply for quick estimate.
2. Derived theoretical probability model of surf parameter and wave height is sensitive to the bandwidth parameter. Broad banded feature is found for the conditional distribu-

tion of surf parameter given low values of wave height.

3. Derived theoretical probability model of surf parameter and wave height gives same qualitative statistical behaviour for breaker index and breakers with parametric model given by [Myrhaug and Fouques \(2012\)](#). However, the marginal and conditional quantities of surf parameter obtained are not in good agreement between these two models, but show the same qualitative behaviour. Hence, theoretical model and parametric model are comparable in qualitative sense.
4. Marginal distributions of wave power from theoretical model and parametric model are in good agreement with each other.
5. Theoretical probability model of wave power and wave height given by [Izadparast and Niedzwecki \(2011\)](#) only compares well with parametric bivariate distribution of wave power and wave height presented by [Myrhaug et al. \(2009\)](#) for large wave height as opposed to the models of wave power and wave period in small wave period.

## 4.2 Recommendation for further work

1. As runup is related to the surf parameter, it is interesting to investigate the conditional distribution of runup for different breakers in further study. Since the empirical relation of runup and surf parameter used in this thesis is only valid for a small range of surf parameter, more advanced form of the relation covering larger range of surf parameter are suggested.
2. Estimates of distributions of wave power from theoretical model and parametric model may be compared with the results from simulated sea state by using the method given by [Izadparast and Niedzwecki \(2011\)](#) in Wave-by-wave analysis part. Expected wave power for the same state from theoretical model, parametric model as well as simulation may be compared with the result of following formula for estimating the mean deepwater wave power in one random sea state ([Falnes \(2002\)](#))

$$J = \frac{\rho g^2}{4\pi} T_{-1} m_0^f; \quad T_{-1} = \frac{m_{-1}^f}{m_0^f} \quad (4.1)$$

where  $T_{-1}$  is energy period,  $m_0^f$  and  $m_{-1}^f$  are moments of wave spectrum. The definitions of wave spectrum and its moment can be found in Chapter 2.  $J$  is dimensional wave power defined in section 3.1.

3. Estimate of averaged wave power in long term in the field of interest is an important parameter for the selection of specific WECs for that area. The value of it may be computed by taking summation of products of mean wave power of each possible sea state and the probability of the sea state in long term. [Izadparast and Niedzwecki \(2011\)](#) utilized the same approach by using a simplified formula based on narrow band approximation, which takes the form

$$p(j_{IN}) = \exp(-j_{IN}) \tag{4.2}$$

where  $j_{IN}$  is dimensionless wave power defined in section 3.2.

The approximation may be inappropriate for evaluation of wave power in long-term sense, since sea states in long term, e.g. seasonally or yearly, are not always narrow banded. Hence, it is necessary to employ the theoretical marginal distribution of wave power without narrow banded assumption, which is obtained by numerical integration with respect to wave height or wave period from theoretical model for wave power, for calculating the long-term averaged wave power.



# Bibliography

- Abramowitz, M. (1954). On the practical evaluation of integrals. *Journal of the Society for Industrial & Applied Mathematics*, 2(1):20–35.
- Baldock, T., Cox, D., Maddux, T., Killian, J., and Faylor, L. (2009). Kinematics of breaking tsunami wavefronts: A data set from large scale laboratory experiments. *Coastal Engineering*, 56(5):506–516.
- Battjes, J. (1974). Surf similarity. *Coastal Engineering Proceedings*, 1(14).
- Carrier, G. and Greenspan, H. (1958). Water waves of finite amplitude on a sloping beach.
- Carroll, J. Numerical differentiation and integration. [http://www.personal.psu.edu/jjb23/web/html/sl455SP12/ch4/CH04\\_5AS.pdf](http://www.personal.psu.edu/jjb23/web/html/sl455SP12/ch4/CH04_5AS.pdf). Retrieved on 28th April 2014.
- Clément, A., McCullen, P., Falcão, A., Fiorentino, A., Gardner, F., Hammarlund, K., Lemonis, G., Lewis, T., Nielsen, K., Petroncini, S., et al. (2002). Wave energy in europe: current status and perspectives. *Renewable and sustainable energy reviews*, 6(5):405–431.
- Cruz, J. (2008). Ocean wave energy. *UK: Springer Series in Green Energy and Technology*.
- Davis, P. J. and Rabinowitz, P. (1984). *Methods of numerical integration*. ACADEMIC PRESS, INC.
- Falcão, A. F. d. O. (2010). Wave energy utilization: A review of the technologies. *Renewable and sustainable energy reviews*, 14(3):899–918.
- Falnes, J. (2002). *Ocean waves and oscillating systems*. Cambridge University Press.
- Falnes, J. (2007). A review of wave-energy extraction. *Marine Structures*, 20(4):185–201.
- Gunn, K. and Stock-Williams, C. (2012). Quantifying the global wave power resource. *Renewable Energy*, 44:296–304.



- Hunt, I.A. (1959). Design of seawalls and breakwaters. *Proceedings of the American Society of Civil Engineers* 85, pages 123 – 152.
- Iribarren Cavanilles, R. and Nogales, C. (1949). Protection des ports. *XVIUfc Int. Congr. Navig. Lisbon*, pages 31–80.
- Izadparast, A. H. and Niedzwecki, J. M. (2011). Estimating the potential of ocean wave power resources. *Ocean Engineering*, 38(1):177–185.
- Kaminsky, G. and Kraus, N. (1994). Evaluation of depth-limited wave breaking criteria. pages 180–1933. American Society of Civil Engineers.
- Lenée-Bluhm, P., Paasch, R., and Özkan-Haller, H. (2011). Characterizing the wave energy resource of the us pacific northwest. *Renewable Energy*, 36(8):2106–2119.
- Longuet-Higgins, M. S. (1983). On the joint distribution of wave periods and amplitudes in a random wave field. *Proceedings of the Royal Society of London. A. Mathematical and Physical Sciences*, 389(1797):241–258.
- Meyer, R. E. (1971). *Waves on beaches and resulting sediment transport: proceedings of an advanced seminar conducted by the Mathematics Research Center, the University of Wisconsin, and the Coastal Engineering Research Center, US Army, at Madison October 11-13, 1971*. Number 28. Academic Press.
- Mørk, G., Barstow, S., Kabuth, A., and Pontes, M. T. (2010). Assessing the global wave energy potential. In *ASME 2010 29th International Conference on Ocean, Offshore and Arctic Engineering*, pages 447–454. American Society of Mechanical Engineers.
- Myrhaug, D. (2006). *TMR4230 Oceanography - Wind and Waves*. Norwegian University of Science and Technology.
- Myrhaug, D. and Fouques, S. (2007). Discussion of “distributions of wave steepness and surf parameter” by M. Aziz Tayfun. *Journal of waterway, port, coastal, and ocean engineering*, 133(3):242–243.
- Myrhaug, D. and Fouques, S. (2010). A joint distribution of significant wave height and characteristic surf parameter. *Coastal Engineering*, 57(10):948–952.
- Myrhaug, D. and Fouques, S. (2012). Joint distributions of wave height with surf parameter and breaker index for individual waves. *Coastal Engineering*, 60:235–247.

- Myrhaug, D. and Kjeldsen, S. P. (1984). Parametric modelling of joint probability density distributions for steepness and asymmetry in deep water waves. *Applied Ocean Research*, 6(4):207–220.
- Myrhaug, D. and Kvålsvold, J. (1995). Comparative study of joint distributions of primary wave characteristics. *Journal of Offshore Mechanics and Arctic Engineering*, 117(2):91–98.
- Myrhaug, D., Leira, B. J., and Holm, H. (2009). Wave power statistics for individual waves. *Applied Ocean Research*, 31(4):246–250.
- Myrhaug, D., Leira, B. J., and Holm, H. (2011). Wave power statistics for sea states. *Journal of Offshore Mechanics and Arctic Engineering*, 133(4):044501.
- Nielsen, P. (2009). *Coastal and estuarine processes*. World Scientific.
- Saulnier, J.-B., Clement, A., Falcão, A. F. d. O., Pontes, T., Prevosto, M., and Ricci, P. (2011). Wave groupiness and spectral bandwidth as relevant parameters for the performance assessment of wave energy converters. *Ocean Engineering*, 38(1):130–147.
- Smith, G., Venugopal, V., and Wolfram, J. (2006). Wave period group statistics for real sea waves and wave energy extraction. *Proceedings of the Institution of Mechanical Engineers, Part M: Journal of Engineering for the Maritime Environment*, 220(3):99–115.
- Sorensen, R. M. (1993). *Basic wave mechanics: for coastal and ocean engineers*. John Wiley & Sons.
- Tayfun, M. A. (2006). Distributions of wave steepness and surf parameter. *Journal of waterway, port, coastal, and ocean engineering*, 132(1):1–9.
- Vicinanza, D., Contestabile, P., and Ferrante, V. (2013). Wave energy potential in the north-west of sardinia (italy). *Renewable Energy*, 50:506–521.



# Appendix A

## Derivation and numerical stability study of the theoretical

### A.1 Erratum in Longuet - Higgins 83 Model

Author found that the Eq. (2.17) presented in [Longuet-Higgins \(1983\)](#) results in probability exceeding unity as Eq. (2.16) is integrated with integral limit from 0 to  $\infty$  for the normalized wave amplitude and wave period. Eq. (2.17) should take the form as:

$$\frac{1}{L(v)} = \frac{2}{v\sqrt{\pi}} \int_0^\infty \int_0^\infty \frac{R_a^2}{t^2} \exp \left[ -R_a^2 \left( 1 + (1 - 1/t)^2 / v^2 \right) \right] dR_a dt \quad (\text{A.1})$$

However, Eqs. A2 ([Longuet-Higgins \(1983\)](#)), Eq. (2.18) in [Longuet-Higgins \(1983\)](#) remain the same. This is verified by manual derivation, Maple and numerical integration in Matlab.

## A.2 Maximum value of theoretical joint distribution of surf parameter and wave height

Extreme points of Eq. (2.10) are found by taking partial differentiations with respect to  $\hat{\xi}$  and  $\hat{h}$ , respectively. After simplification, followings are obtained

$$\begin{aligned} \frac{3}{2}\hat{h}^{1/2}\hat{\xi}^2 - 2\hat{h}^{5/2}\hat{\xi}^2 - \frac{1}{v^2}\left(2\hat{h}^{5/2}\hat{\xi}^2 - 3\hat{h}^2\hat{\xi} + \hat{h}^{3/2}\right) &= 0 \\ \hat{h}^{3/2}\hat{\xi}^2 + \frac{1}{v^2}\left(\hat{h}^3\hat{\xi} - \hat{h}^{5/2}\right) &= 0 \end{aligned} \quad (\text{A.2})$$

Solving Eq. (A.2) by Maple and utilizing the same arguments for obtaining Eqs. (2.12) - (2.13) give the extreme points as follows

$$\begin{aligned} \hat{h}_{max} &= \frac{\sqrt{2}}{4}G(v) \\ \hat{\xi}_{max} &= 2^{3/4}\frac{Q(v)^{1/2}}{W(v)G(v)^{1/2}} \end{aligned} \quad (\text{A.3})$$

which are actually the same as Eqs. (2.12) - (2.13) given by Matlab.

It should be noted an extra solution of Eq. (A.2) is ( $\hat{h} = 0, \hat{\xi} = \hat{\xi}$ ) if one of the criteria for finding maximum value  $p(\hat{\xi}, \hat{h}) > 0$  is loosed to include  $p(\hat{\xi}, \hat{h}) = 0$ , which is the minimum value of pdf in general.

Substituting Eqs. (2.12) - (2.13) into Eq. (2.10), expression of corresponding peak value calculated by Matlab after simplifications is

$$p_{max} = \frac{144115188075855872}{3991211251234741} \frac{\sqrt[4]{2}\sqrt{\mu^2+1}\mu^3 \exp\left(\frac{5\mu^2(-8\mu^2+\sqrt{16\mu^2+25}-5)}{(\sqrt{16\mu^2+25}-5)^2(\sqrt{16\mu^2+25+2\mu^2+5})}\right)}{(1+\sqrt{\mu^2+1})(\sqrt{16\mu^2+25}-5)^2\left(\frac{\sqrt{16\mu^2+25+2\mu^2+5}}{\mu^2+1}\right)^{3/4}} \quad (\text{A.4})$$

which is the same as Eq. 2.15 computed by Maple. Numerical investigation carried out also delivers the coincident results if numeric values of  $v$  are used.

Fig. A.1a shows that  $p(\hat{\xi}, \hat{h})$  from derived LH83 model given by Eq. (A.3) seems to possess singularity while Fig. A.1b illustrates that minimum peak value is located around  $v = 0.97$  (see also section 2.1).

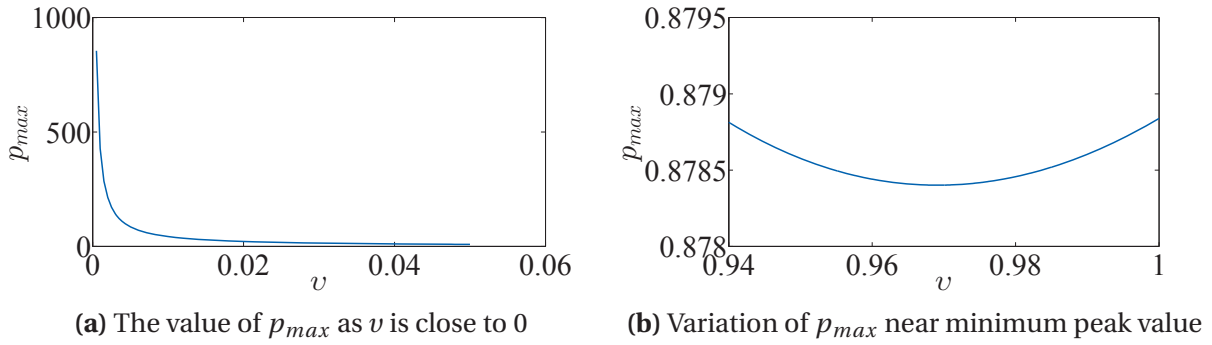


**Figure A.1:** Variation of  $p_{max}$  as  $\nu$  is close to 0 and 1, respectively

### A.3 Connection between different normalized procedure

Two approaches of deriving Eq. (2.35) are presented herein, that is, from definitions of two normalized quantities of  $S$  given in section 2.1 and section 2.3 respectively and from connections of different normalized quantities established in Myrhaug and Kvålsvold (1995).

$$\hat{S} \frac{H_{cr}}{g T_{cr}^2 / (2\pi)} = \hat{S}_{MK} \frac{0.7 H_s}{g T_z^2 / (2\pi)} \quad (\text{A.5})$$

where  $T_{cr}$ ,  $H_{cr}$ ,  $T_z$  are given in Eq. (2.1), (2.2) and (2.29), respectively. Substitute the expressions of  $T_{cr}$ ,  $H_{cr}$ ,  $T_z$  and  $H_s = 4\sqrt{m_0^f}$  into Eq. (A.5), we obtain

$$\hat{S} \frac{2\sqrt{2m_0^\omega}}{(g/(2\pi)) (2\pi m_0^\omega / m_1^\omega)^2} = \hat{S}_{MK} \frac{2.8\sqrt{m_0^f}}{g m_0^f / (2\pi m_2^f)} \quad (\text{A.6})$$

Combine Eq. (A.6) with Eq. (2.33), Eq. (A.6) can be rearranged into

$$\hat{S} = \hat{S}_{MK} \frac{5.6\pi}{4\pi\sqrt{2}} \frac{m_0^f m_2^f}{(m_1^f)^2} \quad (\text{A.7})$$

Further, Eq. (A.7) can be simplified by using Eq. (2.9), and take the form

$$\hat{S} = \hat{S}_{MK} \frac{\gamma_s(1+\nu^2)}{4\pi\sqrt{2}} \quad (\text{A.8})$$

where  $\gamma_s = 5.6\pi = 17.6$ .

Based on definitions of  $\hat{\xi}$  and  $\hat{S}$  given in section 2.1, following is obtained

$$\hat{S} = \frac{1}{\hat{\xi}^2} \quad (\text{A.9})$$

Substitute Eq. (2.6) into Eq. (A.9), relation between  $\hat{S}$  and  $\hat{h}$ ,  $t$  is given by

$$\hat{S} = \frac{\hat{h}}{t^2} \quad (\text{A.10})$$

However, the connection between  $\hat{S}_{MK}$  and  $\hat{h}_{MK}$ ,  $\hat{t}_{MK}$  not necessarily follows the same form. Corresponding derivation will be given in the forthcoming. Eq. (16) in Myrhaug and Kvålsvold (1995) gives

$$t = \left[ \frac{2\pi\gamma_H}{\gamma_S(1+v^2)} \right]^{1/2} \left( \frac{\hat{h}_{MK}}{\hat{S}_{MK}} \right)^{1/2} \quad (\text{A.11})$$

Combine Eq. (A.10) with Eqs. (A.11) and (2.34), Eq. (A.8) is obtained.

As  $\xi = m/\sqrt{S}$ , the connection between  $\hat{\xi}$  and  $\hat{\xi}_{MK}$  is established as shown in Eq. (2.35).

According to the definition of  $\hat{S}_{MK}$  given in section 2.2, it can be expressed as

$$\hat{S}_{MK} = \frac{0.714}{0.7} \frac{HT_z^2}{H_{rms}T^2} \quad (\text{A.12})$$

Hence,

$$\hat{S}_{MK} = \frac{0.714 \hat{h}_{MK}}{0.7\gamma_T^2 \hat{t}_{MK}^2} \quad (\text{A.13})$$

$\hat{\xi}_{MK}$  is connected with  $\hat{S}_{MK}$  in the same form as given in Eq. (A.9). After incorporating the relation with Eq. (A.13), following is obtained

$$\hat{\xi}_{MK} = \left( \frac{0.7\gamma_T^2}{0.714} \right)^{1/2} \frac{\hat{t}_{MK}}{\sqrt{\hat{h}_{MK}}} \quad (\text{A.14})$$

Hereafter,  $(0.7\gamma_T^2/0.714))^{1/2}$  is denoted as  $\gamma_\xi$ . Combine Eq. (A.13) with Eq. (3.11), following is obtained

$$t = \left( \frac{0.714}{0.7(1+v^2)} \right)^{1/2} \left( \frac{\hat{h}_{MK}}{\hat{S}_{MK}} \right)^{1/2} \quad (\text{A.15})$$

Eq. (A.11) and Eq. (A.15) are the same with  $2\pi\gamma_H/\gamma_S = 0.714/0.7$ .

## A.4 Another approach to derive theoretical models for different quantities of interest

### A.4.1 Normalized quantities

With utilization of Eqs. (2.34) and (3.11), LH83 model is transformed with Jacobian  $\left| \frac{\partial \hat{h}}{\partial \hat{h}_{MK}} \cdot \frac{\partial \hat{t}}{\partial \hat{t}_{MK}} \right| = AB$  to have arguments, normalized wave height and wave period as given in Myrhaug and Kjeldsen (1984).

$$p(\hat{h}_{MK}, \hat{t}_{MK}) = \frac{2A^3}{B\sqrt{\pi}v} \left( \frac{\hat{h}_{MK}}{\hat{t}_{MK}} \right)^2 \exp \left[ -(A\hat{h}_{MK})^2 \left( 1 + \left( 1 - \frac{1}{B\hat{t}_{MK}} \right)^2 / v^2 \right) \right] L(v) \quad (\text{A.16})$$

Combining with Eq. (A.14), Eq. (A.16) is transformed into joint distribution of  $(\hat{\xi}_{MK}, \hat{h}_{MK})$  with Jacobian  $\sqrt{\hat{h}_{MK}}/\gamma_\xi$

$$p(\hat{\xi}_{MK}, \hat{h}_{MK}) = \frac{2A^3\gamma_\xi}{B\sqrt{\pi}v} \frac{\hat{h}_{MK}^{3/2}}{\hat{\xi}_{MK}^2} \exp \left[ -(A\hat{h}_{MK})^2 \left( 1 + \left( 1 - \frac{\gamma_\xi}{B\hat{\xi}_{MK}\sqrt{\hat{h}_{MK}}} \right)^2 / v^2 \right) \right] L(v) \quad (\text{A.17})$$

Comparing with Eq. (2.36), it is found that

$$\frac{\gamma_\xi}{B} = \frac{1}{C_m\sqrt{A}} = \sqrt{0.98(1+v^2)} \quad (\text{A.18})$$

$$\frac{A^3\gamma_\xi}{B} = \frac{A^{5/2}}{C_m} = 1.021\sqrt{1+v^2} \quad (\text{A.19})$$

Similar to the definition of  $\hat{h}_{bMK}$ ,  $\hat{h}_b = \hat{\xi}^{k_2}$ . Making a change of variables for Eq. (2.10) from variables  $(\hat{\xi}, \hat{h})$  to  $(\hat{h}_b, \hat{h})$  by using Jacobian  $\left| \frac{\partial \hat{\xi}}{\partial \hat{h}_b} \right| = \hat{h}_b^{1/k_2-1}/k_2$ , joint pdf  $p(\hat{h}_b, \hat{h})$  hence is



given by

$$p(\hat{h}_b, \hat{h}) = \frac{2L(v)}{k_2 \sqrt{\pi} v} \frac{\hat{h}^{1.5}}{\hat{h}_b^{\frac{k_2+1}{k_2}}} \exp \left( -\hat{h}^2 \left[ 1 + \left( 1 - \frac{1}{\hat{h}_b^{1/k_2} \sqrt{\hat{h}}} \right)^2 / v^2 \right] \right) \quad (\text{A.20})$$

By change of variable from Eq. (A.20) using Jacobian  $A C_m^{k_2}$ , the joint distribution of  $(\hat{h}_{bMK}, \hat{h}_{MK})$  is obtained.

#### A.4.2 Dimensional quantities

Performing transformation of Eq. (2.10) from variables  $(\hat{\xi}, \hat{h})$  into  $(\xi, H)$  in the use of Jacobian  $(\xi_{cr} H_{cr})^{-1}$ ,  $p(\xi, H)$  is given by

$$p(\xi, H) = \frac{2\xi_{cr}}{H_{cr}^{5/2} \sqrt{\pi} v} \frac{H^{3/2}}{\xi^2} \exp \left[ -(H/H_{cr})^2 \left( 1 + \left( 1 - \frac{\xi_{cr} \sqrt{H_{cr}}}{\xi \sqrt{H}} \right)^2 / v^2 \right) \right] L(v) \quad (\text{A.21})$$

Further, combining with Eq. (2.46),  $p(R, H)$  is derived from Eq. (A.21) through a change of variables from  $(\xi, H)$  into  $(R, H)$  by utilization of Jacobian  $\left| \frac{\partial \xi}{\partial R} \cdot \frac{\partial H}{\partial H} \right| = \frac{1}{KH}$ , and takes the form

$$p(R, H) = \frac{2K\xi_{cr}}{\sqrt{\pi} v H_{cr}^{2.5}} \frac{H^{2.5}}{R^2} \exp \left[ -(H/H_{cr})^2 \left( 1 + \left( 1 - \frac{K\xi_{cr} (H_{cr} H)^{0.5}}{R} \right)^2 / v^2 \right) \right] L(v) \quad (\text{A.22})$$

Joint pdf of  $(R, \xi)$  can be derived from by combining Eqs. (2.25), (2.26) and (2.46) with Eq. (2.36) through change of variables, and Jacobian calculated is  $\left| \frac{\partial \xi_{MK}}{\partial \xi} \frac{\partial \hat{H}_{MK}}{\partial H} \right| = (K\xi H_{rms} \xi_{rms})^{-1}$ . Hence, Eq. (2.53) is obtained.

## A.5 Numerical Stability Study for surf parameter and runup

### A.5.1 surf parameter

$$E(\hat{\xi}_{MK} | \hat{h}_{MK}) = \int_0^\infty p(\hat{\xi}_{MK} | \hat{h}_{MK}) \hat{\xi}_{MK} d\hat{\xi}_{MK} \quad (\text{A.23})$$

**Table A.1:** Numerical integration by matlab trap built-in function and Simpson method

$\hat{h}_{MK} = 0.01$ $\hat{\xi}_{MK}$	Trapsoidal Method		Simpson Method	
	$E(\hat{\xi}_{MK} \hat{h}_{MK})$	$\sigma(\hat{\xi}_{MK} \hat{h}_{MK})$	$E(\hat{\xi}_{MK} \hat{h}_{MK})$	$\sigma(\hat{\xi}_{MK} \hat{h}_{MK})$
$5 \times 10^{-4} : 5 \times 10^{-4} : 600.0005$	1.5667	10.8249	1.5667	10.8249
$5 \times 10^{-4} : 5 \times 10^{-4} : 700.0005$	1.5975	11.7059	1.5975	11.7059
$5 \times 10^{-4} : 5 \times 10^{-4} : 900.0005$	1.6476	13.2951	1.6476	13.2951
$5 \times 10^{-4} : 5 \times 10^{-4} : 1000.0005$	1.6686	14.0228	1.6686	14.0228
$5 \times 10^{-4} : 5 \times 10^{-4} : 1500.0005$	1.7495	17.2076	1.7495	17.2076
$2 \times 10^{-4} : 2 \times 10^{-4} : 1500.0002$	1.7495	17.2076	1.7495	17.2076

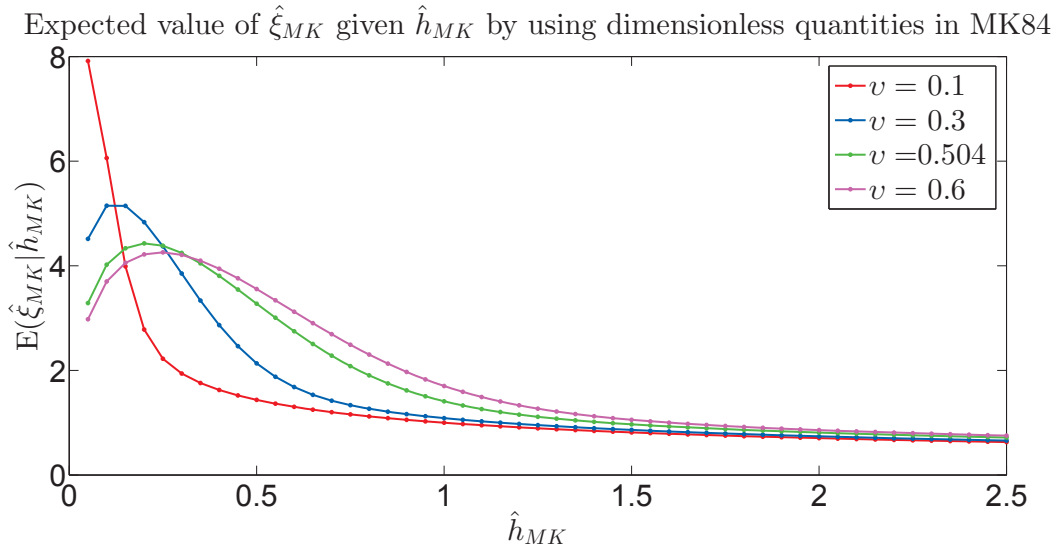


**Figure A.2:**  $E(\hat{\xi}_{MK}|\hat{h}_{MK})$  versus  $\hat{h}_{MK}$   
 $\hat{\xi}_{MK} = 0.0005 : 0.0005 : 400.0005$

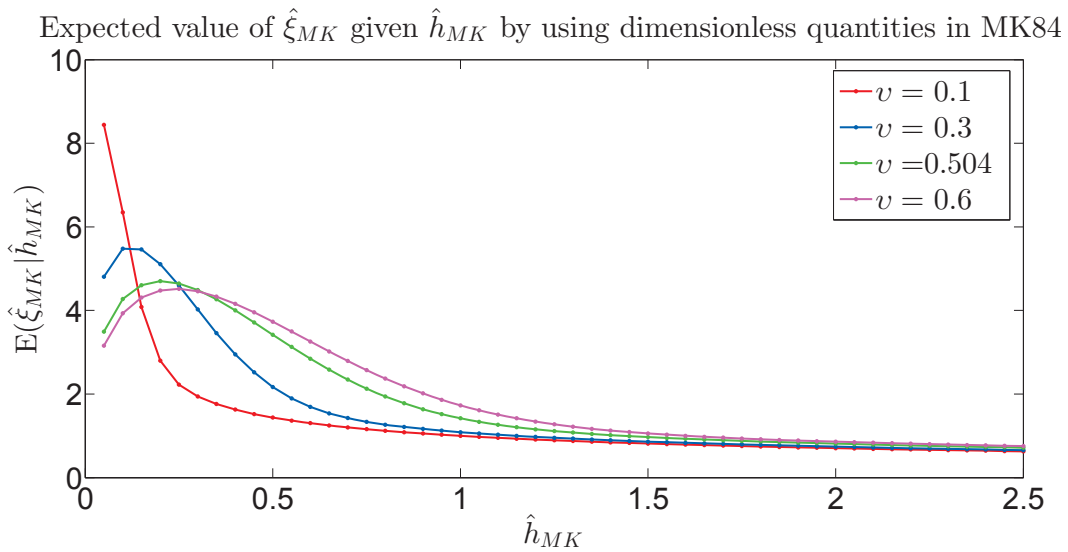


**Figure A.3:**  $E(\hat{\xi}_{MK}|\hat{h}_{MK})$  versus  $\hat{h}_{MK}$   
 $\hat{\xi}_{MK} = 0.0005 : 0.0005 : 600.0005$

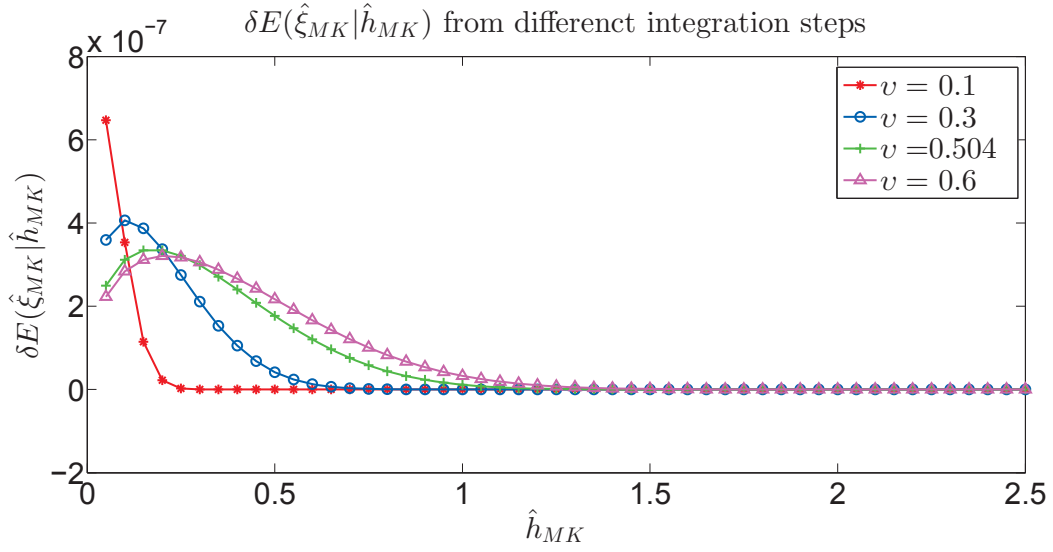


**Figure A.4:**  $\delta E(\hat{\xi}_{MK} | \hat{h}_{MK})$  versus  $\hat{h}_{MK}$   
 $\hat{\xi}_{MK} = 0.0005 : 0.0005 : 600.0005$  and  $\hat{\xi}_{MK} = 0.0002 : 0.0002 : 600.0002$ , respectively

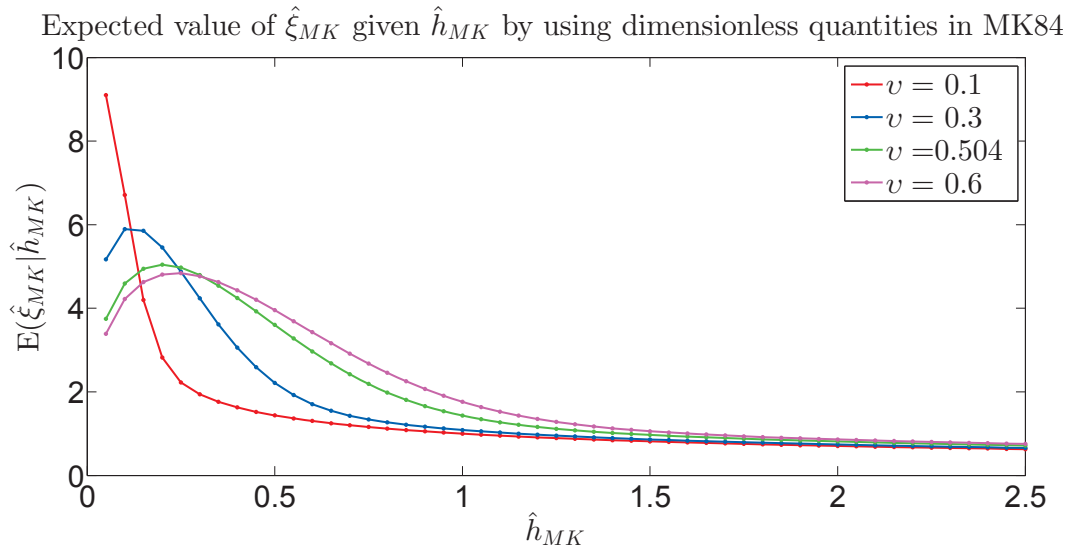


**Figure A.5:**  $E(\hat{\xi}_{MK} | \hat{h}_{MK})$  versus  $\hat{h}_{MK}$   
 $\hat{\xi}_{MK} = 0.0005 : 0.0005 : 1000.0005$

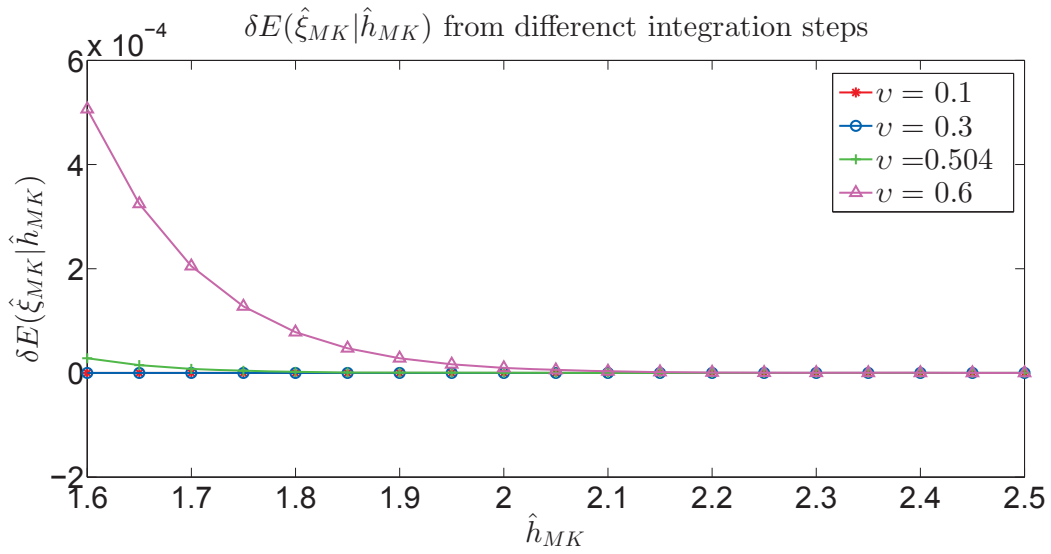


**Figure A.6:**  $\delta E(\hat{\xi}_{MK}|\hat{h}_{MK})$  versus  $\hat{h}_{MK}$   
 $\hat{\xi}_{MK} = 0.0005 : 0.0005 : 600.0005$  and  $\hat{\xi}_{MK} = 0.0005 : 0.0005 : 1000.0005$ , respectively

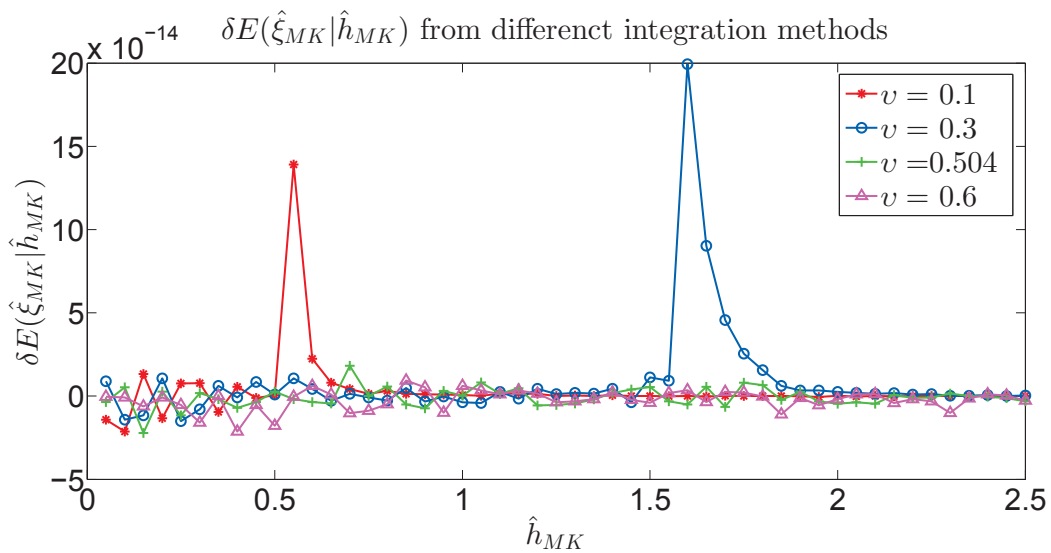


**Figure A.7:**  $\delta E(\hat{\xi}_{MK}|\hat{h}_{MK})$  caused by using Simpson and Romberg integration method, respectively

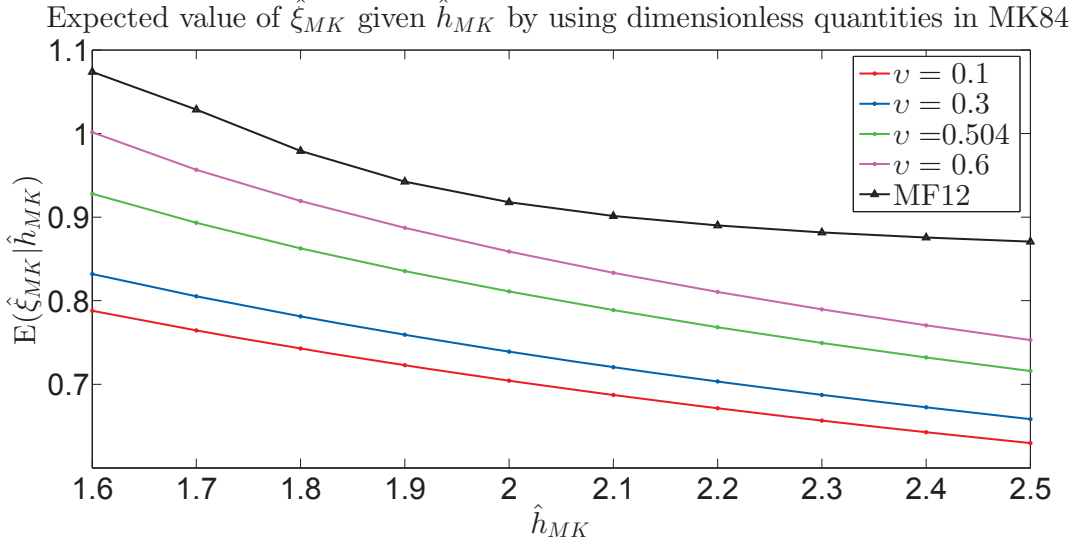


**Figure A.8:** Comparison of  $E(\hat{\xi}_{MK}|\hat{h}_{MK})$  between derived LH83 model and MF12 model  $\hat{\xi}_{MK} = 0.0005 : 0.0005 : 1000.0005$

From Figs. A.2, A.3 and A.5, it is observed that  $E(\hat{\xi}_{MK}|\hat{h}_{MK})$  increases significantly with integration upper limit of  $\hat{\xi}_{MK}$  for small  $\hat{h}_{MK}$ , which reflects the broadening characteristics of joint distribution of  $(\hat{\xi}_{MK}, \hat{h}_{MK})$  at low values of  $\hat{h}_{MK}$ . Eq.(A.23) verifies that the results of integral increase with upper integration limit due to non-negative integrand and integration variable in this case. Fig. A.4 demonstrates that integration with  $\delta\hat{\xi}_{MK}$  is sufficient. It is seen from Fig. A.6 that results converge as  $\hat{\xi}_{MK}$  larger than 1.6. Fig. A.7 shows extremely small difference induced by different numerical integration methods. To summarize, it seems that numerical integration method utilized is not so critical in contrast with variation of upper integration limit and integration step. Numerical integration results of  $E(\hat{\xi}_{MK}|\hat{h}_{MK})$  are credible with  $\hat{h}_{MK}$  being in excess of 1.6.

In the similar manner, numerically calculated standard deviation of  $\hat{\xi}_{MK}$  given  $\hat{h}_{MK}$  grows with numerical upper integral limit (shown by Figs. A.9, A.10 and A.12). It means that conditional  $p(\hat{\xi}_{MK}|\hat{h}_{MK})$  has much lower peak values in smaller wave height than the larger wave height. Therefore, to obtain converged numerically calculated  $\sigma(\hat{\xi}_{MK}|\hat{h}_{MK})$ , higher integration limit approaches infinity is required. As shown by Figs. A.11 and A.13, less evident disparity exists due to 0.0005 and 0.0002 integration step compared to different integration limit.

Comparing Fig. A.7 and Fig. A.14, it is found that Simpson and Romberg integration methods give same results for both  $E(\hat{\xi}_{MK}|\hat{h}_{MK})$  and  $\sigma(\hat{\xi}_{MK}|\hat{h}_{MK})$  to the 12th decimal. Eq. (A.24)

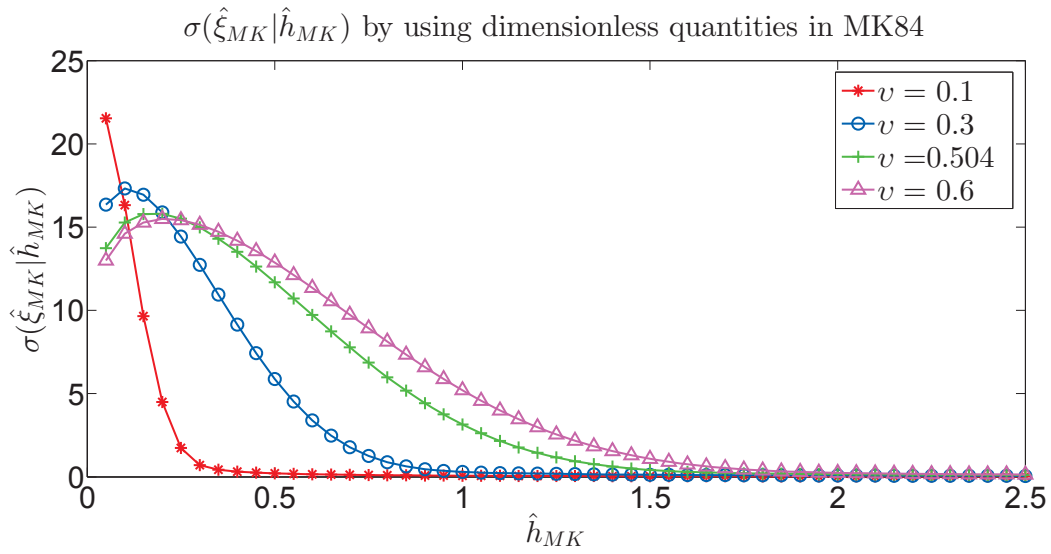


**Figure A.9:**  $\sigma(\hat{\xi}_{MK}|\hat{h}_{MK})$  versus  $\hat{h}_{MK}$   
 $\hat{\xi}_{MK} = 0.0005 : 0.0005 : 400.0005$

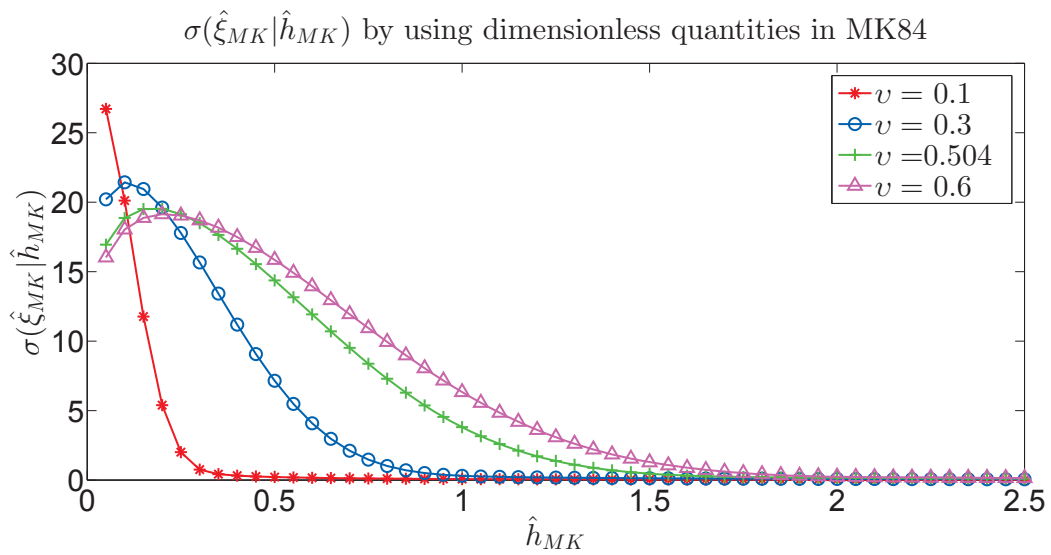


**Figure A.10:**  $\sigma(\hat{\xi}_{MK}|\hat{h}_{MK})$  versus  $\hat{h}_{MK}$   
 $\hat{\xi}_{MK} = 0.0005 : 0.0005 : 600.0005$

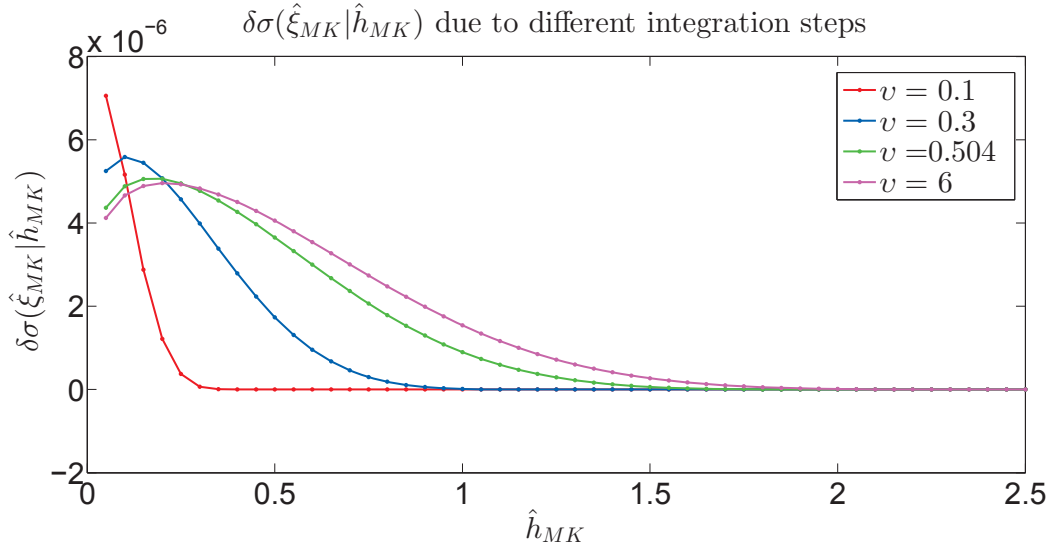


**Figure A.11:**  $\delta\sigma(\hat{\xi}_{MK}|\hat{h}_{MK})$  versus  $\hat{h}_{MK}$   
 $\hat{\xi}_{MK} = 0.0005 : 0.0005 : 600.0005$  and  $\hat{\xi}_{MK} = 0.0002 : 0.0002 : 600.0002$ , respectively

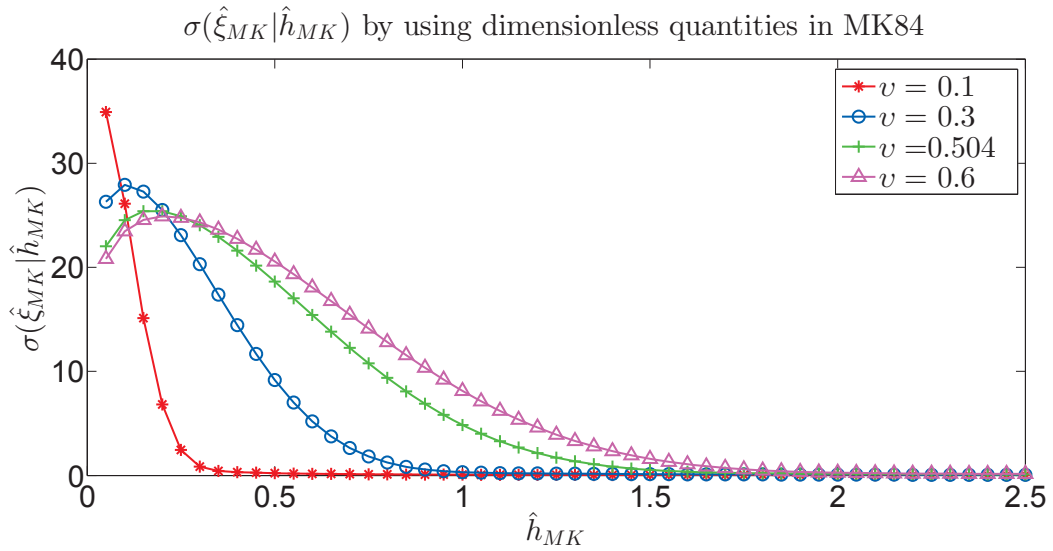


**Figure A.12:**  $E(\hat{\xi}_{MK}|\hat{h}_{MK})$  versus  $\hat{h}_{MK}$   
 $\hat{\xi}_{MK} = 0.0005 : 0.0005 : 1000.0005$

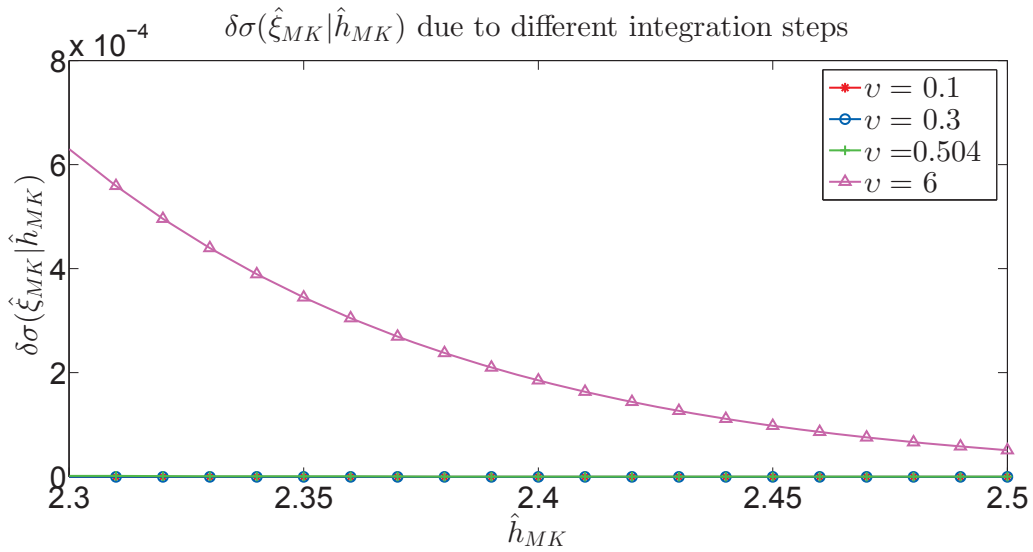


**Figure A.13:**  $\delta\sigma(\hat{\xi}_{MK}|\hat{h}_{MK})$  versus  $\hat{h}_{MK}$   
 $\hat{\xi}_{MK} = 0.0005 : 0.0005 : 600.0005$  and  $\hat{\xi}_{MK} = 0.0005 : 0.0005 : 1000.0005$ , respectively

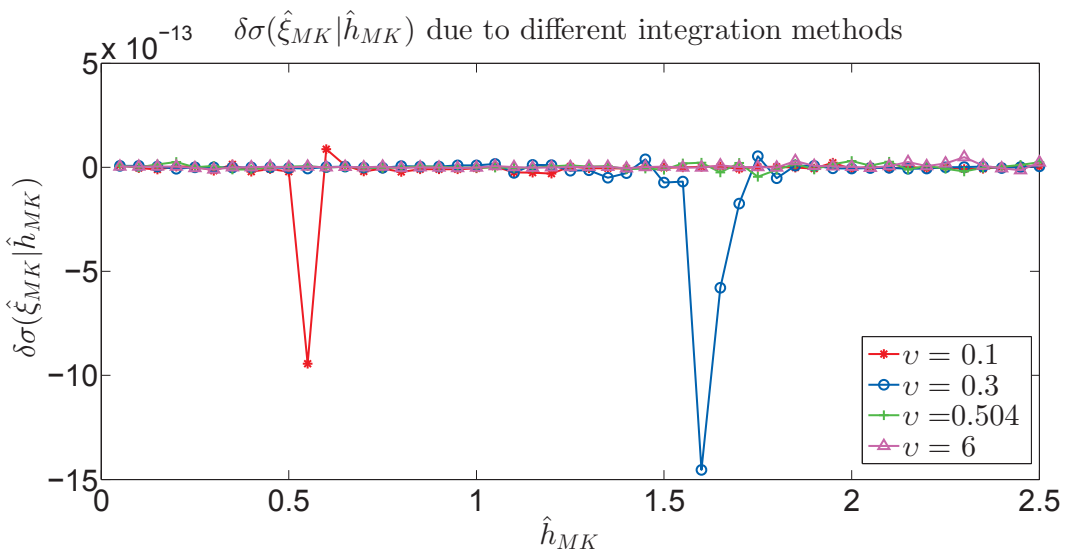


**Figure A.14:**  $\delta\sigma(\hat{\xi}_{MK}|\hat{h}_{MK})$  caused by using Simpson and Romberg integration method, respectively



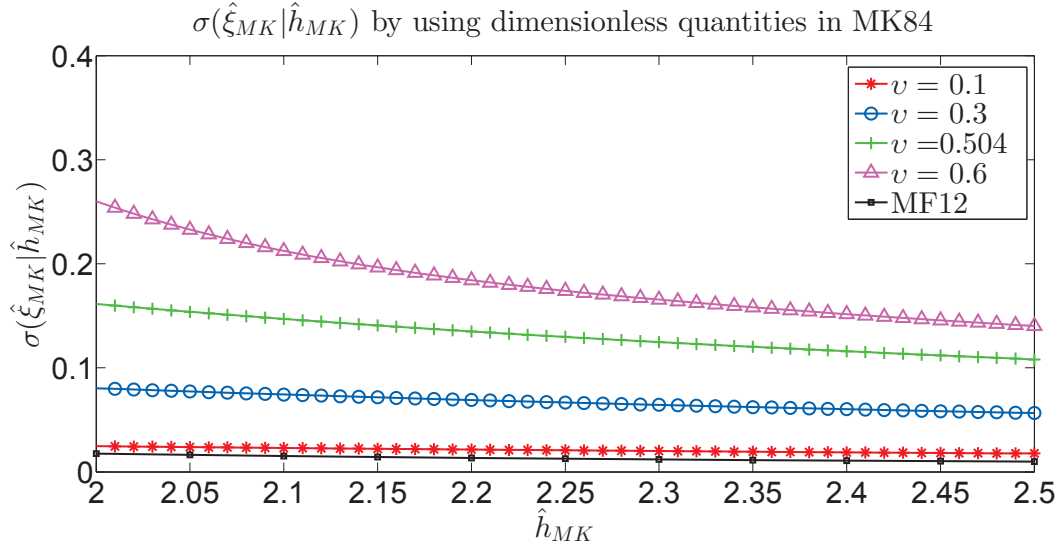


**Figure A.15:** Comparison of  $\sigma(\hat{\xi}_{MK}|\hat{h}_{MK})$  between derived LH83 model and MF12 model  
 $\hat{\xi}_{MK} = 0.0005 : 0.0005 : 1000.0005$

demonstrates that numerically calculated conditional standard deviation of surf parameter given wave height depends on the corresponding mean values of surf parameter given wave height. Consequently,  $\sigma(\hat{\xi}_{MK}|\hat{h}_{MK})$  begins to converge at higher wave height in comparison with corresponding to  $E(\hat{\xi}_{MK}|\hat{h}_{MK})$  if same converged criterion i.e.  $1 \times 10^{-3}$  applies.

$$\sigma(\hat{\xi}_{MK}|\hat{h}_{MK}) = \sqrt{E(\hat{\xi}_{MK}^2|\hat{h}_{MK}) - [E(\hat{\xi}_{MK}|\hat{h}_{MK})]^2} \quad (\text{A.24})$$

## A.5.2 Runup

Fig. A.16 shows that the conditional expected value of  $R$  is converged only for given wave height  $\hat{h}_{MK} = 1.4$  and  $\hat{h}_{MK} = 3.2$  in terms of integration steps utilized. However, it is noted that the calculated expected value for other four wave heights increase with upper integral limit for numerical integration. The variability of the expected conditional runup seems extremely limited by using derived LH83 model.

R = Rstart: (Rend - Rstart)/(2^(JJ-1)) :Rend;			hMK	E (R   hMK)
CDFSp_30.mat			0.25	2.59291156
RsExpRom_30.mat			0.5	3.555973502
RsExpsp_30.mat			1	3.145200512
Rstart = 0.0002			1.4	3.233341598
Rend = 300.0002			2.1	3.766480646
JJ=21				
Thesis_ConCDF_WaveRunUp_Fig17.m				
			hMK	E (R   hMK)
CDFSp_20.mat			0.25	2.444761409
RsExpRom_20.mat			0.5	3.39125659
RsExpsp_20.mat			1	3.122597587
Rstart = 0.0005			1.4	3.232462974
Rend = 200.0005			2.1	3.766480527
JJ=21				
Thesis_ConCDF_WaveRunUp_Fig17.m				
			hMK	E (R   hMK)
CDFSp_18.mat			0.25	2.406236183
RsExpRom_18.mat			0.5	3.348277543
RsExpsp_20.mat			1	3.116586055
Rstart = 0.0005			1.4	3.232222076
Rend = 180.0005			2.1	3.766480491
JJ=19				
Thesis_ConCDF_WaveRunUp_Fig17.m				
			hMK	E (R   hMK)
CDFSp.mat			0.25	2.191002222
RsExpRom.mat			0.5	3.106553152
RsExpsp.mat			1	3.081473297
Rstart = 0.0005			1.4	3.230726223
Rend = 100.0005			2.1	3.76648022
JJ=18				
Thesis_ConCDF_WaveRunUp_Fig17.m				

**Figure A.16:** Numerical stability study for calculation of  $E(R|\hat{h}_{MK})$  from derived LH83 model

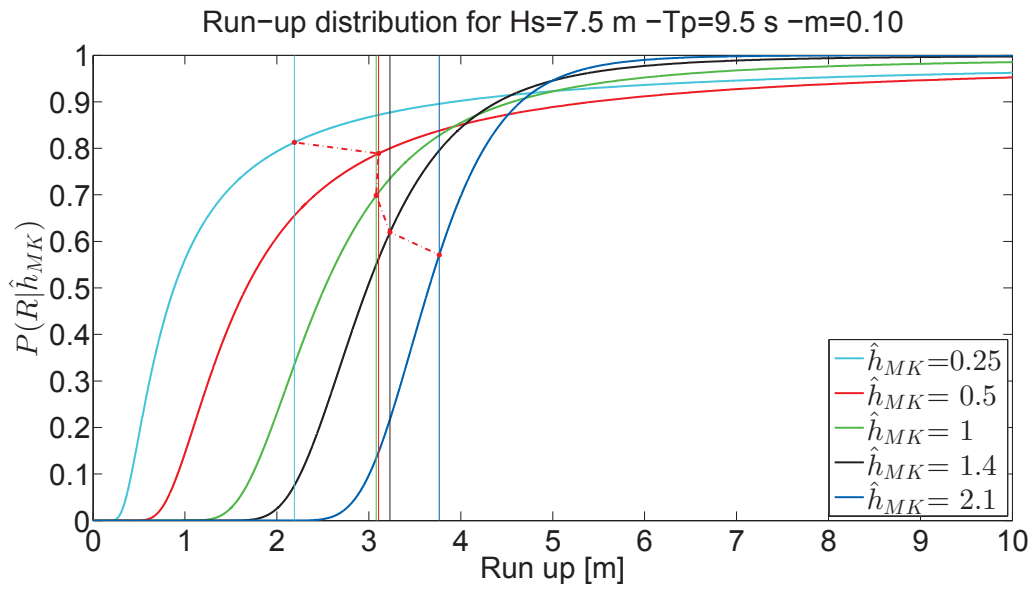


**Figure A.17:** Conditional cumulative distribution of wave run-up given wave height  $P(R|H)$  from derived LH83 model by integration step corresponding with  $R_{end} = 100.0005$  in Fig. A.16

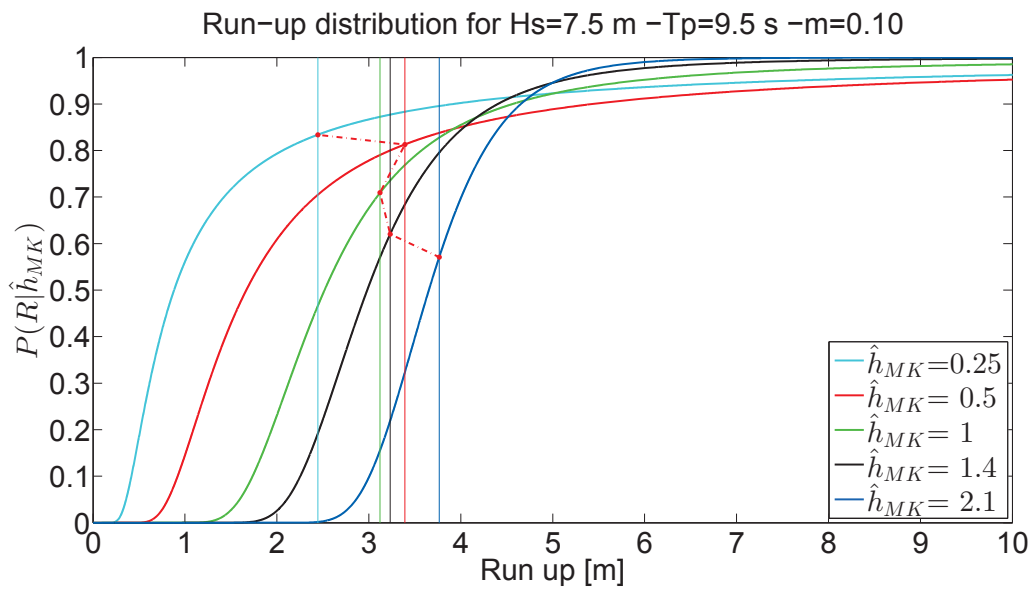


**Figure A.18:** Conditional cumulative distribution of wave run-up given wave height  $P(R|H)$  from derived LH83 model by integration step indicated with  $R_{end} = 200.0005$  in Fig. A.16

# Appendix B

## Derivation and numerical stability study of the theoretical

Appreciable efforts have been putted into to obtain convergent numerically calculated results. Trapezoidal method, Simpson method as well as Romberg method are adopted to compute integrals needed to be evaluated.

The peak value of two bivariate distributions  $p(\hat{h}_{MK}, j_{MK})$  and  $p(\hat{t}_{MK}, j_{MK})$  from IN11 model and MB09 model also investigated numerically. The mesh grids are generated according to the Tables. B.1 and B.4 and numerical peak values are presented there as well. As the grided domain is fined further, peak value of  $p(\hat{h}_{MK}, j_{MK})$  from both models calculated increases dramatically and their positions are closer to origin. Hence, singularity seems to exist.

### B.1 Numerical stability study for MB09 model

Utilizing  $t \geq \alpha$  given in Eq. (3.28) and Eq. (3.23), following connection between  $t_{MK}$  and  $j_{MK}$  is

$$\hat{t}_{MK} \geq [j_{MK}(0.12)^4]^{1/5} \quad (\text{B.1})$$

Note that  $\Delta$  given in Tables. B.1 and B.2 are used to generate  $j_{MK}$  (from  $j \geq \alpha \hat{h}_{MK}^2$  in Eq. (3.22)) and  $\hat{t}_{MK}$  (based on Eq. (B.1)) matrix in Matlab, respectively.

**Table B.1:** Numerical peak value of  $p(\hat{h}_{MK}, j_{MK})$  from MB09 model

$\hat{h}_{MK}$	$\Delta$	$\hat{h}_{MK}^{max}$	$j_{MK}^{max}$	Peak Value
$1 \times 10^{-3} : 1 \times 10^{-3} : 1.4$	$1 \times 10^{-3} : 1 \times 10^{-3} : 2$	0.0600	$1.1 \times 10^{-3}$	40.68
$5 \times 10^{-4} : 5 \times 10^{-4} : 1.4$	$5 \times 10^{-4} : 5 \times 10^{-4} : 2$	0.0435	$5.47 \times 10^{-4}$	51.64
$2 \times 10^{-4} : 2 \times 10^{-4} : 1.4$	$2 \times 10^{-4} : 2 \times 10^{-4} : 2$	0.0282	$2.16 \times 10^{-4}$	70.08
$5 \times 10^{-5} : 5 \times 10^{-5} : 1.4$	$5 \times 10^{-5} : 5 \times 10^{-5} : 2$	0.0144	$5.30 \times 10^{-5}$	109.60

**Table B.2:** Numerical peak value of  $p(\hat{t}_{MK}, j_{MK})$  from MB09 model

$j_{MK}$	$\Delta$	$j_{MK}^{max}$	$\hat{t}_{MK}^{max}$	Peak Value
$2 \times 10^{-4} : 2 \times 10^{-4} : 0.5$	$2 \times 10^{-4} : 2 \times 10^{-4} : 0.8$	$1.2 \times 10^{-3}$	0.236	4.8067
$1 \times 10^{-4} : 1 \times 10^{-4} : 0.5$	$1 \times 10^{-4} : 1 \times 10^{-4} : 0.8$	$1.1 \times 10^{-4}$	0.2334	4.8070
$5 \times 10^{-5} : 5 \times 10^{-5} : 0.5$	$5 \times 10^{-4} : 5 \times 10^{-5} : 0.8$	$1.2 \times 10^{-3}$	0.2347	4.8071
$1 \times 10^{-5} : 1 \times 10^{-5} : 0.002$	$1 \times 10^{-5} : 1 \times 10^{-5} : 0.4$	$1.1 \times 10^{-3}$	0.2342	4.8071
$5 \times 10^{-6} : 5 \times 10^{-6} : 0.0015$	$5 \times 10^{-6} : 5 \times 10^{-6} : 0.3$	$1.1 \times 10^{-3}$	0.2343	4.8071
$2 \times 10^{-6} : 2 \times 10^{-6} : 0.0015$	$2 \times 10^{-6} : 2 \times 10^{-6} : 0.3$	$1.1 \times 10^{-3}$	0.2343	4.8071
$2 \times 10^{-6} : 2 \times 10^{-6} : 0.0030$	$2 \times 10^{-6} : 2 \times 10^{-6} : 0.4$	$1.1 \times 10^{-3}$	0.2343	4.8071

Iso-density curves of  $p(\hat{t}_{MK}, j_{MK})$  from MB09 are plotted by Matlab and Maple and are identical with each other, shown as Figs. B.1a and B.1b. The possibility of distinct isocontour being attributed to different contour plotting algorithms is therefore excluded. In comparison with Fig. 7 in Myrhaug et al. (2009), region neighbouring to ordinate axis shows some discrepancies. Fig. B.1c illustrates that the isocontour is enclosed as opposed to this feature not being shown clearly in Figs. B.1a and B.1b.

## B.2 Numerical Stability Study for IN11 model

Recursive - Romberg method is more efficient compared to basic construction of Romberg method, since function evaluation does not have to repeat. Specifically, more than half of

**Table B.3:** Numerical peak value of  $p(\hat{h}_{MK}, j_{MK})$  from IN11 model

$\hat{h}_{MK}$	$j_{MK}$	$\hat{h}_{MK}^{max}$	$j_{MK}^{max}$	Peak Value
$2 \times 10^{-4} : 2 \times 10^{-4} : 1.5$	$2 \times 10^{-4} : 2 \times 10^{-4} : 1.5$	0.0460	$2 \times 10^{-4}$	109.72
$1 \times 10^{-4} : 2 \times 10^{-4} : 1.5$	$1 \times 10^{-4} : 1 \times 10^{-4} : 1.5$	0.0363	$1 \times 10^{-4}$	203.80
$5 \times 10^{-5} : 5 \times 10^{-5} : 0.75$	$5 \times 10^{-5} : 5 \times 10^{-5} : 0.75$	0.0287	$5 \times 10^{-5}$	316.05
$2 \times 10^{-5} : 2 \times 10^{-5} : 0.75$	$2 \times 10^{-5} : 2 \times 10^{-5} : 0.75$	0.0211	$2 \times 10^{-5}$	568.49
$1 \times 10^{-4} : 1 \times 10^{-4} : 0.1$	$1 \times 10^{-7} : 1 \times 10^{-7} : 1 \times 10^{-4}$	0.0036	$1 \times 10^{-7}$	$1.83 \times 10^4$

**Table B.4:** Numerical peak value of  $p(\hat{t}_{MK}, j_{MK})$  from IN11 model

$\hat{t}_{MK}$	$j_{MK}$	$j_{MK}^{max}$	$\hat{t}_{MK}^{max}$	Peak Value
$2 \times 10^{-4} : 2 \times 10^{-4} : 1.5$	$2 \times 10^{-4} : 2 \times 10^{-4} : 1.5$	$2 \times 10^{-4}$	0.0792	37.14
$1 \times 10^{-4} : 1 \times 10^{-4} : 0.5$	$1 \times 10^{-4} : 1 \times 10^{-4} : 0.5$	$1 \times 10^{-4}$	0.0634	56.49
$5 \times 10^{-5} : 5 \times 10^{-5} : 0.2$	$5 \times 10^{-5} : 5 \times 10^{-5} : 0.2$	$5 \times 10^{-5}$	0.0507	86.67
$2 \times 10^{-5} : 2 \times 10^{-5} : 1.5$	$2 \times 10^{-5} : 2 \times 10^{-5} : 1.5$	$2 \times 10^{-5}$	0.0376	154.20
$1 \times 10^{-5} : 1 \times 10^{-5} : 0.07$	$1 \times 10^{-5} : 1 \times 10^{-5} : 0.07$	$1 \times 10^{-5}$	0.0299	239.90
$1 \times 10^{-5} : 1 \times 10^{-5} : 0.5$	$1 \times 10^{-7} : 1 \times 10^{-7} : 1 \times 10^{-5}$	$1 \times 10^{-7}$	0.0065	$4.86 \times 10^3$

**Table B.5:** Integration steps for numerical stability study of  $\delta E(j_{MK}|\hat{t}_{MK})$  from MB09 model

Legend	value of mm	$j_{MK}^{max}$	integration steps
mm6	$6 \times 10^7$		
mm8	$8 \times 10^7$	$\frac{\hat{t}_{MK}^5}{(0.12)^4} \left(1 - \frac{1}{m}\right)$	$\frac{j_{MK}^{max}}{mm} : \frac{j_{MK}^{max}}{mm} : j_{MK}^{max}$
mm10	$1 \times 10^8$		

**Table B.6:** Numerical integration by matlab built-in function and trapezoidal method for IN11 model

$\hat{h}_{MK}$	$j_{MK}$	$E(j_{MK} \hat{h}_{MK})$	$\sigma(j_{MK} \hat{h}_{MK})$	$p(\hat{h}_{MK})$
0.5	$1 \times 10^{-4} : 2 \times 10^{-4} : 1000.0001$	0.6161	7.1037	0.6269
	$1 \times 10^{-4} : 1 \times 10^{-4} : 2000.0001$	0.6512	10.0537	0.6269
	$1 \times 10^{-4} : 1 \times 10^{-4} : 3000.0001$	0.6717	12.3167	0.6269
	$5 \times 10^{-5} : 5 \times 10^{-5} : 3000.00005$	0.6717	12.3168	0.6269
	$1 \times 10^{-4} : 1 \times 10^{-4} : 4000.0001$	0.6863	14.2243	0.6269

**Table B.7:** Numerical integration by matlab built-in function and Simpson method for IN11 model

$\hat{h}_{MK}$	$j_{MK}$	$E(j_{MK} \hat{h}_{MK})$	$\sigma(j_{MK} \hat{h}_{MK})$	$p(\hat{h}_{MK})$
0.5	$1 \times 10^{-4} : 2 \times 10^{-4} : 1000.0001$	0.6161	7.1037	0.6269
	$1 \times 10^{-4} : 1 \times 10^{-4} : 2000.0001$	0.6512	10.0537	0.6269
	$1 \times 10^{-4} : 1 \times 10^{-4} : 3000.0001$	0.6717	12.3167	0.6269
	$5 \times 10^{-5} : 5 \times 10^{-5} : 3000.00005$	0.6717	12.3168	0.6269
	$1 \times 10^{-4} : 1 \times 10^{-4} : 4000.0001$	0.6863	14.2243	0.6269

**Table B.8:** Numerical integration by matlab built-in function and Romberg method - basic construction for IN11 model

$\hat{h}_{MK}$	$j_{MK}$	$E(j_{MK} \hat{h}_{MK})$	$\sigma(j_{MK} \hat{h}_{MK})$	$p(\hat{h}_{MK})$
0.5	$1 \times 10^{-4} : 1 \times 10^{-4} : 838.8609$	0.6072	6.5045	0.6269
	$1 \times 10^{-4} : 1 \times 10^{-4} : 1677.7217$	0.6423	9.2067	0.6269
	$1 \times 10^{-4} : 1 \times 10^{-4} : 3355.4432$	0.6774	13.0268	0.6269

**Table B.9:** Numerical integration by matlab built-in function and Simpson method for IN11 model

$\hat{h}_{MK}$	$j_{MK}$	$E(j_{MK} \hat{h}_{MK})$	$\sigma(j_{MK} \hat{h}_{MK})$	$p(\hat{h}_{MK})$
	$1 \times 10^{-4} : 1 \times 10^{-4} : 838.8609$	0.6072	6.5045	0.6269
0.5	$1 \times 10^{-4} : 1 \times 10^{-4} : 1677.7217$	0.6423	9.2067	0.6269
	$1 \times 10^{-4} : 1 \times 10^{-4} : 3355.4432$	0.6774	13.0268	0.6269

evaluations of integrand for entry at next row in first column of Romberg table are performed already as composite trapezoidal formulae is applied for neighbouring upper row.

From [Carroll](#), approximations of integral  $\int_a^b f(x)dx$  by composite trapezoidal rule are carried out as following, which generate the entries in first column

$$R_{1,1} = \frac{(b-a)}{2} [f(a) + f(b)] \quad (\text{B.2})$$

$$R_{k,1} = \frac{1}{2} \left[ R_{k-1,1} + h_{k-1} \sum_{i=1}^{2^{k-2}} f(a + (2i-1)h_k) \right]; \quad k = 2, 3, \dots \quad (\text{B.3})$$

where

$$h_k = \frac{b-a}{2^{k-1}} \quad (\text{B.4})$$

Remaining columns are produced by

$$R_{k,j} = R_{k,j-1} + \frac{1}{4^{j-1} - 1} (R_{k,j-1} - R_{k-1,j-1}); \quad k = j, j+1 \dots \quad (\text{B.5})$$

It should be noted that integral step is subdivided until the following tolerances are met

$$|R_{n,n} - R_{n-1,n-1}| < 1e-6 \quad (\text{B.6})$$

$$|R_{n,n} - R_{n,n-1}| < 1e-6 \quad (\text{B.7})$$

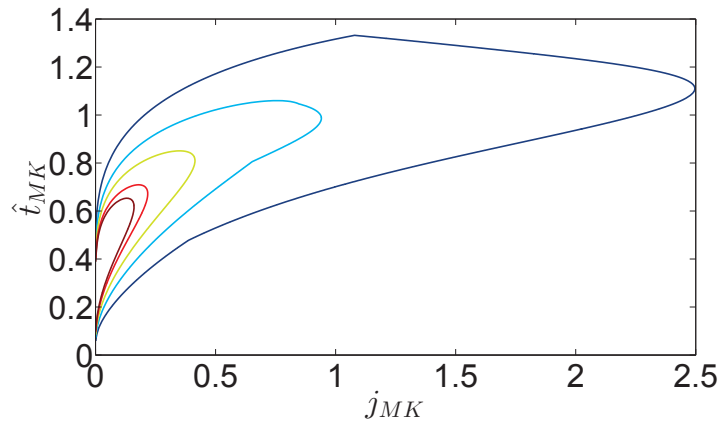
**Table B.10:** Comparison of numerical integration by matlab integral built-in function and recursive Romberg method for IN11 model

$\hat{h}_{MK}$	Romberg		Integral	
	$j_{MK}$	$p(\hat{h}_{MK})$	$j_{MK}$	$p(\hat{h}_{MK})$
0.5	$1 \times 10^{-4} - 1 \times 10^4$	0.4593	$0 - \infty$	0.6269
	$1 \times 10^{-4} - 1.5 \times 10^4$	0.4722		
	$1 \times 10^{-4} - 5 \times 10^4$	0.5104		
	$1 \times 10^{-4} - 2 \times 10^5$	0.5544		
	$1 \times 10^{-4} - 5 \times 10^5$	0.5835		
	$1 \times 10^{-4} - 1 \times 10^6$	0.6055		
	$1 \times 10^{-4} - 1.5 \times 10^6$	0.6184		
	$1 \times 10^{-4} - 1.8 \times 10^6$	0.6242		
	$1 \times 10^{-4} - 2 \times 10^6$	0.6275		
	$1 \times 10^{-4} - 2 \times 10^6$	0.6291		
	$1 \times 10^{-6} - 2 \times 10^6$	0.6291		

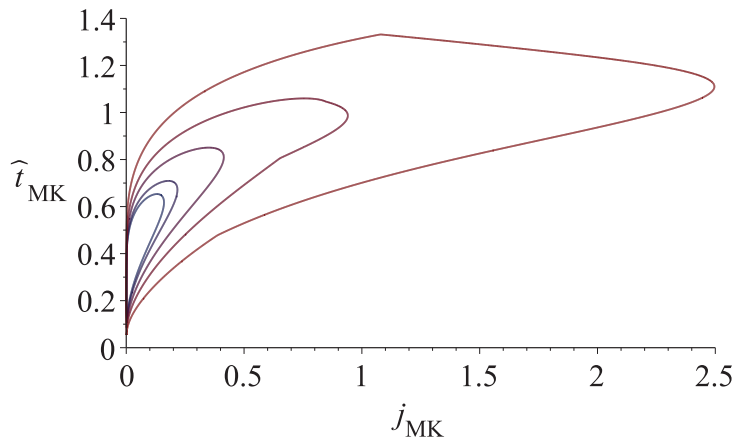
**Table B.11:** Integration steps for numerical stability study of  $\delta E(j_{MK}|\hat{t}_{MK})$  and  $\delta\sigma(j_{MK}|\hat{t}_{MK})$  from IN11 model

Legend	Meaning ( integration steps)
$600_{08}$	$8 \times 10^{-5} : 8 \times 10^{-5} : 600$
$600_1$	$1 \times 10^{-4} : 1 \times 10^{-4} : 600$
$800_1$	$1 \times 10^{-4} : 1 \times 10^{-4} : 800$
$1000_5$	$5 \times 10^{-4} : 5 \times 10^{-4} : 1000$
$1000_2$	$2 \times 10^{-4} : 2 \times 10^{-4} : 1000$
$1200_5$	$5 \times 10^{-4} : 5 \times 10^{-4} : 1200$

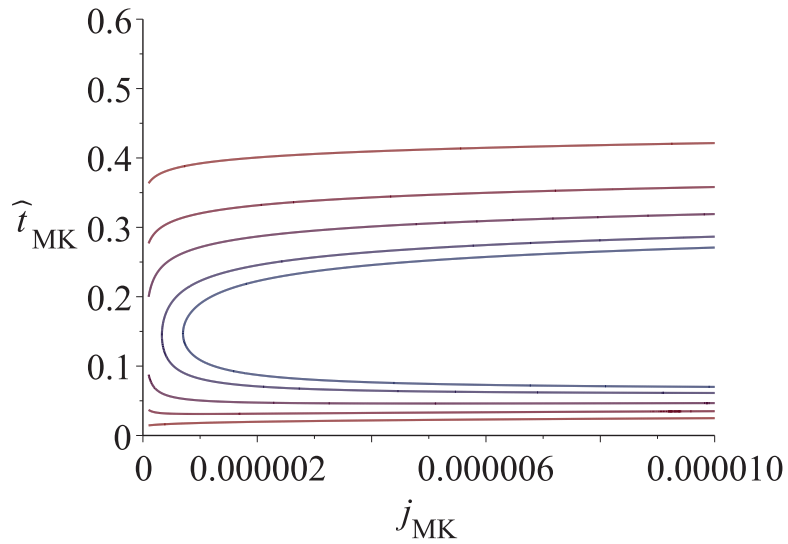




(a) joint pdf of  $(j_{MK}, \hat{t}_{MK})$  plotted by Matlab



(b) joint pdf of  $(j_{MK}, \hat{t}_{MK})$  plotted by Maple



(c) joint pdf of  $(j_{MK}, \hat{t}_{MK})$  plotted by Maple for showing enclosed contour in the proximity of origin

**Figure B.1:** Isocontour of  $p(\hat{t}_{MK}, j_{MK})$  from MB09 model  $p$  takes 0.25, 0.75, 1.25, and 2.0 from outermost to center, respectively

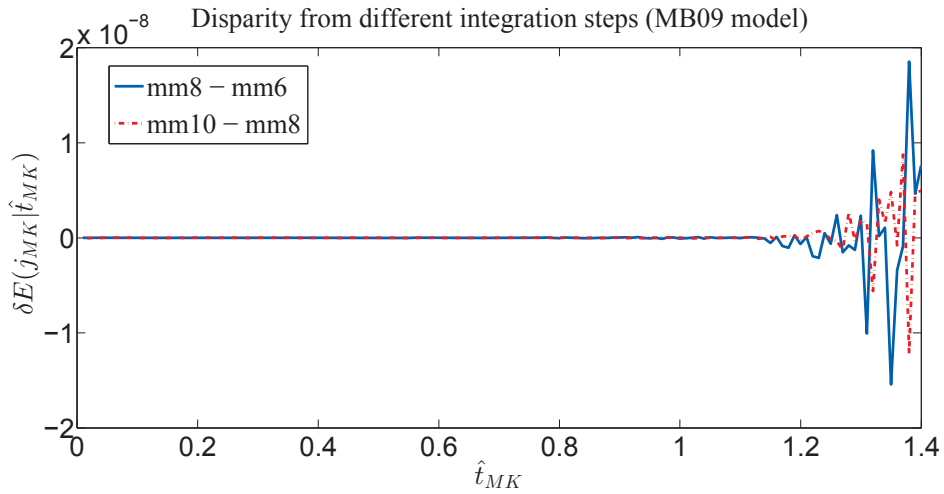


**Figure B.2:**  $\delta E(j_{MK}|\hat{t}_{MK})$  versus  $\hat{t}_{MK}$  from MB09 model

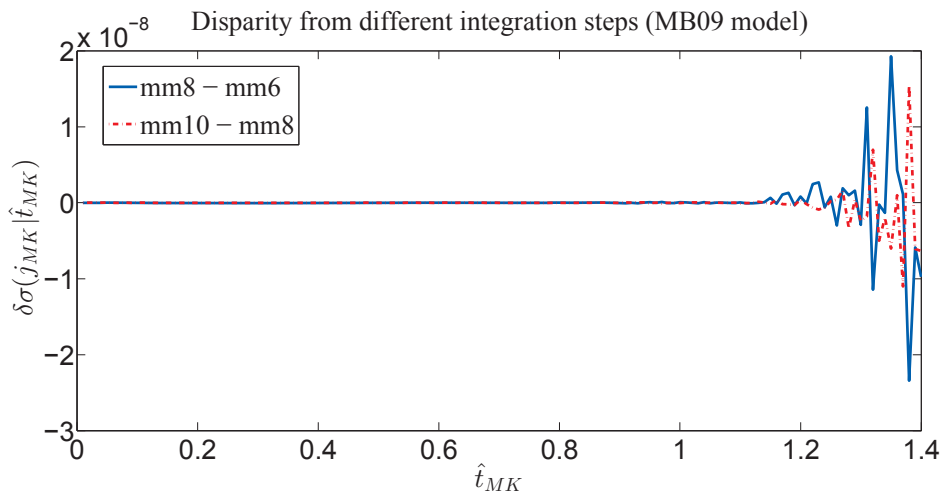


**Figure B.3:**  $\delta \sigma(j_{MK}|\hat{t}_{MK})$  versus  $\hat{t}_{MK}$  from MB09 model

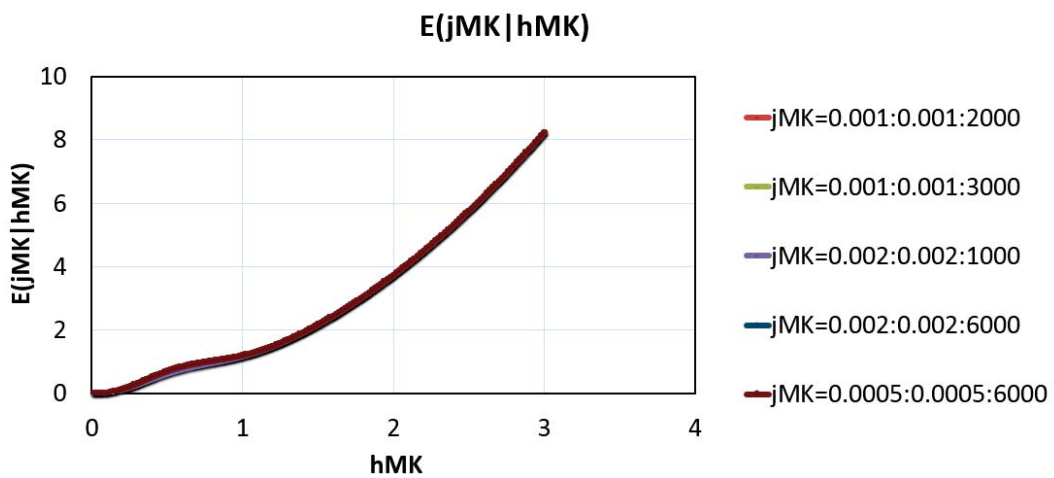


**Figure B.4:**  $E(j_{MK}|\hat{h}_{MK})$  from IN11 model versus  $\hat{h}_{MK}$  ( $h_{MK} \equiv \hat{h}_{MK}$  and  $j_{MK} \equiv j_{MK}$ )

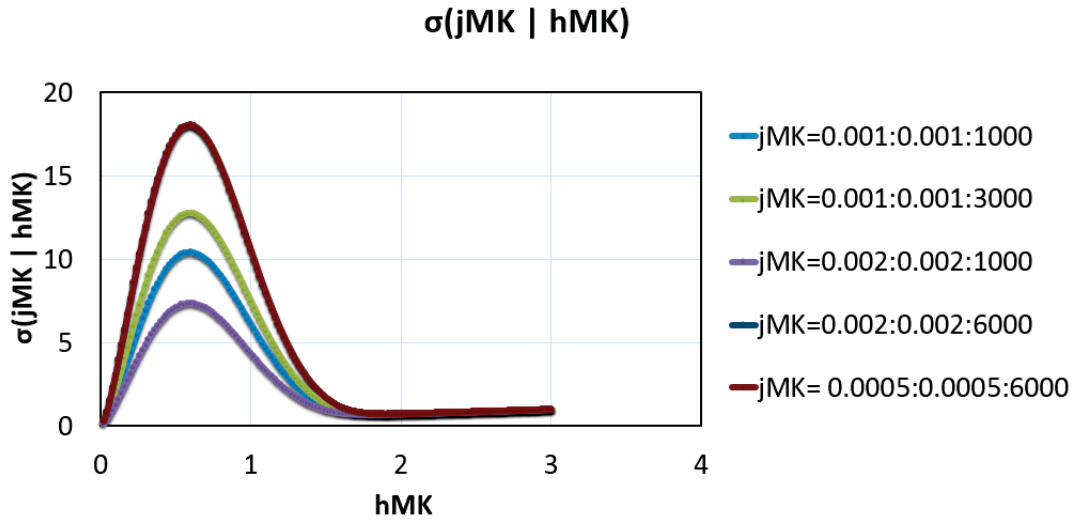


**Figure B.5:**  $\sigma(j_{MK}|\hat{h}_{MK})$  from IN11 model versus  $\hat{h}_{MK}$  ( $h_{MK} \equiv \hat{h}_{MK}$  and  $j_{MK} \equiv j_{MK}$ )

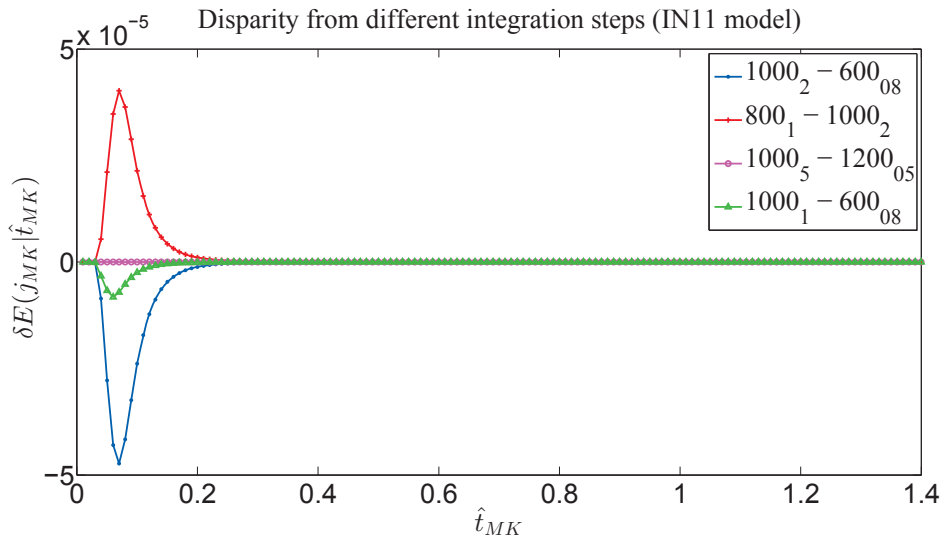


**Figure B.6:**  $\delta E(j_{MK}|\hat{t}_{MK})$  versus  $\hat{t}_{MK}$  from IN11 model

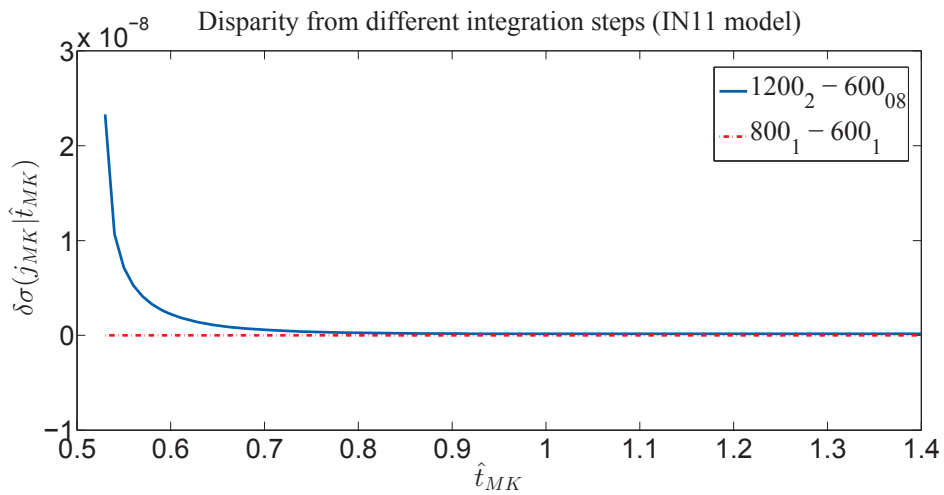


**Figure B.7:**  $\delta\sigma(j_{MK}|\hat{t}_{MK})$  versus  $\hat{t}_{MK}$  from IN11 model

# **Appendix C**

## **Matlab Scripts**

---



---

```

function [pdf] = pdfxiMKhMK(xiMK,hMK,mu)
%%----Joint distribution of surf parameter xiMK and wave height hMK derived
%%----from Logget-Higgins(1983).Normalized quanties are the same as in MK84
%%-----mu is bandwith parameter defined in MK84

%%---Transform to dimensionless quantities used in MK84---
rH=2.8582;
rT=1.2416;
rS = 17.6;
LvIntCC=2/( 1 + (1+mu^2)^(-0.5));
A=rH/(2*sqrt(2));
B=rT/sqrt(1+mu^2);
Cm = sqrt( 4*pi*sqrt(2) / ( rS * (1+mu^2) ) );
%%---Transform to dimensionless quantities used in MK84---

%%----Joint distribution of (xiMK,jMK) derived from Logget-Higgins (1983)
pdf = 2 / (sqrt(pi) * mu) * A^(2.5)/Cm * ...
      (hMK.^(3/2)) ./ (xiMK.^2) .* ...
      exp( (- ( A*hMK).^2) .* ( 1 + ...
      ( 1 - 1./ ( Cm * xiMK.* sqrt(A*hMK) ) ).^2/mu^2))*...
      LvIntCC;
%%----Joint distribution of (xiMK,jMK) derived from Logget-Higgins (1983)

end

```

*Published with MATLAB® R2013a*

---

```

function [intVal,Tol] = RombergInt(funVal,a,b)
%[intVal,Tol] = RombergInt(funVal,a,b)
%Romberg Integration Method: Number of funval n should satisfy log2(n)is
%an integer
%%---Validate against examples in Pages 214 and 215 given by
%%---R. L. Burden and J. D. Faires, Numerical Analysis, 9th edition,
%%---Brooks-Cole, 2010. ISBN-13: 978-0-538-73351-9; ISBN-10: 0-538-73351-9
%%---www.mathstat.dal.ca/~tkolokol/classes/1500/romberg.pdf,
%%---Retrived on May 10, 2014
    nn = length(funVal);
    if mod(nn,2) == 0
        error('myApp:RombergInt','number of funVal for RombertInt should be odd');
    end
    mm = 1+log2(nn-1);
    h = b - a;
    Rtemp=0;
    R2 = h/2 * (funVal(1) + funVal(end));
    kk=1;
    for i = 2:1:mm
        h = h/2;
        R1 = R2;
        Index = 1+2^(mm-i):2^(mm-i):nn-2^(mm-i);
        %%-----Take mm = 5 as an example, extra point needed for first entry of curr
        %%----- 2nd row      9th point -----
        %%-----3rd          5  13 -----
        %%-----4th          3  7  11  15-----
        %%-----5th 2  4  6  8  10  12  14  16-----
        %%--- a = [1 2 3 4], b = [1 3] ---
        %%--- b is excluded from a; [ 2 4]
    Index = Index(~ismember(Index,Rtemp));
        %%--- a = [1 2 3 4], b = [1 3] ---
        %%--- b is excluded from a; [2 4]
    %%*****
        %%---Recursive algorithm, reduce the amount of function evaluations
        %%----First column of Romberg is generated by composite trapezoidal
        R2(1) = R1(1)/2 + h * sum( funVal(Index) );
        %%----First column of Romberg is generated by composite trapezoidal
        %%---Recursive algorithm, reduce the amount of function evaluations
    %%*****
        for k = 2:1:i
            R2(k) = R2(k-1) + ( R2(k-1) - R1(k-1) ) / ( 4^(k-1) -1 );
        end
        %%---Mark previous funtion value evaluated already
        Rtemp = 1+2^(mm-i):2^(mm-i):nn-2^(mm-i);
        %%---Mark previous funtion value evaluated already
    end
    end
    Tol = max( abs(R2(end) - R2(end-1)), abs(R2(end) - R1(end) ));
    intVal = R2(end);

```

---



---

```

clc
clear all
mu=0.504;
LvIntCC=1/2*(1+(1+mu^2)^(-0.5));
%%---Transform to dimensionless quantities used in MK84----
K = 1;
Hs=7.5;
hrms=0.714*Hs;
Hcr = [1 1.4].*hrms;
%%---Parameters-----
Tp=9.5;
Tz=Tp/1.22;
g=9.81;
Sm=Hs/(g*Tz^2/(2*pi));
mslope=0.1;
xirms=mslope/sqrt(0.7*Sm);
%%---Parameters-----
Rstart = 0.0005;
Rend = 250.0005;
JJ = 19;
%%----odd number of elements in R-----
R = Rstart: (Rend - Rstart)/(2^(JJ-1)) :Rend; %% Run-up

NN = length(Hcr);
KK = length(R);
pdf = pdfRH(K,ones(NN,1)*R,Hcr'*ones(1,KK),mu,xirms,hrms);

%%----Integrate over R-----
pdfH = zeros(NN,1);
for i=1:1:NN

    pdfH(i,1) = integral(@(R)pdfRH(K,R,Hcr(i),mu,xirms,hrms),0,inf);

end

%%----Integrate over R-----

%%----Conditional distribution f(R|h)----
conPDF=zeros(NN,KK);
for i=1:1:NN
    conPDF(i,:)=pdf(i,:)/pdfH(i,1);
end
%%----Conditional distribution f(R|h)----

%%---Expected value E(R|hMK)-----
RExpSp=zeros(2,1);
RExpRom = zeros(2,1);
dR = (Rend - Rstart)./(2^(JJ-1));
for i=1:1:2
    %%-----Simpson Method-----

```

---

---

```

RsExpSp(i,1)= dR/3 * ( R(1) * conPDF(i,1) + R(end) * conPDF(i,end) + ...
    4 * sum( R(2:2:end-1).* conPDF(i,2:2:end-1) ) + 2*sum( R(3:2:end-2) .*...
    conPDF(i,3:2:end-2) ) );
%%-----Romberg Method-----
RsExpRom(i,1) = RombergInt( R.*conPDF(i,:),R(1),R(end) );
end
%%---Expected value E(R|hMK)-----

%%-----Find index as R=RsExp-----
colRs=zeros(NN,1);
for i=1:1:NN
    [~,colRs(i,1)]=min(abs(R-RsExpSp(i,1)));
end
%%-----Find index as R=RsExp-----

%%---Verify integral of conditional probability f(R|h) goes to 1--
VCDFxi_h=zeros(NN,1);
for i=1:1:NN

    VCDFxi_h(i)=trapz(R,conPDF(i,:));
end
%%---Verify integral of conditional probability f(R|h) goes to 1--

%%---CDF P(R|h)-----
CDFxi_h=zeros(NN,length(R)-1);

for i=1:1:NN
    for j=2:1:length(R)
        CDFxi_h(i,j-1)=trapz(R(1:j),conPDF(i,1:j));
    end
end

end

for i =1:1:NN
CDFsp(i,1) = CDFxi_h(i,colRs(i,1)-1);
end

%%---Postprocess-----
figure(1);
h_MK = [1 1.4];
colorSig=['r','b','g','k'];
charNum=num2str(h_MK');
cellNum=cellstr(charNum);
headCell=cell(length(colRs),1);
hpNum=zeros(length(colRs),1);
for i=1:1:length(colRs)
    x=R(2:end);
    y=CDFxi_h(i,:);
    headCell{i,1}='$h_{MK}$ = ';

    hpNum(i,1)=plot(x,y,'Color',colorSig(i),'LineWidth',2);
    hold on;
end

```

---



---



---

```

for i=1:1:length(colRs)

    xR=R(colRs(i,1));
    yR=CDFxi_h(i,colRs(i,1)-1);
    plot(xR,yR,'Marker','+','MarkerEdgeColor',colorSig(i),'MarkerSize',16);
    hold on;
end

strLeg=strcat(headCell,cellNum);
grid on;
hpLeg=legend(hpNum,strLeg,'Location','Best','FontSize',12,'FontWeight','bold');
set(hpLeg,'Interpreter','Latex');
xlabel('Run up [m]','interpreter','latex','FontSize',14);
ylabel('Cummulative Distribution ','interpreter','latex','FontSize',14);
title('Run-up distribution for Hs=7.5 m - Tp=9.5 s - m=0.1','Interpreter',...
'Latex','FontSize',14);
%%----Postprocess-----

```

*Published with MATLAB® R2013a*

```
function [hMK,Rv,cdfRH,ExpRH,cdfExp] = MF12Fig17()
%%---- [hMK,Rv,cdfRH,ExpRH,cdfExp] = MF12Fig17()----
%%----Calculate cdf of runup given hMK, expected value E(R|hMK) as well as
%%----its probability
%%----Enlightened by Eqs.(9),(11) and 13 in Dag Myrhaug (2012)

hMK = [ 0.25 0.5 1 1.4 2.1];
Rv = 0.002:0.002:10;
K = 1;
Hs=7.5;          %% significant wave height
Hrms=0.714*Hs;
Tp=9.5;         %% peak period
Tz=Tp/1.22;    %% average zero crossing period
g=9.81;
Sm=Hs/(g*Tz^2/(2*pi));
Srms=0.7*Sm;   %% rms value of wave steepness
mslope=0.1;   %% slope
xirms=mslope/sqrt(Srms);
cdfRH = zeros(length(hMK),length(Rv));
ExpRH = zeros(length(hMK),1);
cdfExp = zeros(length(hMK),1);
for nn = 1:1:length(hMK)
    for kk = 1:1:length(Rv)
        [cdfRH(nn,kk),muR,sigmaR] = funR_H(hMK(nn),Rv(kk),K,xirms,Hrms);
    end
    ExpRH(nn) = exp(muR + 1/2 * sigmaR);
    [~,col] = min(abs(Rv - ExpRH(nn)));

    cdfExp(nn) = cdfRH(nn,col);
end
```

```
function [cdfRH,muR,sigmaR] = funR_H(h,Rv,K,xirms,Hrms)

sigmaS = - 0.15 * atan( 1.75 * ( h - 1.2) ) + 0.225; %% Eq.(5)
sigmaXi = 1/4 * sigmaS; %% Eq.(10)
sigmaR = sigmaXi;
[m,n] = size(h);
muR = zeros(m,n);

for i = 1:1:m
    for k = 1:1:n
        if h(i,k) <= 1.7
            mus = 0.558 * h(i,k)^2 - 1.021 * h(i,k) + 0.096; %% Eq.(4)

        else if h(i,k) > 1.7
            mus = 0.25 * atan( 4 * ( h(i,k) - 1.7) ) - 0.027; %% Eq.(4)
        end
    end

    muR(i,k) = - mus /2 + log( K * xirms * Hrms * h);
    x = (log(Rv) - muR(i,k)) / sqrt(sigmaR); %% Eq.(11)
```

---

---

```
        cdfRH = normcdf(x,0,1);  
    end  
end  
  
end  
end
```

*Published with MATLAB® R2013a*

# Appendix D

## Example of visual basic code for Excel

```
Sub ConvergedStudy()  
Dim i As Long  
Dim j As Long  
For j = 1 To 2 Step 1  
For i = 1 To 1999 Step 1  
Cells(2 + i, 9 + j).Value = Abs(Cells(2 + i, 1 + j).Value - Cells(5 + (i - 1) * 2, 5 + j).Value)  
Next i  
Next j  
End Sub
```

In the user interface of Excel, following command is useful to find the exact cell storing maximum value in one column: '=ADDRESS(MATCH(MAX(K:K),K:K,0),COLUMN(K:K))'

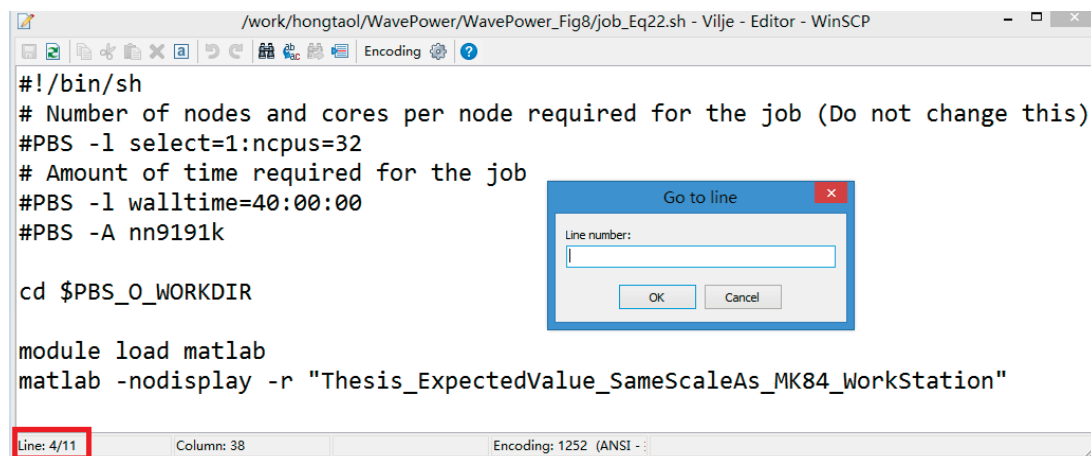
# Appendix E

## Example of bash script for using on supercomputer

Useful short-cut is the Ctrl + G to open the 'Go to File' window to locate at a specific line. The line number the cursor at is indicated as shown by the red rectangular region in Fig. E.1.

In putty software, useful commands include

- cd ../XX, XX represents the directory to be changed into under the same parent directory as the current directory is in
- qsub job\_Eq22.sh, submit job\_Eq22.sh to run Matlab script Thesis\_ExpectedValue\_SameScaleAsMK84\_WorkStation.m
- qstat, check current status of files run on server, including the time elapsed for running
- qdel 2440517.server2 , delete job 2440517 run on number 2 server



The screenshot shows a WinSCP editor window titled "/work/hongtaol/WavePower/WavePower\_Fig8/job\_Eq22.sh - Vilje - Editor - WinSCP". The editor contains a bash script with the following content:

```
#!/bin/sh
# Number of nodes and cores per node required for the job (Do not change this)
#PBS -l select=1:ncpus=32
# Amount of time required for the job
#PBS -l walltime=40:00:00
#PBS -A nn9191k

cd $PBS_O_WORKDIR

module load matlab
matlab -nodisplay -r "Thesis_ExpectedValue_SameScaleAs_MK84_WorkStation"
```

A "Go to line" dialog box is overlaid on the script, with a text input field for "Line number:" and "OK" and "Cancel" buttons. A red rectangular box highlights the status bar at the bottom left, which shows "Line: 4/11".

Figure E.1: Example of bash script